European Journal of Mineralogy

Fe-rich antigorite: A rock-forming mineral from low-temperature/high-pressure meta-ophicarbonates

--Manuscript Draft--

Manuscript Number:	ejm190029R1
Article Type:	Research paper
Full Title:	Fe-rich antigorite: A rock-forming mineral from low-temperature/high-pressure meta-ophicarbonates
Short Title:	Fe-rich antigorite from LT-HP meta-ophicarbonates
Corresponding Author:	Chiara Groppo University of Torino Torino, ITALY
Corresponding Author E-Mail:	chiara.groppo@unito.it
Order of Authors:	Simonpietro Di Pierro
	Chiara Groppo
	Roberto Compagnoni
	Giancarlo Capitani
	Marcello Mellini
Abstract:	This study provides the first characterization of Fe-rich antigorite (FeOtot up to 12 wt%), a rock-forming mineral occurring in ophicarbonate rocks from different low-temperature/high-pressure meta-ophiolitic suites: Acceglio (Traversiera Valley, external Piemonte Zone, NW Italy), Macedonia and Verias (Thessaloniki and Vurinos-Kozani ophiolitic complexes, NE Greece), Tinos (Tinos Island, Cyclades Archipelago, Greece). Fe-rich antigorite has been characterized through optical and transmission electron microscopy, and its mineral chemistry has been investigated by means of WDS and TEM-EDS techniques. In thin section, Fe-rich antigorite is characterized by a strong, peculiar pleochroism (α = green to dark green; γ = bright-yellow to orange). It occurs in both mesh and bastite microstructures, and it is locally associated with relics of lizardite and/or chrysotile. The modulated lattice parameters of disordered Fe-rich antigorites have been determined by electron diffraction in the transmission electron microscope. The values are highly variable, even within each ophicarbonate sample. Verias dominantly has a superlattice parameter a clustering around 43.5 Å (corresponding to the m = 17 polysome); Tinos and Macedonia have around 35.4 Å (m = 14); Acceglio may even go down to 29 Å (m = 12). Globally, the disorder features (i.e., reduced size of crystals, polysomatic faults, wobbling, misalignment among sublattice and superlattice reflections, etc.) increase from Macedonia to Verias, Tinos and Acceglio, respectively. The analyzed Fe-rich antigorites accommodate up to 12 wt% FeOtot: Macedonia and Acceglio are richer in Fe than Tinos and Verias, with XFe values [XFe=Fetot/(Mg+Fetot)] in the range 0.10-0.16 for Macedonia, 0.05-0.17 for Acceglio, 0.10-0.12 for Tinos and 0.05-0.10 for Verias. The intensity of the pleochroism seems to be directly correlated with the Fe content, with the Fe-richer samples showing the deeper absorption colours. Mineral relationships and TEM observations suggest that Fe-rich antigorite replaces former mesh and bastite microstructures consisting of lizardite ± chrysotile, only locally preserved as relict phases. The thermodynamic modelling approach (i.e., P/T-X(CO2) pseudosection) qualitatively shows that the stability of Fe-rich antigorite is compatible with low-temperature, high-pressure conditions (i.e., blueschist-facies metamorphic conditions), and is enhanced by the occurrence of CO2 in the fluid, consistent with the systematic occurrence of this mineral in meta-ophicarbonate rocks.
Keywords:	Fe-rich antigorite; meta-ophicarbonates; Transmission Electron Microscopy; thermodynamic modelling; blueschist-facies metamorphism; H2O-CO2 fluid
Manuscript Region of Origin:	ITALY
Requested Editor:	Patrick Cordier, Editor-in-Chief

Additional Information:	
Question	**Response**
Author Comments:	Dear Editor, the two reviewers and your own constructive comments have been carefully considered in order to improve the revised version of our manuscript. Please, find in the attached pdf file (ANSWERS TO EDITOR AND REVIEWERS) how and where the editor + reviewers comments have been incorporated in the manuscript (comments, suggestions and criticisms from the reviewers are shown in black; answers and comments from the authors are shown in red). We hope that the manuscript now meets your approval for publication in European Journal of Mineralogy. With best regards, Chiara Groppo and co-authors
Response to Reviewers:	See the attached pdf file (ANSWERS TO EDITOR AND REVIEWERS)

Cover Page

Title: **Fe-rich antigorite: A rock-forming mineral from low-temperature/high-pressure meta-ophicarbonates**

Running title
Fe-rich antigorite from LT-HP meta-ophicarbonates

Detailed plan of the article:

Corresponding author:
Chiara Groppo
Dept. of Earth Sciences, University of Torino
Via Valperga Caluso, 35, 10125 Torino (Italy)
chiara.groppo@unito.it
Tel. +39/0116705106
Fax: +39/0116705128

Title Page

Fe-rich antigorite: A rock-forming mineral from low-temperature/high-pressure meta-ophicarbonates

Simonpietro Di Pierro[1,2§], Chiara Groppo[1,3*], Roberto Compagnoni[1], Giancarlo Capitani[4] and Marcello Mellini[5]

[1] Department of Earth Sciences, University of Turin, via Valperga Caluso 35, 10125 Torino, Italy
[2] Institut de Minéralogie et Pétrographie, Université de Fribourg, Switzerland
[§] Present address: Saint-Gobain Recherche, Paris, France. E-mail: simonpietro.dipierro@saint-gobain.com
[3] CNR-IGG, via Valperga Caluso 35, 10125 Torino, Italy
[4] Department of Earth and Environmental Sciences (DISAT), University of Milano Bicocca, Italy
[5] Department of Earth Sciences (now Dept. of Physical Sciences, Earth and Environment), University of Siena, Italy
*Corresponding author: chiara.groppo@unito.it

Abstract

This study provides the first characterization of Fe-rich antigorite (FeO_{tot} up to 12 wt%), a rock-forming mineral occurring in ophicarbonate rocks from different low-temperature/high-pressure meta-ophiolitic suites: *Acceglio* (Traversiera Valley, external Piemonte Zone, NW Italy), *Macedonia* and *Verias* (Thessaloniki and Vurinos-Kozani ophiolitic complexes, NE Greece), *Tinos* (Tinos Island, Cyclades Archipelago, Greece). Fe-rich antigorite has been characterized through optical and transmission electron microscopy, and its mineral chemistry has been investigated by means of WDS and TEM-EDS techniques.

In thin section, Fe-rich antigorite is characterized by a strong, peculiar pleochroism (α = green to dark green; γ = bright-yellow to orange). It occurs in both mesh and bastite microstructures, and it is locally associated with relics of lizardite and/or chrysotile. The modulated lattice parameters of disordered Fe-rich antigorites have been determined by electron diffraction in the transmission electron microscope. The values are highly variable, even within each ophicarbonate sample. *Verias* dominantly has a superlattice parameter *a* clustering around 43.5 Å (corresponding to the *m* = 17 polysome); *Tinos* and *Macedonia* have around 35.4 Å (*m* = 14); *Acceglio* may even go down to 29 Å (*m* = 12). Globally, the disorder features (*i.e.*, reduced size of crystals, polysomatic faults, wobbling, misalignment among sublattice and superlattice reflections, etc.) increase from *Macedonia* to *Verias*, *Tinos* and *Acceglio*, respectively. The analyzed Fe-rich antigorites accommodate up to 12 wt% FeO_{tot}: *Macedonia* and *Acceglio* are richer in Fe than *Tinos* and *Verias*, with X_{Fe} values [$X_{Fe}=Fe_{tot}/(Mg+Fe_{tot})$] in the range 0.10-0.16 for *Macedonia*, 0.05-0.17 for *Acceglio*, 0.10-0.12 for *Tinos* and 0.05-0.10 for *Verias*. The intensity of the pleochroism seems to be directly correlated with the Fe content, with the Fe-richer samples showing the deeper absorption colours.

Mineral relationships and TEM observations suggest that Fe-rich antigorite replaces former mesh and bastite microstructures consisting of lizardite ± chrysotile, only locally preserved as relict phases. The thermodynamic modelling approach (*i.e.*, *P/T*-$X(CO_2)$ pseudosection) qualitatively shows that the stability of Fe-rich antigorite is compatible with low-temperature, high-pressure conditions (*i.e.*, blueschist-facies metamorphic conditions), and is enhanced by the occurrence of CO_2 in the fluid, consistent with the systematic occurrence of this mineral in meta-ophicarbonate rocks.

Key-words

Fe-rich antigorite, meta-ophicarbonates, Transmission Electron Microscopy, thermodynamic modelling, blueschist-facies metamorphism, H_2O-CO_2 fluid

1. Introduction

The serpentine minerals are composed of Si_2O_5 tetrahedral sheets alternating with $Mg_3(OH)_4$ octahedral sheets, stacked along the *c* axis (Wicks & O'Hanley, 1988; Evans *et al*., 2013, and references therein). The different serpentine minerals are not real polymorphs. Lizardite, polygonal serpentine and chrysotile have the ideal general formula $^{VI}M_3{}^{IV}T_2O_5(OH)_4$, where M = Mg, Fe^{2+}, Ni, Al, and T = Si, Al, Fe^{3+}; antigorite deviates because of discrete $Mg(OH)_2$ loss (Mellini *et al*., 1987). The structure of lizardite is based upon flat 1:1 layers (Mellini & Viti, 1994). Chrysotile has a cylindrical structure resulting from curled 1:1 layers (Wicks & O'Hanley, 1988). Antigorite has a modulated wave-like 1:1 layer, with polarity inversion every half wavelength (Capitani & Mellini, 2004). The variable modulation gives rise to a polysomatic series, with general formula $M_{3m-3}T_{2m}O_{5m}(OH)_{4m-6}$, *m* being the number of tetrahedra within a wavelength (Mellini *et al*., 1987; Otten, 1993).

In undeformed ultramafic rocks, serpentine resulting from peridotite hydration develops microstructures typical of retrograde metamorphic conditions, namely mesh and bastite microstructures after olivine and orthopyroxene, respectively (Moody, 1976; Dungan, 1979a,b; O'Hanley & Dyar, 1993). Lizardite dominates in the mesh rims, whereas mesh cores and bastites mainly consist of lizardite, polygonal serpentine and chrysotile (Viti & Mellini, 1998). Conversely, antigorite is the typical metamorphic serpentine mineral, stable from greenschist- to low-amphibolite- and eclogite-facies conditions (Trommsdorff & Evans, 1972, 1977a,b; Dungan, 1979b; Mellini *et al*., 1987; Evans, 2004).

We now report the occurrence of a rock-forming Fe-rich antigorite (up to 12 wt% FeO_{tot}) replacing former mesh and bastite microstructures consisting of lizardite ± chrysotile, these last only locally preserved as relict phases. Fe-rich antigorite is easily recognizable in thin section for its marked pleochroism, variable from green to bright-yellow and orange. Serpentine minerals with similar optical features have been previously reported by other authors (*e.g*., Frondel, 1962; Dietrich, 1972; Driesner, 1993; Groppo, 2005), but their unambiguous identification as antigorite was not given. This study thus provides the first characterization of this rock-forming mineral by means of different techniques (*i.e.,* optical microscopy, transmission electron microscopy and wavelength-dispersive electron microprobe). The systematic occurrence of Fe-rich antigorite in low-temperature/high-pressure (LT-HP) meta-ophicarbonate rocks (serpentinite breccias with carbonate cement) suggests that its stability could be favoured by LT-HP metamorphic conditions and could be enhanced by the presence of CO_2-bearing fluids, as further confirmed, at least qualitatively, by the thermodynamic modelling approach.

2. Samples and methods

2.1 Samples

Fe-rich antigorite has been identified during the systematic study of ophicarbonates used as dimension stones (Di Pierro, 1997). Various ophicarbonate samples from four different localities contain Fe-rich antigorite. The first ophicarbonate, trade name *Verde Acceglio*, is quarried near Acceglio village, Val Maira (ca. 44°28'51''N, 6°58'51''E), from the roof of the serpentinitic basement of the meta-ophiolitic complex of the Traversiera Valley (Schwartz *et al*., 2000). The *Verde Acceglio* ophicarbonate belongs to the external Piemonte Zone, Western Alps, which underwent peak metamorphism under medium-temperature (350-400°C) blueschist-facies conditions (Schwartz *et al*., 2000, 2013). The second ophicarbonate (*Green Tinos*) is quarried in the northern portion of Tinos Island (ca. 37°40'29''N, 25°00'28''E), Cyclades Archipelago, Greece. The *Tinos* ophicarbonate is part of an ophiolitic sequence, including also serpentinized harzburgite and metagabbro (Stolz *et al*., 1997). The ultramafic rocks reported from the Island of Tinos consist of antigorite-bearing serpentinites and ophicarbonates partly assigned to the low-*T* and high-*P* eclogite- to blueschists-facies units of the Cyclades Archipelago (Stolz *et al*., 1997; Ring & Layer, 2003). The other two samples (*Green Macedonia* and *Green Verias*) are ophicarbonates from NW Macedonia, Greece. *Green Macedonia* belongs

to the Thessaloniki ophiolite nappes, and *Green Verias* to the Vurinos-Kozani ophiolitic complex, located respectively west and est of the city of Veria (ca. 41°31'10''N, 22°12'07''E) (Tsikouras & Hatzipanagiotou, 1998). The *Green Verias* and the *Green Macedonia* are both derived from blueschist-facies units.

2.2 Microscopy and microanalysis

The rocks were studied in polished thin sections by optical microscopy and electron microprobe microanalysis (Cameca SX 50 Electron Microprobe, EMPA) with wavelength dispersive spectrometers, WDS, at the Geologisches Institut, the University of Bern. Operating conditions were 15 kV and 20 nA. The following natural silicates and oxides were used as standards: almandine (Fe), spinel (Mg), orthoclase (K, Si), anorthite (Ca, Al), eskolaite (Cr), tephroite (Mn), albite (Na), ilmenite (Ti) and bunsenite (Ni). Transmission electron microscopy (TEM) analyses were carried out at the Department of Physical Sciences, Earth and Environment, the University of Siena, on polished thin sections (ion-milled to electron transparency) by a JEOL 2010 microscope working at 200 kV, equipped with an energy dispersive spectrometer (EDS).

2.3 Thermodynamic modelling

A *P/T-X*(CO_2) pseudosection was calculated in the CFMAS-HC (CaO-FeO-MgO-Al_2O_3-SiO_2-H_2O-CO_2) system along a 7°C km^{-1} gradient, compatible with the blueschist-facies metamorphism experienced by the studied samples. O_2 was neglected, due to the current unavailability of a solution model considering the Fe^{3+} exchange in antigorite. A generic lherzolitic bulk composition (SiO_2=41, Al_2O_3=1, MgO=50, FeO=5, CaO=3 mol%) was used, and the binary H_2O-CO_2 fluid was considered in excess. The pseudosection was calculated using Perplex 6.8.6 (version February 2019; Connolly, 1990, 2005, 2009), the internally consistent thermodynamic dataset of Holland & Powell (2011) (ds62) and the equation of state for H_2O-CO_2 fluid of Holland & Powell (1998). The following solution models were used: olivine (Holland & Powell, 1998), antigorite (Padrón-Navarta *et al*., 2013), clinopyroxene and orthopyroxene (Holland & Powell, 1996), chlorite (Holland *et al*., 1998), tremolite, talc and brucite (ideal models; Connolly, 1990). Aragonite was considered as a pure phase.

3. Results

3.1 Optical properties

Only *Green Macedonia* will be described in detail, because the optical properties of Fe-rich antigorite are the same in the four studied ophicarbonates. Structurally, the rock is a breccia composed of serpentinite fragments cemented by a network of calcite veins. Serpentine, more than 50 vol%, occurs both in mesh and bastite microstructures (Fig. 1), apparently pseudomorphous after olivine and orthopyroxene, respectively (Viti & Mellini, 1998). The mesh microstructure consists of a pleochroic serpentine (mostly identified as Fe-rich antigorite under the TEM, see section 3.2), and minor carbonate and magnetite (Fig. 1). This serpentine has a lamellar habit and defines a mesh microstructure characterized by two sets of orientations cross-cutting each other at about 60°, most likely due to moderate tectonic deformation. Carbonate and minor subhedral magnetite occur in the mesh core, with magnetite mostly localized at the intermesh boundaries. Bastites, mainly consisting of a similar pleochroic serpentine (also identified as Fe-rich antigorite at the TEM), normally do not show magnetite and carbonate (Figs. 1a,b). Accessory diopside, locally replaced by tremolite, and Cr-rich spinel replaced by magnetite at the rims (the so-called "ferritchromite"; *e.g*., Mellini *et al*., 2005) are present as well. The relative proportions of mesh and bastite, which correspond in the peridotite protolith to olivine and orthopyroxene, respectively, and the limited presence of clinopyroxene relics, suggest either a Cpx-poor lherzolite or a harzburgite protolith. Representative microstructures for *Green Macedonia* and *Acceglio* are shown in Fig. 1.

Unlike common antigorite, normally colourless to pale green, Fe-rich antigorite is strongly pleochroic with α = green to dark green and γ = bright yellow to orange (Fig. 1), has low relief (consistent with that of "normal" antigorite; Deer *et al*., 1992), no evident cleavage, and positive elongation. Under crossed polarizers, in the mesh pseudomorphs, Fe-rich antigorite shows low to very-low birefringence with anomalous brownish-yellow to grey-green interference colours (Figs. 1c,f), whereas in the bastite pseudomorphs birefringence is higher (δ = 0.025, Fig. 1c). The difference in birefringence is possibly due to different chemical compositions (see EMPA data in section 3.3). In the veins, Fe-rich antigorite looks fibrous with fiber elongation orthogonal to the vein selvages (Fig. 1f). Fe-rich antigorite is biaxial with $2V_\alpha \approx 20°$, definitely smaller than in "normal" antigorite ($2V_\alpha \approx 37$ - 61°; Deer *et al*., 1992). Due to the very fine grain-size of both mesh and bastite microstructures, the above reported optical characteristics (in particular the 2V) must be considered with care, having been obtained not from a single crystal but from fine-grained aggregates of sub-microscopic intergrowth of crystals with a preferred orientation. Chrysotile and fine-grained colourless antigorite have additionally been observed in veins of *Green Tinos*.

3.2 Transmission electron microscopy (TEM) characterization

Reliable characterization of serpentine minerals may be obtained by transmission electron microscopy (TEM). In fact, chrysotile, lizardite, polygonal serpentine and antigorite often occur as fine-grained, intimately intergrown crystals (Wicks & O'Hanley, 1988; O'Hanley, 1996; Mellini *et al*., 2002), thus preventing their unambiguous identification by means of optical microscopy or scanning electron microscopy.

TEM images and diffraction patterns along with EDS analyses confirmed the presence of Fe-rich antigorite in all the ophicarbonate samples, with remarkable differences both from sample to sample and within the same sample. Fe-rich antigorite is almost the only serpentine mineral in *Green Macedonia* and *Green Verias*, where it occurs as lath-shaped, submicrometer sized, highly faulted crystals (*e.g*., Fig. 2a), whereas it is the dominant serpentine phase in *Green Tinos* and *Acceglio* samples, where it forms smaller, fish-shaped, poorly ordered crystals, always associated with relict chrysotile and lizardite (*e.g*., Fig. 2b).

Reliable, statistically significant determination of the superlattice parameter *a* was markedly hampered by the limited order of these antigorites, suffering from tiny crystal size, important polysomatic disorder, evident offset effects (*i.e.*, mutual rotation between sublattice and superlattice vectors; e.g., inset of Fig. 2a). These are features typical of poorly annealed antigorite, suffering from concerted polysomatic faults, known as wobbling (*e.g*., Otten, 1993). Globally, *a* values range from ~43.5 Å to ~29.1 Å, with the most recurrent values close to 35.4 Å. *Verias* dominantly has a superlattice parameter *a* clustering around 43.5 Å (*m* = 17 polysome); *Tinos* and *Macedonia* have around 35.4 Å (*m* = 14); *Acceglio* may even go down to 29 Å (*m* = 12). The disorder features increase from *Macedonia* to *Verias*, *Tinos* and *Acceglio*, respectively.

Mellini *et al*. (1987) and Padrón-Navarta *et al*. (2008) reported low *m* values, in the range 13-17 for HT metamorphic antigorites (Valmalenco and Cerro del Almirez antigorites, respectively), whereas higher *m* values, up to 23, are reported by Mellini *et al*. (1987) for LT antigorites, suggesting the existence of an inverse relation between *m* parameter and metamorphic annealing. The same general correlation has been confirmed for synthetic antigorite by Wunder *et al*. (2001). However, *m* values between 13 and 19 (namely, shorter than expected) are common also in the low- to very-low-grade vein antigorites from Elba (Viti & Mellini, 1996). Similarly, *m* values between 12 and 16 have been reported for oceanic serpentinites from the Mid-Atlantic Ridge, for which a formation temperature < 300°C was estimated based on oxygen isotope data (Ribeiro da Costa *et al*., 2008); in that case, the low *m* values combined with the highly disordered state of the analyzed antigorite were interpreted to be related to low temperature, incipient crystallization rather than as a sign that antigorite formed at high temperatures. Finally, *m* values in the range 16-21 are reported

for HP antigorites from the western Alps (Monviso Massif; Auzende *et al*., 2006). Our data seem to duplicate the latter cases, showing low *m* values even in rocks from LT-HP settings.

3.3 Mineral chemistry (WDS and TEM-EDS)

Selected representative EMPA analyses are reported in Table 1; the complete sets of analyses for the four studied samples are reported as supplementary material in Tables SM1-SM4 and plotted in Fig. 3. Antigorite analyses have been normalized on the basis of the total cations (a.p.f.u.) corresponding to each polysome (*i.e.*, Σcat=4.824 for the *m*=17 *Verias* antigorite, Σcat=4.786 for the *m*=14 *Macedonia* and *Tinos* antigorites and Σcat=4.750 for the *m*=12 *Acceglio* antigorite). Chemical compositions of Fe-rich antigorite are quite homogeneous, with low standard deviations (≈1 wt%). The SiO_2 content, in the range 41-42 wt%, is obviously lower than in Fe-poor antigorite, in which it is generally around 45 wt% (Trommsdorff & Evans, 1972; Dungan, 1979b; Uehara & Shirozu, 1985). MgO ranges from 33.4 to 38.2 wt% and seems to be unevenly distributed between mesh and bastite domains. MnO is present as traces, max 0.11 wt%, while NiO, up to 0.52 wt%, is more significant. Substantial amounts of Cr_2O_3 occur in the Fe-rich antigorite from the *Macedonia* bastites, up to 0.32 wt%, and *Tinos* mesh, max 0.68 wt%. Al_2O_3 and Cr_2O_3 contents are generally significantly lower in mesh than in bastite antigorite (*e.g*., *Macedonia*, Table 1 and Fig. 3b). Similar systematic Al and Cr enrichment in bastite serpentine relative to Ni-rich mesh serpentine is known from the Durrington-Sultan Complex retrograde serpentinites, California (Dungan, 1979b), and from Elba Island, Italy (Viti & Mellini, 1998). These values have been interpreted as inherited from the pristine compositions of the former olivine and orthopyroxene.

The most unusual feature of Fe-rich antigorite is its iron content. The *Macedonia* and *Acceglio* Fe-rich antigorites accommodate up to 12 wt% FeO_{tot}, in contrast with the average FeO_{tot} content of 2-4 wt.% reported elsewhere for antigorite (*e.g*., Evans, 1972, 1977a,b; Dungan, 1979b; Uehara & Kamata, 1994; O'Hanley, 1996; Viti & Mellini, 1996; Trommsdorff & Trommsdorff *et al*., 1998; Mellini *et al.,* 2002; Capitani & Mellini, 2004; Padrón-Navarta *et al*., 2008; Evans *et al*., 2012; Debret *et al*., 2014). Overall, *Macedonia* and *Acceglio* antigorites are richer in Fe than *Tinos* and *Verias* antigorites, with X_{Fe} values [$X_{Fe}=Fe_{tot}/(Mg+Fe_{tot})$] in the range 0.10-0.16 for *Macedonia*, 0.05-0.17 for *Acceglio*, 0.10-0.12 for *Tinos* and 0.05-0.10 for *Verias* (Fig. 3a). The Fe content of Fe-rich antigorite seems to control the intensity of the pleochroic absorption: the deeper orange and green colours, in fact, have been noted in the Fe-richer samples (*Macedonia* and *Acceglio*), whereas the Fe-poorer *Verias* antigorite has lighter absorption colours.

The most recent Mössbauer (Evans *et al*., 2012) and micro-XANES (Debret *et al*., 2014, 2015) data on antigorite samples show that Fe can occur in both bivalent and trivalent states. Therefore, the question of the Fe oxidation state in the studied Fe-rich antigorites cannot be ignored. Assuming an ideal Tschermak's $(Fe^{3+},Al)_2Mg_{-1}Si_{-1}$ substitution, as suggested by Evans *et al*. (2012), the Fe^{3+} content in antigorite may be tentatively calculated from microprobe analyses as Fe^{3+} a.p.f.u. = 2×(2-Si-Al/2-Cr/2). This assumption is based on the hypothesis that half of all trivalent cations inversely correlate 1:1 with Si, and that Al^{3+} and Fe^{3+} are equally distributed in the tetrahedral and octahedral sites. Fig. 3b shows that most of the analyzed Fe-rich antigorites are characterized by a deficiency in the occupation of the T sites, which is potentially a measure of half the total Fe^{3+}, except for the bastite Fe-rich antigorites, which mostly plot along the ideal Tschermakite substitution line or slightly above it. It is worth noting that such a calculation may be affected by numerous uncertainties, well explained by Evans *et al*. (2012), and should be therefore considered with care. Apart from the possible analytical uncertainties, false x-values in Fig. 3b may be due to: (i) the presence of undetected amounts of chrysotile or lizardite impurities, as suggested by observations under TEM (see section 3.2) and/or (ii) the use of an inappropriate total cations formula, *i.e.* the presence of *m* values locally (at the point analysis) different from the most frequent value used for the normalization purpose. Both these possible

sources of uncertainties are very probable in the studied samples, and may partially explain the sub-horizontal trends that characterize most of the samples in Fig. 3b. Fig. 3c is a direct derivative of Fig. 3b and is a plot of the calculated Fe^{3+} (a.p.f.u.) vs. the measured Fe_{tot} (a.p.f.u.). Fig. 3c shows that: (i) the measured Fe_{tot} is in the range 0.12-0.48 a.p.f.u.; (ii) for most of the analyzed antigorites the calculated Fe^{3+} is positive, except for the bastite antigorites (differentiated from mesh antigorite only for the *Macedonia* sample) that have a negative Fe^{3+}, suggesting that they do not respect the assumption of an ideal Tschermak's substitution; (iii) the calculated Fe^{3+}/Fe_{tot} ratio is highly variable, ranging between 0.0 and 0.8, with relatively high average values between 0.3 and 0.5, depending on samples; the *Acceglio* and *Tinos* Fe-rich antigorites have the highest and lowest Fe^{3+}/Fe_{tot} ratios, respectively. Evans *et al*. (2012) showed that the Fe^{3+} calculated from microprobe analyses is generally overestimated with respect to Fe^{3+} measured by Mössbauer spectroscopy. Therefore, we can argue that the Fe^{3+}/Fe_{tot} ratios calculated for the studied Fe-rich antigorites represent maximum values. Although the reliability of Fe^{3+} measurement/calculation in serpentine minerals is still a highly debated issue (*e.g*., Evans *et al*., 2013; Beard & Frost, 2017), it is worth noting that the Fe^{3+}/Fe_{tot} ratios calculated for the studied Fe-rich antigorite are comparable to those measured in blueschist- to eclogite-facies antigorite samples from the western Alps using the micro-XANES technique (Debret *et al*., 2014, 2015).

Further detailed analyses aimed at the direct measurement of the Fe^{3+} content are clearly needed to correctly estimate the iron oxidation state in the studied Fe-rich antigorite samples. These estimates are complicated by the fine-grained and disordered nature of the antigorite crystals and are definitively well beyond the aim of this work; however, as suggested by Evans *et al*. (2012), the formula plots of Figs. 3b,c are at best first approximations when the goal is to assess the content of Fe^{3+} in individual antigorites.

4. Discussion

4.1 Other occurrences of Fe-rich antigorite reported in the literature

Antigorites are normally reported as Fe-poor serpentines. Considering that Wicks & O'Hanley (1988) suggested a maximum value of the Fe^{2+} for Mg substitution in antigorite of about 10 wt%, a few published examples effectively show anomalous FeO_{tot} content:

(i) Frondel (1962) reported jenkinsite, a ferroan-antigorite with more than 20 wt% FeO_{tot}, associated with magnetite and occurring in veins of the O'Neil's mine, New York State. However, Dietrich (1972) questioned the identification of jenkinsite as antigorite.

(ii) Dietrich & Peters (1971) and Dietrich (1972) reported "Kluft" (vein) Fe-antigorite, pleochroic from yellow to green, associated with greenalite, calcite and dolomite from fissures in ophicarbonate rocks from the Oberhalbstein ophiolitic complex, associated with low-grade lizardite-chrysotile serpentinites. The authors reported FeO_{tot} values up to 12.3 wt%, and confirmed the mineral identification by XRD.

(iii) Wicks & Plant (1979) reported two antigorite samples (samples 18540 and T179) from prograde serpentinites from Quebec, with FeO_{tot} ranging from 8.4 to 10 wt% and 4.3 to 10.1 wt%, respectively. The authors, unfortunately, did not report the optical features of their Fe-rich antigorite.

(iv) Uehara & Shirozu (1985) reported antigorite from the Nishisonogi area, Japan, with $FeO_{tot} \approx 9$ wt% (samples N81 and NIA), but they did not mention its optical features.

(v) Driesner (1993) reported Fe-rich antigorite (up to 7.9 wt% of FeO_{tot}) from an ophicarbonate from Châtillon, Aosta Valley, western Alps, and described also mesh-antigorite pseudomorphs after olivine and antigorite + calcite pseudomorphs after orthopyroxene in the ophicalcite clasts.

(vi) Anselmi *et al.* (2000) reported an unusual Fe-rich serpentine mineral, with FeO_{tot} up to 15 wt% and pleochroism from yellow to blue, from the Monti Livornesi serpentinites, Italy, but the authors did not identify the mineral.

(vii) Groppo (2005) reported Fe-rich antigorite from an ophicarbonate from the Argentiera Valley (Cesana, western Alps, external Piemontese Zone) with FeO_{tot} up to 14.5 wt%. Fe-rich antigorite, characterized by a strong pleochroism from yellow to deep green, occurs in both mesh and bastite microstructures, with higher FeO_{tot} values in mesh rims. In the mesh core, Fe-rich antigorite is often associated with aragonite and/or partially replaced by fine-grained tremolite. Antigorite and aragonite were identified based on their micro-Raman spectra.

(viii) In a systematic study of natural serpentinites from the western Alps, sampled in order to represent a wide range of metamorphic *P-T* conditions, Schwartz *et al*. (2013) and Lafay *et al*. (2013) reported unusual Fe-rich antigorite for a serpentinite collected from the medium-temperature (360-390°C, 10-12 kbar) blueschist domain of the Schistes lustrés complex (External Piemonte Zone, Eychassier massif). The FeO_{tot} content ranges from 5.41 to 7.64 wt%; unfortunately, the optical features of this antigorite are not mentioned. Antigorite was identified using micro-Raman spectrometry.

4.2 Factors enhancing the stability of Fe-rich antigorite

Although the studied samples come from different geological settings, they share the following features: (i) they all experienced LT-HP, blueschist-facies metamorphism, and (ii) all of them are ophicarbonate rocks. Similarly, most of the Fe-rich antigorite reported in the literature comes from ophicarbonate lithologies and/or from LT-HP metamorphic settings. This suggests that the stability of Fe-rich antigorite could be somehow influenced by the *P-T* conditions of metamorphism and/or by the occurrence of CO_2 in the metamorphic fluid. In order to test this hypothesis, a thermodynamic approach was used. The approach remains qualitative, due to the current lack of a reliable solution model that considers the Fe^{3+} substitution in antigorite [note that a ferric iron end-member was preliminary incorporated in the antigorite solution model by Evans & Powell (2015), but details on the model are not provided yet]. However, because the studied Fe-rich antigorites are Fe^{2+}-rich (on average the Fe^{3+}/Fe_{tot} ratio ranges from 0.3 to 0.5), the available solution model can be used as a first approximation and the results of thermodynamic modelling are therefore useful to broadly predict the factors controlling the stability of Fe-rich antigorite.

The modelled *P/T-X*(CO_2) pseudosection (Fig. 4) is dominated by three- and four-variant fields, with minor two-variant fields. Antigorite is predicted to be stable in the whole *P/T-X*(CO_2) range of interest; olivine appears at about 400°C in the absence of CO_2, but the olivine-in boundary is shifted to significantly higher *P-T* conditions for small amounts of CO_2 in the fluid [*i.e.,* to 560°C for $X(CO_2)\geq0.003$]. Diopside, tremolite and talc are stable at similar *P-T* conditions but at different $X(CO_2)$ values, diopside being the phase stable at lower $X(CO_2)$ conditions and talc at higher $X(CO_2)$ conditions (*e.g*., Groppo & Compagnoni, 2007). Orthopyroxene appears at $T>490$°C in the presence of CO_2 and at $T>580$°C in the absence of CO_2. For this specific bulk composition, the chlorite stability field is limited to very low $X(CO_2)$ values at $T < 470$°C. A carbonate mineral (aragonite) is predicted to be stable even at very low values of $X(CO_2)$, especially at low *P-T* conditions.

The equilibrium mineral assemblage observed in the studied samples (antigorite + diopside + carbonate) is predicted to be stable in a relatively narrow *P/T-X*(CO_2) range of $T<500$°C, $P< 20$ kbar and $X(CO_2)<0.0015$. The modelled modal amounts of these minerals (Atg: 92; Di: 6; Arg: 2 vol%) are consistent with petrographic observations. The maximum X_{Fe} in antigorite predicted by the modelled compositional isopleths is 0.09, at least for this specific bulk composition. An increase of the FeO content in the bulk composition would result in the increase of X_{Fe} in antigorite [*e.g*., X_{Fe}(Atg) up to 0.13 for a bulk FeO of 10 mol%]. The increase of Al_2O_3 in the bulk composition has the opposite effect, favouring the stability of chlorite, which subtracts FeO from the system [*e.g.*, X_{Fe}(Atg) down to 0.05 for a bulk Al_2O_3 of 5 mol%].

Although the results of the modelled *P/T-X*(CO_2) pseudosection should be considered as qualitative, the following points are worth mentioning: (1) the Fe content in antigorite is inversely proportional to the

metamorphic temperature, reaching maximum values at temperatures in the range 300-500°C, depending on the $X(CO_2)$ of the fluid. The appearance of olivine or orthopyroxene in equilibrium with antigorite invariably coincides with a decrease of X_{Fe} in antigorite (Figs. 4a,b); (2) even small amounts of CO_2 in the fluid enhance the stability of Fe-rich antigorite. At 350°C the predicted X_{Fe}(Atg) is ~0.06 in the absence of CO_2, whereas it is significantly higher (up to ~0.09) for $X(CO_2) > 0.00001$ (Fig. 4c); the difference between CO_2-absent and CO_2-present conditions is even greater at higher temperatures [*e.g.*, at 400°C, X_{Fe}(Atg) increases from ~0.05 to ~0.09 if a small amount of CO_2 is present in the fluid]; (3) due to the impossibility of implementing Fe^{+3}-bearing end-members in the antigorite solution model, the X_{Fe}(Atg) values predicted by the pseudosection modelling are obviously lower than those measured in the studied antigorites. However, the order of magnitude is the same, thus confirming the hypothesis that LT-HP metamorphic conditions and a fluid slightly enriched in CO_2 are key factors favouring the stability of Fe-rich antigorite.

5. Conclusions

Thermodynamic modelling suggests that Fe-rich antigorite formed from the breakdown of lizardite and/or chrysotile, under relatively low-*T* and high-*P* conditions and in the presence of a CO_2-bearing fluid. This model is consistent with the TEM observations of chrysotile and lizardite relics, and fits the regional geotectonic settings of the studied ophicarbonates, reported in the literature as re-equilibrated at blueschist-facies conditions. Hence, Fe-rich antigorite should be considered as a mineral that forms at low geothermal gradients (such as those of subduction zones), under blueschist-facies metamorphic conditions, possibly common in meta-ophicarbonate rocks with similar geodynamic origin and evolution.

Acknowledgements

The three Greek samples have been acquired from producers at the International Traded Marbles and Stones Exhibition annually held in Verona, Italy. The firms Psofaki S.A. of Athens and Thassos Marble S.A. of Vrilissia, Greece, are kindly acknowledged for providing the *Green Tinos* and *Macedonia,* respectively. The *Verde Acceglio* specimen has been kindly provided by Bruno Lombardo (IGG-CNR, Torino), and initially characterized by Elena Belluso, University of Torino. Electron-microprobe analyses, performed at the University of Bern, were supported by Schweizerischer Nationalfonds (credit 21-26579.89). Edwin Gnos, Cecilia Viti, Bernard Grobéty, Paulo Bourqui, Vincent Serneels, and Stelios Giannousopoulos are all thanked for lab assistance and useful discussions. The authors are very grateful to Bernard Evans for a critical reading of an early version of this paper. Two anonymous reviewers are acknowledged for their constructive comments, which improved the manuscript; the Guest Editor is warmly thanked for its detailed editorial handling.

References

Anselmi, B., Mellini, M., Viti, C. (2000): Chlorine in the Elba, Monti Livornesi and Murlo serpentinites: Evidence for sea-water interaction. *Eur. J. Mineral*., **12**, 137–146.

Auzende, A., Guillot, S., Devouard, B., Baronnet, A. (2006): Serpentinites in an Alpine convergent setting: effects of metamorphic grade and deformation on microstructures. *Eur. J.. Mineral.*, **18**, 21–33.

Beard, J.S. & Frost, B.R. (2017): The stoichiometric effects of ferric iron substitutions in serpentine from microprobe data. *Int. Geol. Rev*., **59**, 541–547.

Capitani, G.C. & Mellini, M. (2004): The modulated crystal structure of antigorite: the *m*=17 polysome. *Am. Mineral*., **89**, 147–158.

Connolly (1990): Multivariable phase diagrams: an algorithm based on generalized thermodynamics. *Am. J. Sci*., **290**, 666–718.

— (2005): Computation of phase equilibria by linear programming: A tool for geodynamic modeling and its application to subduction zone decarbonation. *Earth Planet. Sci. Lett*., **236**, 524–541.

— (2009): The geodynamic equation of state: what and how. *Geochem. Geophys. Geosyst*., **10**, Q10014.

Debret, B., Andreani, M., Muñoz, M., Bolfan-Casanova, N., Carlut, J., Nicollet, Ch., Schwartz, S., Trcera, N. (2014): Evolution of Fe redox state in serpentine during subduction. *Earth Planet. Sci. Lett*., **400**, 206–218.

Debret, N., Bolfan-Casanova, N., Padrón-Navarta, J.A., Martín-Hernández, F., Andreani, M., Garrido, C.J., López-Sánchez Vizcaíno, V., Gómez-Pugnaire, M.T., Muñoz, M., Trcera, N. (2015): Redox state of iron during high pressure serpentinite dehydration. *Contrib. Mineral. Petrol.*, **169**, 1–18.

Deer, W.A., Howie, R.A., Zussman, J. (1992): An introduction to the rock-forming minerals. 2nd Edition. 696 pp., Longman Ltd.

Di Pierro, S. (1997): Studio geologico-petrografico del marmo Verde Alpi Cesana e confronto petrografico con analoghe rocce oficarbonatiche di provenienza straniera. Unpubl. M.Sc. Thesis, Univ. Torino, Italy, 140 pp.

Di Pierro, S., Compagnoni, R., Mellini, M., Groppo, C., Capitani, G., Belluso, E. (2007). Rock forming Fe-rich antigorite from low-grade meta-ophicarbonates. In: Journées Tématiques “Serpentines” (SGF), 1-12 October 2007, Grenoble: UJF. *Abs. Vol.*

Dietrich, V.J. (1972): Ilvait, Ferroantigorit und Greenalith als Begleiter oxidisch-sulfidischer Vererzungen in den Oberhalbsteiner Serpentiniten. *Schweiz. Mineral. Petr. Mitt*., **52**, 57–74.

Dietrich, V.J. & Peters, T. (1971): Regionale Verteilung der Mg-Phyllosilikate in den Serpentiniten des Oberhalbsteins (ein Vergleich: Natur - Experiment). *Schweiz. Mineral. Petr. Mitt.*, **51**, 329–348.

Driesner, T. (1993): Aspects of petrographical, structural and stable isotope geochemical evolution of ophicarbonate breccias from ocean floor to subduction and uplift: an example from Châtillon, Middle Aosta Valley, Italian Alps. *Schweiz. Mineral. Petr. Mitt.*, **73**, 69–84.

Dungan, M.A. (1979a): Bastite pseudomorphs after orthopyroxene, clinopyroxene and tremolite. *Can. Mineral.*, **17**, 729–740.

— (1979b): A microprobe study of antigorite and some serpentine pseudomorphs. *Can. Mineral.*, **17**, 771–784.

Evans, B.W. (2004): The serpentinite multisystem revisited: chrysotile is metastable. *Int. Geol. Rev*., **46**, 479–506.

Evans, B.W., Dyar, D.M., Kuehner, S.M. (2012): Implication of ferrous and ferric iron in antigorite. *Am. Mineral*., **97**, 184–196.

Evans, B.W., Hattori, K., Baronnet, A. (2013): Serpentinite: what, why, where? *Elements*, **9**, 99-106.

Evans, K.A. & Powell, R. (2015): The effect of subduction on the sulphur, carbon and redox budget of lithospheric mantle. *J. metamorphic Geol*., **33**, 649–670.

Frondel, C. (1962): Ferroan antigorite (Jenkinsite). *Am. Mineral*., **47**, 783–784.

Fuchs, Y., Linares, J., Mellini, M. (1998): Mössbauer and infrared spectrometry of lizardite-1T from Monte Fico, Elba. *Physics Chem. Min*., **26**, 111–115.

Groppo, C. (2005): Asbestos hazard in Western Alps: petrology, characterization and quantitative determination of fibrous minerals in the asbestos-bearing serpentinites of the Piemonte Zone (Susa and Lanzo valleys). Unpubl. PhD Thesis, Univ. Torino, Italy, 179 pp.

Groppo, C. & Compagnoni, R. (2007). Metamorphic veins from the serpentinites of the Piemonte Zone, western Alps, Italy: a review. *Per. Mineral*., **76**, 127-153.

Holland, T.J.B. & Powell, R. (1996): Thermodynamics of order-disorder in minerals.2. Symmetric formalism applied to solid solutions. *Am. Mineral*., **81**, 1425–1437.

—, — (1998): An internally consistent thermodynamic dataset for phases of petrological interest. *J. metamorphic Geol*., **16**, 309–343.

—, — (2011): An improved and extended internally consistent thermodynamic dataset for phases of petrological interest, involving a new equation of state for solids. *J. metamorphic Geol*., **29**, 333–383.

Holland, T.J.B., Baker, J., Powell, R. (1998): Mixing properties and activity-composition relationships of chlorites in the system MgO-FeO-Al_2O_3-SiO_2-H_2O. *Eur. J. Mineral*., **10**, 395–406.

Lafay, R., Deschamps, F., Schwartz, S., Guillot, S., Godard, G., Debret, B., Nicollet, C. (2013): High-pressure serpentinites, a trap-and-release system controlled by metamorphic conditions: Example from the Piedmont zone of the western Alps. *Chem. Geol*., **343**, 38–54.

Mellini, M. & Viti, C. (1994): Crystal structure of lizardite-1*T* from Elba, Italy. *Am. Mineral*., **79**, 1194–1198.

Mellini, M., Fuchs, Y., Viti, C., Lemaire, C., Linares, J. (2002): Insights into the antigorite structure from Mössbauer and FTIR spectroscopies. *Eur. J. Mineral*., **14**, 97–104.

Mellini, M., Rumori, C., Viti, C. (2005): Hydrothermally reset magmatic spinels in retrograde serpentinites: Formation of "ferritchromit" rims and chlorite aureoles. *Contrib. Mineral. Petrol*., **149**, 266–275.

Mellini, M., Trommsdorff, V., Compagnoni, R. (1987): Antigorite polysomatism: behaviour during progressive metamorphism. *Contrib. Mineral. Petrol*., **97**, 147–155.

Moody, J.B. (1976): An experimental study on the serpentinization of iron-bearing olivines. *Can. Mineral*., **14**, 462–478.

O'Hanley, D.S. (1996): Serpentinites. Records of tectonic and petrological history. *Oxford Monographs on Geology and Geophysics*, **34**, 277 pp., Oxford University Press, New York.

O'Hanley, D.S. & Dyar, M.D. (1993): The composition of lizardite *1T* and the formation of magnetite in serpentinites. *Am. Mineral*., **78**, 391–404.

Otten, M.T. (1993): High-resolution transmission electron microscopy of polysomatism and stacking defects in antigorite. *Am. Mineral*., **78**, 75–84.

Padrón-Navarta, J.A., López Sánchez-Vizcaíno, V., Garrido, C.J., Gómez-Pugnaire, M.T., Jabaloy, A., Capitani, G.C., Mellini, M. (2008): Highly ordered antigorite from Cerro del Almirez HP-HT serpentinites, SE Spain. *Contrib. Mineral. Petrol.*, **156**, 679–688.

Padrón-Navarta, J.A., López Sánchez-Vizcaíno, V., Hermann, J., Connolly, J.A.D., Garrido, C.J., Gómez-Pugnaire, M.T., Marchesi, C. (2013): Tschermak's substitution in antigorite and consequences for phase relations and water liberation in high-grade serpentinites. *Lithos*, **178**, 186–196.

Ribeiro da Costa, I., Barriga, F.J.A.S., Viti, C., Mellini, M., Wicks, F.J. (2008): Antigorite in deformed serpentinites from the Mid-Atlantic Ridge. *Eur. J. Mineral*., **20**, 563–572.

Ring, U. & Layer, P.W. (2003): High-pressure metamorphism in the Aegean, eastern Mediterranean: Underplating and exhumation from the Late Cretaceous until the Miocene to Recent above the retreating Hellenic subduction zone. *Tectonics*, **22**, 1022 (6-1: 6-23).

Schwartz, S., Lardeaux, J.M., Tricart, P. (2000): La zone d'Acceglio (Alpes cottiennes) : Un nouvel exemple de croûte continentale éclogitisée dans les Alpes occidentales. *C. Rend. Acad. Sci. Paris, Série IIA, Earth Planet. Sci.*, **330**, 859–866.

Schwartz, S., Guillot, S., Reynard, B., Lafay, R., Debret, B., Nicollet, C., Lanari, P., Auzende, A.L. (2013): Pressure–temperature estimates of the lizardite/antigorite transition in high pressure serpentinites. *Lithos*, **178**, 197–210.

Stolz, J., Engi, M., Rickli, M. (1997): Tectonometamorphic evolution of SE Tinos, Cyclades, Greece. *Schweiz. mineral. petr. Mitt.*, **77**, 209–231.

Trommsdorff, V. & Evans, B.W. (1972): Progressive metamorphism of antigorite schist in the Bergell tonalite aureole (Italy). *Am. J. Sci*., **272**, 423–437.

—, — (1977a): Antigorite-ophicarbonates: Contact metamorphism in Valmalenco, Italy. *Contrib. Mineral. Petrol.*, **62**, 301–312.

—, — (1977b): Antigorite-ophicarbonates: Phase relations in a portion of the system CaO-MgO-SiO_2-H_2O-CO_2. *Contrib. Mineral. Petrol.*, **60**, 39–56.

Trommsdorff, V., López Sánchez-Vizcaíno, V., Gómez-Pugnaire, M.T., Müntener, O. (1998): High pressure breakdown of antigorite to spinifex-textured olivine and orthopyroxene, SE Spain. *Contrib. Mineral. Petrol.*, **132**, 139–148.

Tsikouras, B. & Hatzipanagiotou, K. (1998): Two alternative solutions for the development of a marginal basin in NE Greece. *Ofioliti*, **23**, 83–92.

Uehara, S. & Kamata, K. (1994): Antigorite with a large supercell from Saganoseki, Oita prefecture, Japan. *Can. Mineral*., **32**, 93–103.

Uehara, S. & Shirozu, H. (1985): Variations in chemical composition and structural properties of antigorites. *Mineral. J*., **12**, 299–318.

Viti, C. & Mellini, M. (1996): Vein antigorites from Elba Island, Italy. *Eur. J. Mineral*., **8**, 423–434.

—, — (1998): Mesh texture and bastite in the Elba retrograde serpentinites. *Eur. J. Mineral*., **10**, 1341–1359.

Whitney, D.L. & Evans, B.W. (2010): Abbreviations for names of rock-forming minerals. *Am. Mineral.*, **95**, 185–187.

Wicks, F.J. & O'Hanley, D.S. (1988): Serpentine minerals: structures and petrology. *In:* "Phyllosilicates (exclusive of micas)", S.W. Bailey, Ed., *Reviews in Mineralogy*, **19**, 91–167.

Wicks, F.J. & Plant, A.G. (1979): Electron-microprobe and X-ray-microbeam studies of serpentine textures. *Can. Mineral*., **17**, 785–830.

Wunder, B., Wirth, R., Gottschalk, M. (2001): Antigorite: Pressure and temperature dependence of polysomatism and water content. *Eur. J. Mineral*., **13**, 485–495.

Figure captions

Fig. 1 (**a-c)** – Photomicrographs of *Verde Macedonia*: mesh microstructures (M) composed of lamellar Fe-rich antigorite (orange to green), subhedral magnetite (black) and carbonate (colourless), this last mostly concentrated in the mesh cores. Bastites (B) are entirely composed of Fe-rich antigorite. Plane Polarized Light (PPL) with vibration plane parallel to γ of Fe-rich antigorite (a), parallel to α (b), and under crossed polarizers (XPL, c). **(d-f)** Photomicrographs of *Verde Acceglio*, where a deformed mesh microstructure is visible, composed of lamellar Fe-rich antigorite (orange to green), crosscut by discontinuous carbonate veins (colourless). PPL parallel to Fe-rich antigorite γ (d), parallel to α (e), and XPL (f). Mineral abbreviations are according Withney & Evans (2010).

Fig. 2. **(a)** TEM image (bright field) of the *Verias* ophicarbonate showing two lath-shaped Fe-rich antigorite crystals (dark because in Bragg conditions) with a high density of (001) planar defects (indicated by arrows), nearly perpendicular to the (100) superstructure lattice fringes. Note also the offset affecting superstructure diffraction spots around subcell reflections (inset). **(b)** TEM image of the *Tinos* ophicarbonate with diffraction pattern (inset). Fish-shaped Fe-rich antigorite crystals occur in pseudo-parallel orientation. Some of them, due to the suitable diffracting conditions, show the typical wide-spaced (100) lattice fringes of the superlattice modulation (indicated by arrows).

Fig. 3. (a) Fe-rich antigorite compositions plotted in the Mg-Fe_{tot}-(Al+Cr) diagram. Note that *Macedonia* and *Acceglio* antigorites have higher *X*Fe values than *Tinos* and *Verias* antigorites. The bulk composition used for the pseudosection modelling is also plotted (black diamond). **(b)** Si vs. (Al+Cr)/2 a.p.f.u. plot for EMPA analyses of antigorite. The dashed line represents ideal Tschermak's substitution of R^{3+} cations on the T site. See Evans et al. (2012) (their Fig. 1) for further explanations. **(c)** Calculated Fe^{3+} vs. total Fe a.p.f.u. See Evans et al. (2012) (their Fig. 2) for further explanations. ACC: *Acceglio*; MAC-m: *Macedonia* (mesh antigorite); MAC-b: *Macedonia* (bastite antigorite); TIN: *Tinos*; VER: *Verias*.

Fig. 4. **(a)** *P/T-X*(CO_2) pseudosection calculated in the CFMAS-HC system along a 7°C km^{-1} geothermal gradient, contoured for *X*Fe(Atg) (x100). **(b)** and **(c)** are different enlargements of (a). White, light and dark grey fields are two-, three- and four-variant fields, respectively.

Fig.1

Click here to access/download;Figure;Fig1.TIF

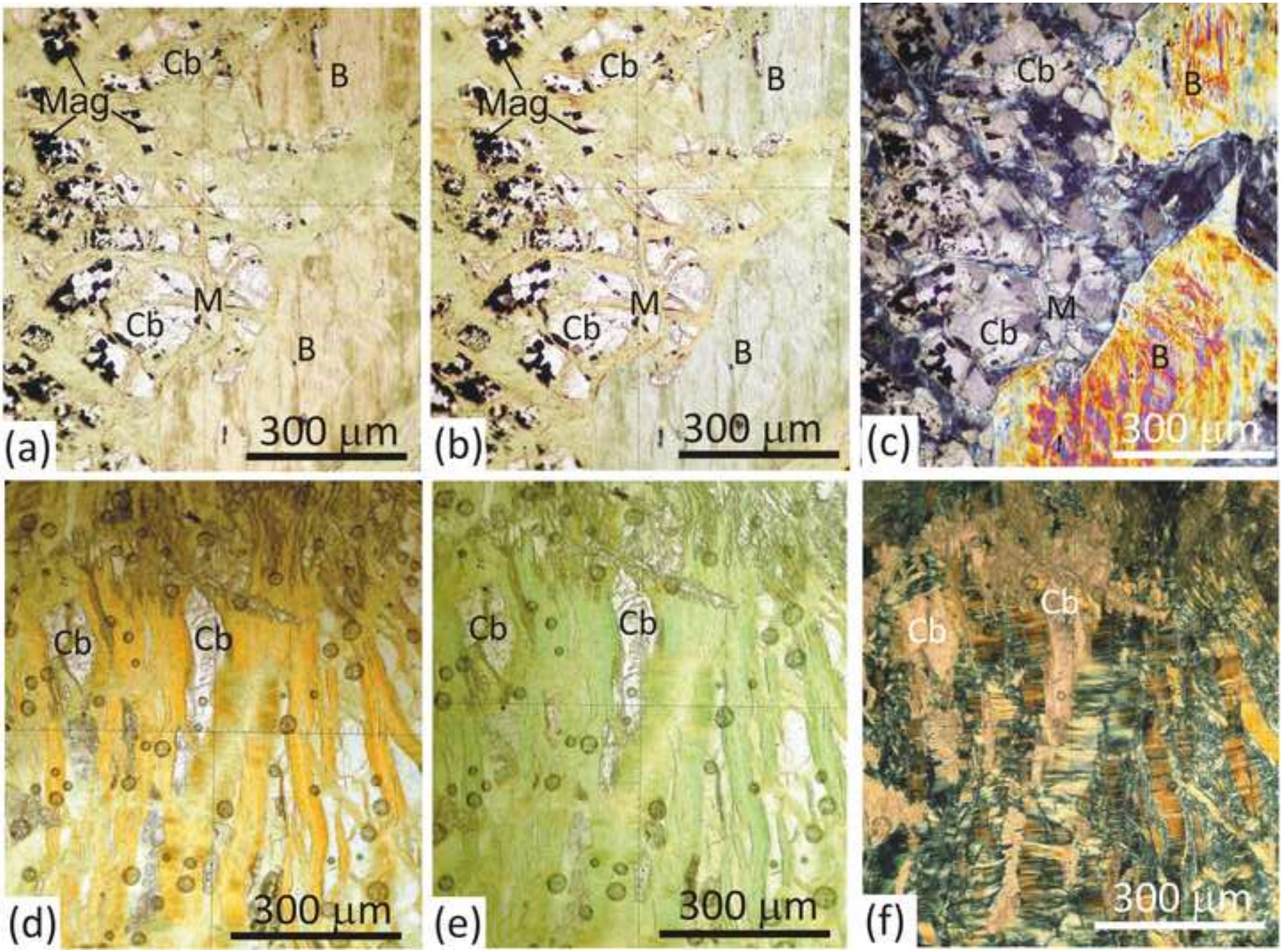

Fig.2

Click here to access/download;Figure;Fig2.TIF

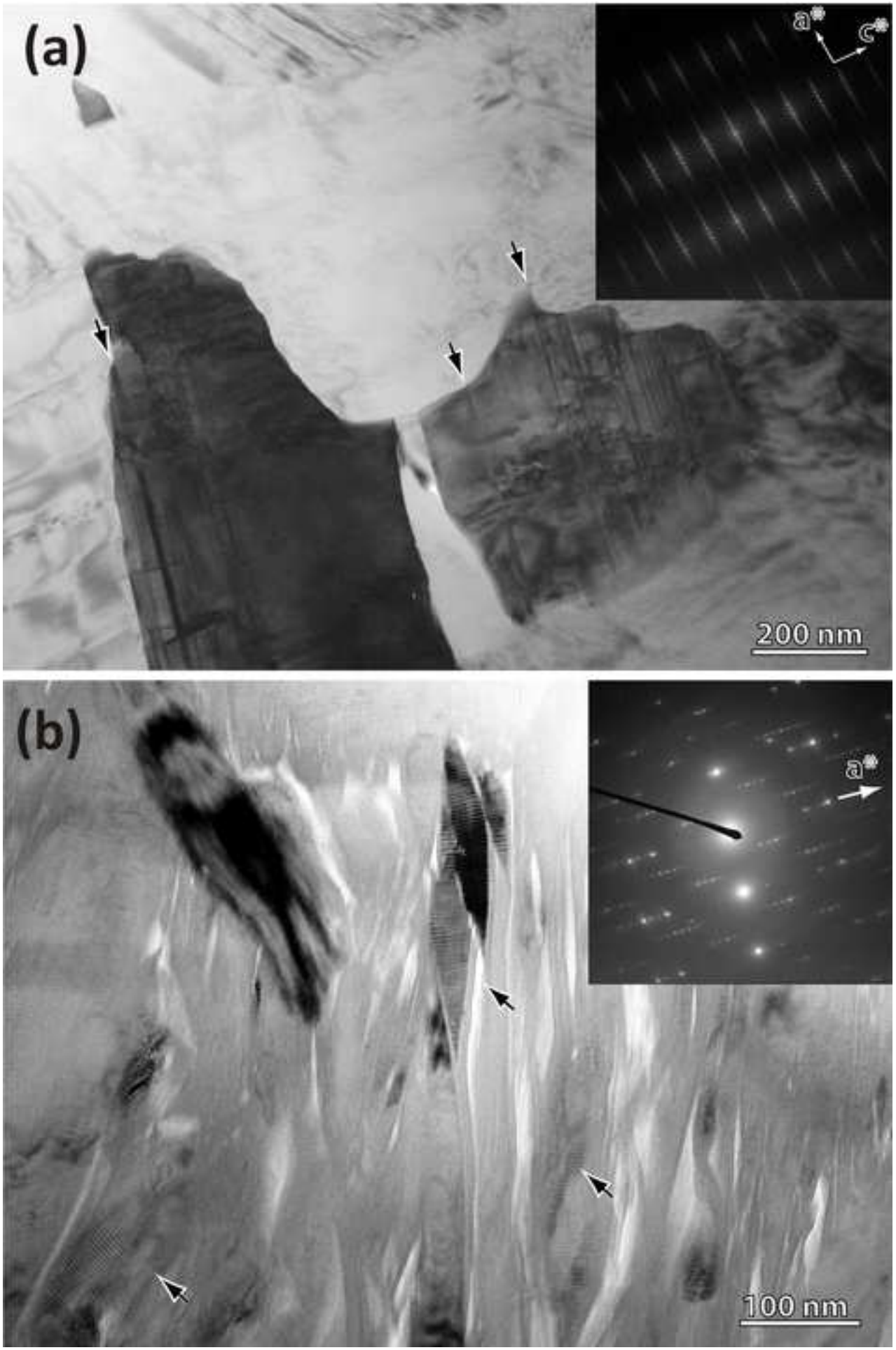

Fig.3

Click here to access/download;Figure;Fig3.TIF

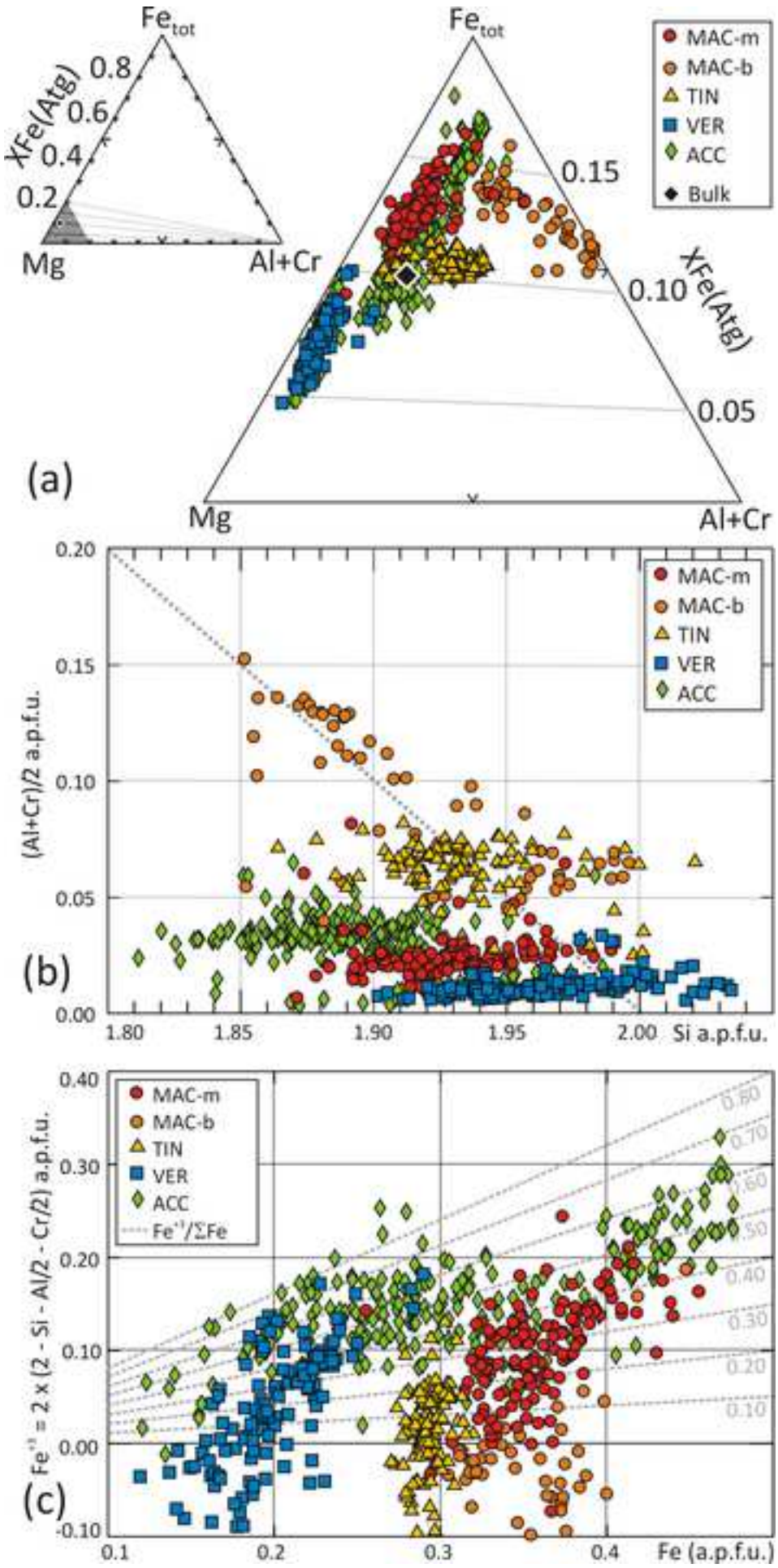

Fig.4

Click here to access/download;Figure;Fig4.TIF

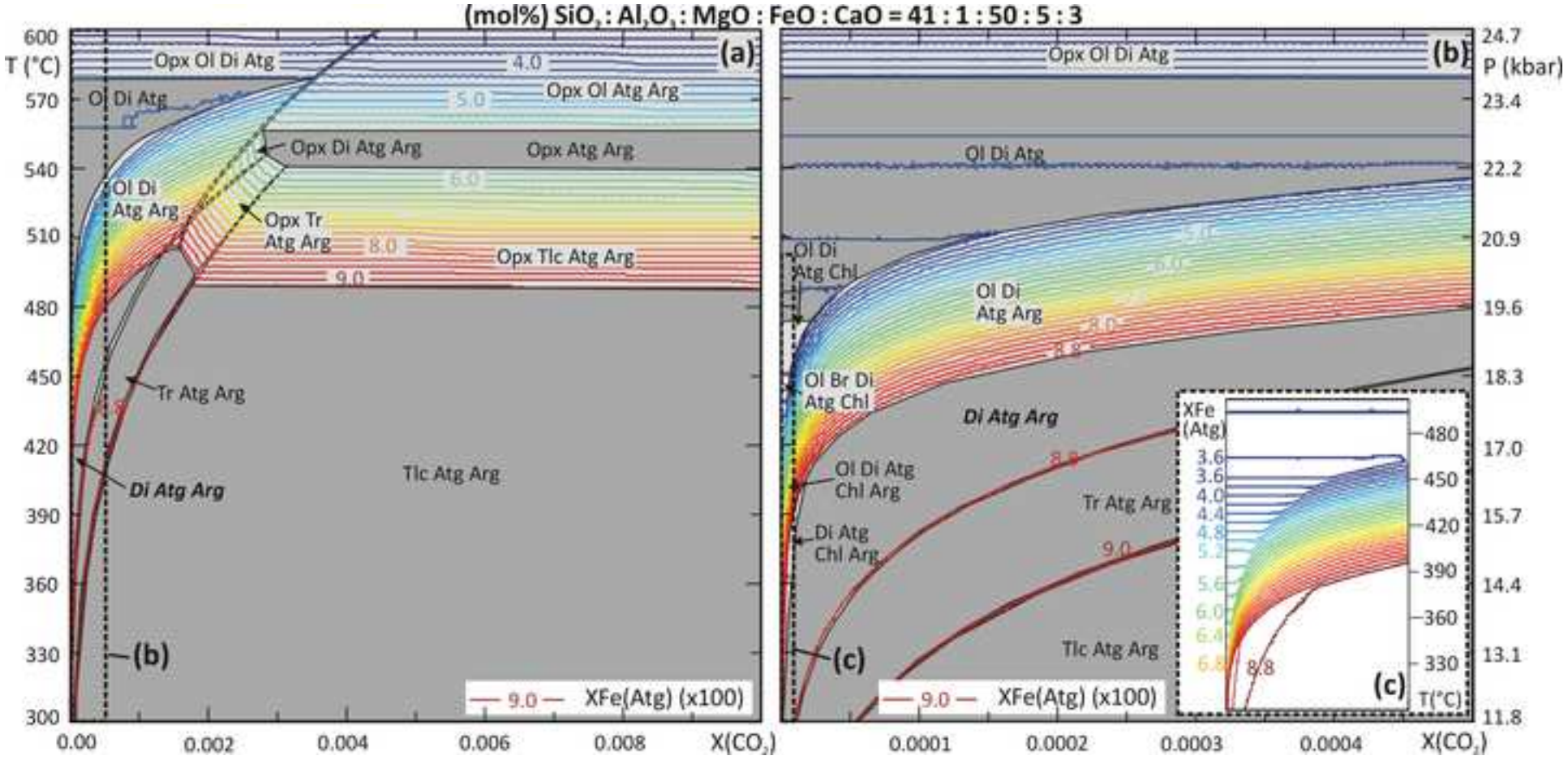

Table1

Table 1. Representative EMPA analyses of Fe-rich antigorite

Σcat	4.786	4.786	4.786	4.786	4.786	4.786	4.786	4.786	4.824	4.824	4.824	4.750	4.750	4.750	4.750
m paramet	14	14	14	14	14	14	14	14	17	17	17	12	12	12	12
Sample	MAC	MAC	MAC	MAC	TIN	TIN	TIN	TIN	VER	VER	VER	ACC	ACC	ACC	ACC
Analyses	85/m	97/m	183/b	187/b	124	127	137	156	47	78	55	71	160	247	250
SiO_2	41.68	40.45	40.78	40.93	40.53	40.08	41.26	40.53	41.30	41.15	42.26	40.29	40.60	40.21	39.85
TiO_2	0.00	0.03	0.02	0.02	0.02	0.02	0.00	0.02	0.00	0.02	0.01	0.03	0.00	0.05	0.00
Al_2O_3	0.80	1.29	2.86	2.09	1.97	1.86	2.02	2.08	0.20	0.38	0.28	1.23	2.20	1.17	1.05
Cr_2O_3	0.09	0.00	0.28	0.32	0.35	0.36	0.68	0.38	0.03	0.04	0.02	0.00	0.00	0.05	0.07
FeO_{tot}	9.09	11.23	9.50	9.96	7.29	7.46	8.05	7.44	7.30	5.04	5.71	8.46	6.47	11.31	12.23
MnO	0.07	0.10	0.11	0.13	0.06	0.00	0.05	0.03	0.07	0.05	0.07	0.03	0.06	0.06	0.02
MgO	36.10	33.84	33.70	34.75	34.04	35.11	34.75	34.67	37.55	38.20	38.65	36.01	37.07	34.27	33.94
NiO	0.41	0.33	0.32	0.28	0.20	0.23	0.26	0.30	0.52	0.41	0.37	0.07	0.24	0.34	0.11
CaO	0.22	0.26	0.22	0.37	0.35	0.14	0.07	0.17	0.03	0.10	0.08	0.04	0.05	0.05	0.07
Total	88.46	87.52	87.77	88.83	84.81	85.25	87.15	85.62	87.00	85.39	87.45	86.16	86.69	87.50	87.33
Si	1.903	1.889	1.892	1.874	1.929	1.890	1.916	1.908	1.911	1.921	1.932	1.865	1.851	1.861	1.853
Ti	0.000	0.001	0.001	0.001	0.001	0.001	0.000	0.001	0.000	0.001	0.000	0.001	0.000	0.002	0.000
Al	0.043	0.071	0.156	0.113	0.110	0.104	0.110	0.115	0.011	0.021	0.015	0.067	0.118	0.064	0.057
Cr	0.002	0.000	0.007	0.008	0.004	0.005	0.008	0.005	0.001	0.002	0.001	0.000	0.000	0.002	0.003
Fe_{tot}	0.347	0.438	0.368	0.381	0.290	0.294	0.313	0.293	0.282	0.197	0.218	0.327	0.247	0.437	0.475
Mn	0.003	0.004	0.004	0.005	0.002	0.000	0.002	0.001	0.003	0.002	0.003	0.001	0.002	0.002	0.001
Mg	2.456	2.354	2.328	2.370	2.413	2.466	2.404	2.430	2.588	2.656	2.633	2.483	2.518	2.362	2.352
Ni	0.020	0.017	0.016	0.014	0.010	0.011	0.013	0.015	0.026	0.021	0.018	0.003	0.012	0.017	0.006
Ca	0.011	0.013	0.011	0.018	0.018	0.007	0.003	0.008	0.002	0.005	0.004	0.002	0.002	0.002	0.003
Σcat	4.785	4.786	4.783	4.782	4.777	4.777	4.769	4.777	4.824	4.824	4.824	4.750	4.750	4.750	4.750
XFe	0.124	0.157	0.137	0.139	0.107	0.106	0.115	0.107	0.098	0.069	0.077	0.116	0.089	0.156	0.168
Fe^{+3}calc	0.148	0.151	0.054	0.132	0.028	0.112	0.049	0.064	0.166	0.136	0.119	0.203	0.180	0.212	0.233
$Fe^{+3}/\Sigma Fe$	0.43	0.35	0.15	0.35	0.10	0.38	0.16	0.22	0.59	0.69	0.55	0.62	0.73	0.48	0.49

Table SM1. EMPA analyses of Fe-rich antigorite from *Green Macedonia* meta-ophicarbonate

WDS analyses																					
Σcat	4.786	4.786	4.786	4.786	4.786	4.786	4.786	4.786	4.786	4.786	4.786	4.786	4.786	4.786	4.786	4.786	4.786	4.786	4.786	4.786	4.786
m paramete	14	14	14	14	14	14	14	14	14	14	14	14	14	14	14	14	14	14	14	14	14
Sample	MAC	MAC	MAC	MAC	MAC	MAC	MAC	MAC	MAC	MAC	MAC	MAC	MAC	MAC	MAC	MAC	MAC	MAC	MAC	MAC	MAC
Analyses	85/m	97/m	183/b	187/b	#1	#2	#3	#4	#5	#8	#9	#10	#11	#12	#13	#14	#15	#16	#17	#18	#19
SiO_2	41.68	40.45	40.78	40.93	42.00	41.48	42.10	41.43	41.60	42.13	41.94	42.78	41.67	41.58	42.03	41.40	41.65	43.27	42.70	42.53	41.84
TiO_2	0.00	0.03	0.02	0.02	0.03	0.01	0.01	0.00	0.04	0.00	0.01	0.01	0.03	0.01	0.02	0.01	0.00	0.01	0.03	0.01	0.00
Al_2O_3	0.80	1.29	2.86	2.09	0.75	0.58	2.10	0.88	0.78	0.84	0.68	0.96	0.75	0.76	0.78	0.70	0.75	0.87	0.99	0.79	0.86
Cr_2O_3	0.09	0.00	0.28	0.32	0.07	0.06	0.36	0.17	0.06	0.12	0.04	0.06	0.00	0.00	0.04	0.00	0.00	0.04	0.00	0.06	0.05
FeO_{tot}	9.09	11.23	9.50	9.96	9.33	9.16	9.36	9.30	9.52	9.19	8.99	8.81	9.27	8.41	8.32	9.09	9.76	7.74	8.41	8.57	9.10
MnO	0.07	0.10	0.11	0.13	0.05	0.05	0.13	0.07	0.10	0.10	0.06	0.13	0.10	0.05	0.06	0.12	0.08	0.04	0.11	0.06	0.08
MgO	36.10	33.84	33.70	34.75	35.24	35.64	32.83	34.77	35.19	35.04	36.02	35.56	35.13	35.48	35.48	34.93	35.05	35.83	35.57	35.32	35.38
NiO	0.41	0.33	0.32	0.28	-	-	-	-	-	-	-	-	-	-	-	-	-	-	-	-	-
CaO	0.22	0.26	0.22	0.37	0.18	0.16	0.45	0.22	0.26	0.17	0.17	0.21	0.26	0.21	0.20	0.32	0.19	0.21	0.25	0.24	0.30
Total	88.46	87.52	87.77	88.83	87.64	87.13	87.34	86.83	87.54	87.58	87.90	88.52	87.20	86.50	86.94	86.58	87.48	88.01	88.05	87.58	87.63
Si	1.903	1.889	1.892	1.874	1.942	1.924	1.972	1.935	1.927	1.951	1.927	1.957	1.936	1.939	1.952	1.937	1.932	1.983	1.960	1.965	1.933
Ti	0.000	0.001	0.001	0.001	0.001	0.000	0.000	0.000	0.001	0.000	0.000	0.000	0.001	0.000	0.001	0.000	0.000	0.000	0.001	0.000	0.000
Al	0.043	0.071	0.156	0.113	0.041	0.032	0.116	0.048	0.043	0.046	0.037	0.052	0.041	0.042	0.043	0.039	0.041	0.047	0.054	0.043	0.047
Cr	0.003	0.000	0.010	0.012	0.003	0.002	0.013	0.006	0.002	0.004	0.002	0.002	0.000	0.000	0.001	0.000	0.000	0.001	0.000	0.002	0.002
Fe_{tot}	0.347	0.438	0.368	0.381	0.361	0.355	0.367	0.363	0.369	0.356	0.345	0.337	0.360	0.328	0.323	0.356	0.379	0.296	0.323	0.331	0.351
Mn	0.003	0.004	0.004	0.005	0.002	0.002	0.005	0.003	0.004	0.004	0.002	0.005	0.004	0.002	0.002	0.005	0.003	0.001	0.004	0.002	0.003
Mg	2.456	2.354	2.328	2.370	2.428	2.462	2.291	2.420	2.428	2.417	2.465	2.423	2.431	2.465	2.454	2.434	2.422	2.446	2.432	2.431	2.435
Ni	0.020	0.017	0.016	0.014	0.000	0.000	0.000	0.000	0.000	0.000	0.000	0.000	0.000	0.000	0.000	0.000	0.000	0.000	0.000	0.000	0.000
Ca	0.011	0.013	0.011	0.018	0.009	0.008	0.022	0.011	0.013	0.008	0.008	0.010	0.013	0.010	0.010	0.016	0.009	0.011	0.012	0.012	0.015
Σcat	4.786	4.786	4.786	4.786	4.786	4.786	4.786	4.786	4.786	4.786	4.786	4.786	4.786	4.786	4.786	4.786	4.786	4.786	4.786	4.786	4.786
XFe	0.124	0.157	0.137	0.139	0.129	0.126	0.138	0.130	0.132	0.128	0.123	0.122	0.129	0.117	0.116	0.127	0.135	0.108	0.117	0.120	0.126
Fe^{+3}calc	0.147	0.151	0.050	0.128	0.072	0.117	-0.073	0.075	0.101	0.048	0.108	0.033	0.087	0.080	0.053	0.087	0.095	-0.014	0.026	0.025	0.085
$Fe^{+3}/\Sigma Fe$	0.423	0.346	0.137	0.336	0.199	0.329	-0.199	0.207	0.275	0.135	0.314	0.098	0.241	0.244	0.163	0.246	0.251	-0.048	0.082	0.076	0.243

4.786	4.786	4.786	4.786	4.786	4.786	4.786	4.786	4.786	4.786	4.786	4.786	4.786	4.786	4.786	4.786	4.786	4.786	4.786	4.786	4.786	4.786	4.786
14	14	14	14	14	14	14	14	14	14	14	14	14	14	14	14	14	14	14	14	14	14	14
MAC #20	MAC #21	MAC #22	MAC #23	MAC #24	MAC #25	MAC #26	MAC #27	MAC #28	MAC #29	MAC #30	MAC #31	MAC #32	MAC #33	MAC #34	MAC #35	MAC #36	MAC #37	MAC #38	MAC #39	MAC #40	MAC #41	MAC #42
43.28	42.25	41.99	41.73	41.90	42.19	42.07	41.41	41.46	41.50	41.90	42.00	41.82	41.45	41.60	42.79	42.07	41.66	41.26	41.02	41.23	41.89	41.10
0.00	0.01	0.02	0.01	0.01	0.03	0.02	0.02	0.01	0.04	0.02	0.00	0.02	0.01	0.01	0.03	0.00	0.01	0.03	0.00	0.01	0.00	0.02
1.02	0.78	1.02	0.92	0.84	1.09	0.86	0.95	0.91	0.97	0.76	0.66	0.70	0.63	0.65	0.95	0.73	1.09	0.88	0.84	0.85	0.65	0.80
0.02	0.02	0.01	0.00	0.01	0.04	0.00	0.01	0.01	0.01	0.00	0.07	0.08	0.04	0.05	0.06	0.02	0.03	0.00	0.12	0.00	0.00	0.06
7.54	8.68	9.05	9.40	9.13	9.08	8.45	9.87	9.61	9.52	9.10	8.31	8.38	8.82	9.11	7.97	8.19	8.84	9.72	9.41	8.99	8.66	9.25
0.08	0.05	0.05	0.08	0.05	0.08	0.10	0.06	0.04	0.09	0.05	0.07	0.07	0.05	0.05	0.08	0.00	0.11	0.07	0.10	0.09	0.08	0.12
35.96	35.47	34.88	34.95	35.09	34.74	35.68	34.40	35.00	34.58	35.23	35.92	35.82	35.29	35.58	35.50	35.82	34.76	34.72	34.97	35.42	35.72	34.98
-	-	-	-	-	-	-	-	-	-	-	-	-	-	-	-	-	-	-	-	-	-	-
0.25	0.24	0.22	0.24	0.21	0.28	0.20	0.26	0.22	0.26	0.19	0.19	0.16	0.17	0.20	0.22	0.26	0.29	0.21	0.24	0.25	0.18	0.18
88.13	87.50	87.24	87.33	87.22	87.53	87.38	86.98	87.25	86.96	87.25	87.22	87.03	86.46	87.24	87.59	87.09	86.78	86.89	86.71	86.83	87.18	86.50
1.979	1.952	1.951	1.938	1.946	1.956	1.943	1.936	1.927	1.938	1.944	1.941	1.938	1.938	1.928	1.973	1.947	1.944	1.927	1.917	1.918	1.940	1.924
0.000	0.000	0.001	0.000	0.000	0.001	0.001	0.001	0.000	0.002	0.001	0.000	0.001	0.000	0.000	0.001	0.000	0.000	0.001	0.000	0.000	0.000	0.001
0.055	0.042	0.056	0.050	0.046	0.060	0.047	0.052	0.050	0.053	0.042	0.036	0.038	0.035	0.035	0.051	0.040	0.060	0.048	0.046	0.046	0.035	0.044
0.001	0.001	0.000	0.000	0.000	0.001	0.000	0.000	0.000	0.000	0.000	0.002	0.003	0.001	0.002	0.002	0.001	0.001	0.000	0.004	0.000	0.000	0.002
0.288	0.335	0.351	0.365	0.355	0.352	0.326	0.386	0.373	0.371	0.353	0.321	0.324	0.345	0.353	0.307	0.317	0.345	0.380	0.368	0.350	0.335	0.362
0.003	0.002	0.002	0.003	0.002	0.003	0.004	0.002	0.002	0.004	0.002	0.003	0.003	0.002	0.002	0.003	0.000	0.004	0.003	0.004	0.003	0.003	0.005
2.449	2.441	2.414	2.417	2.427	2.399	2.455	2.395	2.423	2.405	2.435	2.473	2.472	2.457	2.456	2.438	2.469	2.417	2.416	2.435	2.455	2.464	2.439
0.000	0.000	0.000	0.000	0.000	0.000	0.000	0.000	0.000	0.000	0.000	0.000	0.000	0.000	0.000	0.000	0.000	0.000	0.000	0.000	0.000	0.000	0.000
0.012	0.012	0.011	0.012	0.010	0.014	0.010	0.013	0.011	0.013	0.010	0.010	0.008	0.008	0.010	0.011	0.013	0.014	0.011	0.012	0.013	0.009	0.009
4.786	4.786	4.786	4.786	4.786	4.786	4.786	4.786	4.786	4.786	4.786	4.786	4.786	4.786	4.786	4.786	4.786	4.786	4.786	4.786	4.786	4.786	4.786
0.105	0.121	0.127	0.131	0.127	0.128	0.117	0.139	0.134	0.134	0.127	0.115	0.116	0.123	0.126	0.112	0.114	0.125	0.136	0.131	0.125	0.120	0.129
-0.013	0.052	0.042	0.074	0.062	0.027	0.067	0.075	0.096	0.071	0.070	0.079	0.084	0.089	0.107	0.001	0.066	0.051	0.097	0.115	0.117	0.085	0.106
-0.045	0.156	0.120	0.204	0.176	0.077	0.205	0.195	0.258	0.191	0.199	0.246	0.258	0.257	0.304	0.003	0.208	0.147	0.255	0.313	0.333	0.255	0.292

		TEM-EDS analyses																			
4.786	4.786	Σcat	4.786	4.786	4.786	4.786	4.786	4.786	4.786	4.786	4.786	4.786	4.786	4.786	4.786	4.786	4.786	4.786	4.786	4.786	4.786
14	14	m paramet	14	14	14	14	14	14	14	14	14	14	14	14	14	14	14	14	14	14	14
MAC	MAC	Sample	MAC-m	MAC-m	MAC-m	MAC-m	MAC-m	MAC-m	MAC-m	MAC-m	MAC-m	MAC-m	MAC-m	MAC-m	MAC-m	MAC-m	MAC-m	MAC-m	MAC-m	MAC-m	MAC-m
#43	#44	Analyses	71	72	73	74	75	76	77	78	79	80	81	82	83	84	85	86	87	88	89
41.13	42.18	SiO_2	41.87	41.29	41.73	42.63	42.10	41.97	41.13	41.53	42.39	42.19	42.17	42.12	41.90	41.27	41.68	41.86	42.18	41.77	42.24
0.01	0.00	TiO_2	-	-	-	-	-	-	-	-	-	-	-	-	-	-	-	-	-	-	-
0.90	0.48	Al_2O_3	0.72	0.77	0.77	0.68	0.78	1.15	0.97	0.89	1.77	0.92	0.83	0.77	1.09	0.89	0.80	0.78	0.88	0.69	0.89
0.06	0.00	Cr_2O_3	-	-	-	-	-	-	-	-	-	-	-	-	-	-	-	-	-	-	-
9.76	8.52	FeO_{tot}	9.14	10.67	9.80	8.48	8.63	9.20	10.57	9.92	9.00	9.31	9.21	8.47	9.10	9.85	9.09	8.69	8.58	8.97	8.64
0.06	0.12	MnO	-	-	-	-	-	-	-	-	-	-	-	-	-	-	-	-	-	-	-
34.50	33.78	MgO	36.06	35.83	36.01	36.58	36.27	34.43	34.88	35.05	35.34	36.10	35.69	36.23	35.33	34.85	36.10	36.12	36.06	36.17	36.05
-	-	NiO	0.37	0.43	0.42	0.34	0.37	0.30	0.31	0.44	0.35	0.34	0.33	0.36	0.45	0.35	0.41	0.37	0.31	0.31	0.34
0.55	1.67	CaO	-	-	-	-	-	-	-	-	-	-	-	-	-	-	-	-	-	-	-
86.96	86.76	Total	88.16	89.00	88.72	88.71	88.15	87.06	87.86	87.84	88.85	88.86	88.23	87.95	87.87	87.21	88.08	87.82	88.00	87.91	88.16
1.922	1.978	Si	1.918	1.883	1.904	1.936	1.925	1.957	1.904	1.920	1.932	1.920	1.934	1.930	1.930	1.921	1.910	1.922	1.933	1.917	1.933
0.000	0.000	Ti	0.000	0.000	0.000	0.000	0.000	0.000	0.000	0.000	0.000	0.000	0.000	0.000	0.000	0.000	0.000	0.000	0.000	0.000	0.000
0.050	0.027	Al	0.039	0.041	0.041	0.037	0.042	0.063	0.053	0.048	0.095	0.049	0.045	0.042	0.059	0.049	0.043	0.042	0.047	0.037	0.048
0.002	0.000	Cr	0.000	0.000	0.000	0.000	0.000	0.000	0.000	0.000	0.000	0.000	0.000	0.000	0.000	0.000	0.000	0.000	0.000	0.000	0.000
0.381	0.334	Fe_{tot}	0.350	0.407	0.374	0.322	0.330	0.359	0.409	0.383	0.343	0.354	0.353	0.324	0.350	0.383	0.348	0.334	0.329	0.344	0.331
0.002	0.005	Mn	0.000	0.000	0.000	0.000	0.000	0.000	0.000	0.000	0.000	0.000	0.000	0.000	0.000	0.000	0.000	0.000	0.000	0.000	0.000
2.401	2.359	Mg	2.461	2.434	2.447	2.475	2.471	2.392	2.405	2.413	2.399	2.446	2.438	2.473	2.424	2.416	2.464	2.470	2.462	2.472	2.457
0.000	0.000	Ni	0.018	0.021	0.020	0.017	0.018	0.015	0.015	0.022	0.017	0.017	0.016	0.018	0.022	0.018	0.020	0.018	0.015	0.015	0.016
0.027	0.084	Ca	0.000	0.000	0.000	0.000	0.000	0.000	0.000	0.000	0.000	0.000	0.000	0.000	0.000	0.000	0.000	0.000	0.000	0.000	0.000
4.786	4.786	Σcat	4.786	4.786	4.786	4.786	4.786	4.786	4.786	4.786	4.786	4.786	4.786	4.786	4.786	4.786	4.786	4.786	4.786	4.786	4.786
0.137	0.124	XFe	0.125	0.143	0.132	0.115	0.118	0.130	0.145	0.137	0.125	0.126	0.126	0.116	0.126	0.137	0.124	0.119	0.118	0.122	0.119
0.105	0.018	Fe^{+3}calc	0.125	0.193	0.152	0.091	0.108	0.022	0.139	0.113	0.041	0.112	0.088	0.099	0.081	0.110	0.137	0.115	0.087	0.129	0.085
0.275	0.055	$Fe^{+3}/\Sigma Fe$	0.356	0.474	0.406	0.283	0.326	0.061	0.341	0.294	0.119	0.315	0.248	0.305	0.230	0.287	0.392	0.344	0.264	0.374	0.257

4.786	4.786	4.786	4.786	4.786	4.786	4.786	4.786	4.786	4.786	4.786	4.786	4.786	4.786	4.786	4.786	4.786	4.786	4.786	4.786	4.786	4.786	4.786
14	14	14	14	14	14	14	14	14	14	14	14	14	14	14	14	14	14	14	14	14	14	14
MAC-m	MAC-m	MAC-m	MAC-m	MAC-m	MAC-m	MAC-m	MAC-m	MAC-m	MAC-m	MAC-m	MAC-m	MAC-m	MAC-m	MAC-m	MAC-m	MAC-m	MAC-m	MAC-m	MAC-m	MAC-m	MAC-m	MAC-m
90	91	92	93	94	95	96	97	98	99	100	101	102	103	104	105	106	107	108	109	110	111	112
42.07	42.30	42.07	41.13	41.90	40.97	41.17	40.45	41.33	42.59	41.94	41.53	41.29	41.11	41.03	41.00	41.32	42.27	42.36	40.90	41.42	40.92	41.31
-	-	-	-	-	-	-	-	-	-	-	-	-	-	-	-	-	-	-	-	-	-	-
1.00	0.89	0.79	0.71	1.11	0.87	0.85	1.29	0.80	0.90	0.84	0.72	0.83	0.70	0.83	0.73	0.63	0.43	0.61	0.25	0.74	0.86	0.88
-	-	-	-	-	-	-	-	-	-	-	-	-	-	-	-	-	-	-	-	-	-	-
8.60	8.61	8.64	10.28	9.16	8.63	9.94	11.23	10.06	8.49	9.11	9.56	10.49	9.84	10.18	10.84	10.45	6.73	8.49	9.76	9.26	10.01	10.62
-	-	-	-	-	-	-	-	-	-	-	-	-	-	-	-	-	-	-	-	-	-	-
35.84	36.86	36.45	35.56	35.25	33.66	35.25	33.84	35.15	35.61	35.86	35.44	35.37	35.78	34.93	35.56	35.85	38.12	36.98	36.78	36.21	35.06	35.06
0.32	0.43	0.35	0.34	0.32	0.34	0.40	0.33	0.28	0.34	0.41	0.30	0.31	0.33	0.33	0.28	0.30	0.33	0.33	0.44	0.34	0.37	0.39
-	-	-	-	-	-	-	-	-	-	-	-	-	-	-	-	-	-	-	-	-	-	-
87.83	89.08	88.30	88.02	87.74	84.47	87.60	87.14	87.62	87.92	88.16	87.54	88.28	87.75	87.31	88.40	88.55	87.87	88.77	88.13	87.98	87.22	88.25
1.933	1.911	1.920	1.895	1.934	1.967	1.905	1.896	1.914	1.957	1.923	1.921	1.899	1.895	1.908	1.883	1.892	1.917	1.919	1.871	1.900	1.903	1.904
0.000	0.000	0.000	0.000	0.000	0.000	0.000	0.000	0.000	0.000	0.000	0.000	0.000	0.000	0.000	0.000	0.000	0.000	0.000	0.000	0.000	0.000	0.000
0.054	0.047	0.042	0.038	0.060	0.049	0.046	0.071	0.043	0.049	0.045	0.039	0.045	0.038	0.046	0.039	0.034	0.023	0.033	0.013	0.040	0.047	0.048
0.000	0.000	0.000	0.000	0.000	0.000	0.000	0.000	0.000	0.000	0.000	0.000	0.000	0.000	0.000	0.000	0.000	0.000	0.000	0.000	0.000	0.000	0.000
0.330	0.325	0.330	0.396	0.353	0.346	0.384	0.440	0.390	0.326	0.349	0.370	0.403	0.379	0.396	0.416	0.400	0.255	0.321	0.373	0.355	0.389	0.409
0.000	0.000	0.000	0.000	0.000	0.000	0.000	0.000	0.000	0.000	0.000	0.000	0.000	0.000	0.000	0.000	0.000	0.000	0.000	0.000	0.000	0.000	0.000
2.453	2.482	2.477	2.440	2.423	2.407	2.430	2.362	2.425	2.438	2.449	2.442	2.423	2.457	2.420	2.433	2.445	2.575	2.496	2.507	2.474	2.428	2.407
0.016	0.021	0.017	0.017	0.016	0.017	0.020	0.017	0.014	0.017	0.020	0.015	0.015	0.016	0.017	0.014	0.015	0.016	0.016	0.022	0.017	0.019	0.019
0.000	0.000	0.000	0.000	0.000	0.000	0.000	0.000	0.000	0.000	0.000	0.000	0.000	0.000	0.000	0.000	0.000	0.000	0.000	0.000	0.000	0.000	0.000
4.786	4.786	4.786	4.786	4.786	4.786	4.786	4.786	4.786	4.786	4.786	4.786	4.786	4.786	4.786	4.786	4.786	4.786	4.786	4.786	4.786	4.786	4.786
0.119	0.116	0.117	0.140	0.127	0.126	0.137	0.157	0.138	0.118	0.125	0.131	0.143	0.134	0.141	0.146	0.141	0.090	0.114	0.130	0.126	0.138	0.145
0.080	0.130	0.118	0.172	0.072	0.018	0.143	0.137	0.129	0.037	0.109	0.119	0.156	0.171	0.138	0.194	0.182	0.143	0.128	0.244	0.161	0.147	0.145
0.241	0.400	0.359	0.435	0.205	0.051	0.373	0.312	0.330	0.114	0.313	0.323	0.388	0.451	0.349	0.465	0.454	0.561	0.399	0.654	0.452	0.379	0.355

4.786	4.786	4.786	4.786	4.786	4.786	4.786	4.786	4.786	4.786	4.786	4.786	4.786	4.786	4.786	4.786	4.786	4.786	4.786	4.786	4.786	4.786	4.786
14	14	14	14	14	14	14	14	14	14	14	14	14	14	14	14	14	14	14	14	14	14	14
MAC-m	MAC-m	MAC-m	MAC-m	MAC-m	MAC-m	MAC-m	MAC-m	MAC-m	MAC-m	MAC-m	MAC-m	MAC-m	MAC-m	MAC-m	MAC-m	MAC-m	MAC-m	MAC-m	MAC-m	MAC-m	MAC-m	MAC-m
113	114	115	116	117	118	119	120	121	122	123	124	125	126	127	128	129	130	131	132	133	134	135
41.13	40.87	40.74	41.58	41.14	41.18	40.31	41.53	41.86	42.34	42.14	42.90	41.52	41.67	41.19	41.62	42.50	41.26	41.99	42.50	42.58	41.79	41.64
-	-	-	-	-	-	-	-	-	-	-	-	-	-	-	-	-	-	-	-	-	-	-
0.74	0.82	0.59	0.52	0.85	0.53	0.86	0.55	0.73	0.98	0.62	0.87	0.93	0.97	0.95	0.77	1.29	0.74	0.67	0.76	0.64	0.89	0.71
-	-	-	-	-	-	-	-	-	-	-	-	-	-	-	-	-	-	-	-	-	-	-
10.11	9.78	10.72	9.12	10.43	9.48	10.76	9.65	9.74	9.44	8.63	8.90	10.27	9.95	10.17	9.86	9.18	10.80	8.94	8.49	8.37	9.62	9.67
-	-	-	-	-	-	-	-	-	-	-	-	-	-	-	-	-	-	-	-	-	-	-
35.19	35.13	35.55	36.76	35.41	36.36	33.16	35.71	35.65	35.20	36.53	36.01	35.51	35.32	35.14	35.61	34.57	34.83	36.11	36.41	36.52	35.71	35.36
0.40	0.36	0.43	0.36	0.29	0.25	0.37	0.39	0.33	0.38	0.38	0.32	0.31	0.43	0.41	0.33	0.30	0.34	0.38	0.22	0.39	0.46	0.45
-	-	-	-	-	-	-	-	-	-	-	-	-	-	-	-	-	-	-	-	-	-	-
87.58	86.96	88.02	88.33	88.12	87.80	85.46	87.82	88.31	88.34	88.29	88.99	88.55	88.35	87.87	88.19	87.84	87.96	88.08	88.38	88.49	88.46	87.84
1.906	1.904	1.878	1.896	1.895	1.892	1.927	1.914	1.920	1.944	1.923	1.949	1.903	1.914	1.903	1.912	1.965	1.910	1.924	1.938	1.938	1.913	1.921
0.000	0.000	0.000	0.000	0.000	0.000	0.000	0.000	0.000	0.000	0.000	0.000	0.000	0.000	0.000	0.000	0.000	0.000	0.000	0.000	0.000	0.000	0.000
0.040	0.045	0.032	0.028	0.046	0.029	0.048	0.030	0.040	0.053	0.033	0.046	0.050	0.052	0.052	0.041	0.070	0.040	0.036	0.041	0.034	0.048	0.039
0.000	0.000	0.000	0.000	0.000	0.000	0.000	0.000	0.000	0.000	0.000	0.000	0.000	0.000	0.000	0.000	0.000	0.000	0.000	0.000	0.000	0.000	0.000
0.392	0.381	0.413	0.348	0.402	0.364	0.430	0.372	0.373	0.362	0.329	0.338	0.393	0.382	0.393	0.379	0.355	0.418	0.342	0.324	0.318	0.368	0.373
0.000	0.000	0.000	0.000	0.000	0.000	0.000	0.000	0.000	0.000	0.000	0.000	0.000	0.000	0.000	0.000	0.000	0.000	0.000	0.000	0.000	0.000	0.000
2.429	2.438	2.441	2.497	2.429	2.489	2.362	2.451	2.436	2.408	2.483	2.437	2.424	2.417	2.418	2.437	2.381	2.402	2.465	2.473	2.476	2.435	2.430
0.020	0.018	0.021	0.017	0.014	0.012	0.019	0.019	0.016	0.019	0.019	0.016	0.015	0.021	0.020	0.016	0.015	0.017	0.019	0.011	0.019	0.023	0.022
0.000	0.000	0.000	0.000	0.000	0.000	0.000	0.000	0.000	0.000	0.000	0.000	0.000	0.000	0.000	0.000	0.000	0.000	0.000	0.000	0.000	0.000	0.000
4.786	4.786	4.786	4.786	4.786	4.786	4.786	4.786	4.786	4.786	4.786	4.786	4.786	4.786	4.786	4.786	4.786	4.786	4.786	4.786	4.786	4.786	4.786
0.139	0.135	0.145	0.122	0.142	0.128	0.154	0.132	0.133	0.131	0.117	0.122	0.140	0.137	0.140	0.135	0.130	0.148	0.122	0.116	0.114	0.131	0.133
0.149	0.147	0.211	0.180	0.165	0.187	0.097	0.142	0.120	0.059	0.121	0.056	0.144	0.120	0.142	0.134	-0.001	0.141	0.116	0.084	0.090	0.126	0.118
0.379	0.385	0.511	0.519	0.410	0.512	0.227	0.383	0.321	0.162	0.369	0.164	0.366	0.314	0.363	0.354	-0.002	0.336	0.338	0.259	0.282	0.343	0.318

4.786	4.786	4.786	4.786	4.786	4.786	4.786	4.786	4.786	4.786	4.786	4.786	4.786	4.786	4.786	4.786	4.786	4.786	4.786	4.786	4.786	4.786	4.786
14	14	14	14	14	14	14	14	14	14	14	14	14	14	14	14	14	14	14	14	14	14	14
MAC-m	MAC-m	MAC-m	MAC-m	MAC-m	MAC-m	MAC-m	MAC-m	MAC-m	MAC-m	MAC-m	MAC-m	MAC-m	MAC-m	MAC-m	MAC-m	MAC-m	MAC-m	MAC-m	MAC-m	MAC-m	MAC-b	MAC-b
136	191	192	193	194	195	196	197	198	199	200	201	202	203	204	205	206	207	208	209	210	137	138
42.75	40.55	41.67	42.15	43.61	41.92	42.32	41.97	41.65	42.07	42.64	42.77	43.14	42.66	41.75	41.85	42.20	42.58	42.54	42.01	41.36	40.40	39.62
-	-	-	-	-	-	-	-	-	-	-	-	-	-	-	-	-	-	-	-	-	-	-
1.09	0.94	0.76	0.63	1.01	0.97	1.73	0.42	0.60	0.63	0.75	1.14	1.06	0.78	0.89	1.17	1.47	0.90	0.95	0.81	0.73	4.99	4.91
-	-	-	-	-	-	-	-	-	-	-	-	-	-	-	-	-	-	-	-	-	-	-
9.56	11.67	9.46	9.03	7.71	9.72	8.59	8.66	10.11	8.85	8.22	8.67	8.66	9.09	9.75	8.99	9.47	8.45	8.53	9.27	11.33	7.47	8.64
-	-	-	-	-	-	-	-	-	-	-	-	-	-	-	-	-	-	-	-	-	-	-
34.91	34.06	35.68	36.48	35.86	35.24	34.79	36.83	35.55	36.29	36.15	35.22	35.54	35.79	35.10	35.50	34.20	35.54	35.13	35.70	35.18	34.10	32.98
0.40	0.37	0.42	0.36	0.24	0.29	0.34	0.37	0.40	0.41	0.31	0.33	0.36	0.34	0.31	0.36	0.29	0.28	0.41	0.18	0.45	0.39	0.37
-	-	-	-	-	-	-	-	-	-	-	-	-	-	-	-	-	-	-	-	-	-	-
88.72	87.59	87.99	88.65	88.43	88.14	87.77	88.25	88.31	88.24	88.07	88.11	88.75	88.65	87.80	87.87	87.64	87.75	87.57	87.97	89.04	87.36	86.52
1.959	1.893	1.916	1.918	1.989	1.929	1.953	1.914	1.913	1.923	1.951	1.965	1.967	1.947	1.929	1.926	1.959	1.960	1.966	1.932	1.893	1.864	1.856
0.000	0.000	0.000	0.000	0.000	0.000	0.000	0.000	0.000	0.000	0.000	0.000	0.000	0.000	0.000	0.000	0.000	0.000	0.000	0.000	0.000	0.000	0.000
0.059	0.052	0.041	0.034	0.054	0.052	0.094	0.023	0.032	0.034	0.040	0.062	0.057	0.042	0.048	0.063	0.080	0.049	0.052	0.044	0.039	0.271	0.271
0.000	0.000	0.000	0.000	0.000	0.000	0.000	0.000	0.000	0.000	0.000	0.000	0.000	0.000	0.000	0.000	0.000	0.000	0.000	0.000	0.000	0.000	0.000
0.366	0.455	0.364	0.344	0.294	0.374	0.331	0.330	0.388	0.338	0.315	0.333	0.330	0.347	0.377	0.346	0.368	0.325	0.330	0.356	0.434	0.288	0.338
0.000	0.000	0.000	0.000	0.000	0.000	0.000	0.000	0.000	0.000	0.000	0.000	0.000	0.000	0.000	0.000	0.000	0.000	0.000	0.000	0.000	0.000	0.000
2.383	2.368	2.444	2.473	2.437	2.416	2.391	2.502	2.433	2.471	2.464	2.410	2.414	2.434	2.416	2.433	2.365	2.438	2.418	2.445	2.399	2.343	2.302
0.020	0.018	0.021	0.018	0.012	0.014	0.017	0.018	0.020	0.020	0.015	0.016	0.017	0.016	0.016	0.018	0.014	0.014	0.020	0.009	0.022	0.019	0.018
0.000	0.000	0.000	0.000	0.000	0.000	0.000	0.000	0.000	0.000	0.000	0.000	0.000	0.000	0.000	0.000	0.000	0.000	0.000	0.000	0.000	0.000	0.000
4.786	4.786	4.786	4.786	4.786	4.786	4.786	4.786	4.786	4.786	4.786	4.786	4.786	4.786	4.786	4.786	4.786	4.786	4.786	4.786	4.786	4.786	4.786
0.133	0.161	0.130	0.122	0.108	0.134	0.122	0.117	0.138	0.120	0.113	0.121	0.120	0.125	0.135	0.124	0.135	0.118	0.120	0.127	0.153	0.109	0.128
0.024	0.163	0.127	0.130	-0.033	0.089	0.000	0.150	0.141	0.120	0.057	0.008	0.008	0.063	0.093	0.085	0.002	0.030	0.016	0.093	0.175	0.001	0.016
0.065	0.359	0.348	0.379	-0.112	0.239	0.001	0.453	0.364	0.355	0.181	0.025	0.025	0.183	0.248	0.246	0.005	0.093	0.048	0.260	0.404	0.004	0.048

4.786	4.786	4.786	4.786	4.786	4.786	4.786	4.786	4.786	4.786	4.786	4.786	4.786	4.786	4.786	4.786	4.786	4.786	4.786	4.786	4.786	4.786	4.786
14	14	14	14	14	14	14	14	14	14	14	14	14	14	14	14	14	14	14	14	14	14	14
MAC-b	MAC-b	MAC-b	MAC-b	MAC-b	MAC-b	MAC-b	MAC-b	MAC-b	MAC-b	MAC-b	MAC-b	MAC-b	MAC-b	MAC-b	MAC-b	MAC-b	MAC-b	MAC-b	MAC-b	MAC-b	MAC-b	MAC-b
139	140	141	142	143	144	145	146	147	148	149	150	151	152	153	154	155	156	157	158	159	160	161
40.48	42.20	42.10	42.20	41.09	40.31	40.41	40.61	41.99	41.58	40.43	41.81	42.35	40.39	40.49	39.94	40.54	40.64	42.91	41.94	41.77	42.41	41.44
-	-	-	-	-	-	-	-	-	-	-	-	-	-	-	-	-	-	-	-	-	-	-
3.94	2.01	2.14	2.37	3.22	4.84	4.40	4.98	2.53	3.56	4.02	2.14	2.50	4.62	4.86	5.58	3.99	3.19	2.36	2.23	1.78	2.12	2.05
-	-	-	-	-	-	-	-	-	-	-	-	-	-	-	-	-	-	-	-	-	-	-
7.40	9.38	9.96	9.18	9.23	8.06	7.60	7.71	9.54	8.18	8.61	9.49	8.71	8.20	8.37	8.02	8.76	9.14	9.16	9.81	9.78	8.76	9.36
-	-	-	-	-	-	-	-	-	-	-	-	-	-	-	-	-	-	-	-	-	-	-
34.44	33.29	33.28	32.60	32.51	33.57	34.89	33.89	32.90	33.40	33.31	32.85	32.86	33.11	33.39	33.32	33.16	32.47	33.44	33.05	33.53	33.09	32.05
0.43	0.33	0.32	0.24	0.40	0.29	0.34	0.31	0.41	0.37	0.37	0.39	0.30	0.32	0.35	0.38	0.41	0.30	0.30	0.28	0.23	0.28	0.28
-	-	-	-	-	-	-	-	-	-	-	-	-	-	-	-	-	-	-	-	-	-	-
86.67	87.20	87.80	86.59	86.44	87.07	87.63	87.50	87.37	87.08	86.74	86.67	86.71	86.64	87.45	87.24	86.85	85.73	88.16	87.31	87.09	86.65	85.17
1.880	1.973	1.959	1.990	1.938	1.872	1.855	1.874	1.963	1.937	1.890	1.969	1.990	1.889	1.876	1.851	1.895	1.931	1.985	1.962	1.955	1.994	1.989
0.000	0.000	0.000	0.000	0.000	0.000	0.000	0.000	0.000	0.000	0.000	0.000	0.000	0.000	0.000	0.000	0.000	0.000	0.000	0.000	0.000	0.000	0.000
0.216	0.110	0.117	0.132	0.179	0.265	0.238	0.270	0.139	0.195	0.221	0.119	0.138	0.254	0.265	0.305	0.220	0.179	0.129	0.123	0.098	0.117	0.116
0.000	0.000	0.000	0.000	0.000	0.000	0.000	0.000	0.000	0.000	0.000	0.000	0.000	0.000	0.000	0.000	0.000	0.000	0.000	0.000	0.000	0.000	0.000
0.287	0.367	0.387	0.362	0.364	0.313	0.291	0.297	0.373	0.319	0.336	0.374	0.342	0.320	0.324	0.311	0.342	0.363	0.354	0.383	0.383	0.344	0.375
0.000	0.000	0.000	0.000	0.000	0.000	0.000	0.000	0.000	0.000	0.000	0.000	0.000	0.000	0.000	0.000	0.000	0.000	0.000	0.000	0.000	0.000	0.000
2.382	2.319	2.307	2.290	2.284	2.322	2.385	2.329	2.291	2.317	2.320	2.305	2.300	2.306	2.304	2.300	2.309	2.298	2.304	2.303	2.338	2.317	2.291
0.021	0.017	0.016	0.012	0.020	0.014	0.017	0.015	0.021	0.018	0.019	0.020	0.015	0.016	0.017	0.019	0.020	0.015	0.015	0.014	0.012	0.014	0.014
0.000	0.000	0.000	0.000	0.000	0.000	0.000	0.000	0.000	0.000	0.000	0.000	0.000	0.000	0.000	0.000	0.000	0.000	0.000	0.000	0.000	0.000	0.000
4.786	4.786	4.786	4.786	4.786	4.786	4.786	4.786	4.786	4.786	4.786	4.786	4.786	4.786	4.786	4.786	4.786	4.786	4.786	4.786	4.786	4.786	4.786
0.108	0.136	0.144	0.136	0.137	0.119	0.109	0.113	0.140	0.121	0.127	0.139	0.129	0.122	0.123	0.119	0.129	0.136	0.133	0.143	0.141	0.129	0.141
0.025	-0.057	-0.035	-0.112	-0.056	-0.008	0.053	-0.018	-0.065	-0.068	-0.001	-0.057	-0.119	-0.032	-0.016	-0.007	-0.009	-0.041	-0.098	-0.047	-0.008	-0.104	-0.094
0.087	-0.156	-0.090	-0.310	-0.154	-0.026	0.181	-0.061	-0.173	-0.214	-0.004	-0.154	-0.347	-0.099	-0.051	-0.023	-0.028	-0.112	-0.277	-0.122	-0.022	-0.303	-0.251

4.786	4.786	4.786	4.786	4.786	4.786	4.786	4.786	4.786	4.786	4.786	4.786	4.786	4.786	4.786	4.786	4.786	4.786	4.786	4.786	4.786	4.786	4.786
14	14	14	14	14	14	14	14	14	14	14	14	14	14	14	14	14	14	14	14	14	14	14
MAC-b	MAC-b	MAC-b	MAC-b	MAC-b	MAC-b	MAC-b	MAC-b	MAC-b	MAC-b	MAC-b	MAC-b	MAC-b	MAC-b	MAC-b	MAC-b	MAC-b	MAC-b	MAC-b	MAC-b	MAC-b	MAC-b	MAC-b
162	163	164	165	166	167	168	169	170	171	172	173	175	176	177	178	179	180	181	182	183	184	185
42.43	40.84	41.18	39.70	42.35	40.58	41.96	40.61	40.84	40.53	40.00	41.21	40.36	39.79	41.44	41.03	42.00	41.03	39.91	42.16	40.78	40.41	40.98
-	-	-	-	-	-	-	-	-	-	-	-	-	-	-	-	-	-	-	-	-	-	-
1.69	4.06	2.81	4.64	2.33	4.69	3.13	4.76	3.66	4.75	4.45	3.70	1.45	1.99	1.85	1.80	2.50	4.24	4.63	1.97	2.86	3.77	4.71
-	-	-	-	-	-	-	-	-	-	-	-	-	-	-	-	-	-	-	-	-	-	-
9.05	8.33	9.58	8.03	9.39	8.09	8.88	8.06	9.22	8.16	8.39	8.89	10.74	11.50	10.25	9.85	9.51	8.48	8.12	9.65	9.50	8.97	7.90
-	-	-	-	-	-	-	-	-	-	-	-	-	-	-	-	-	-	-	-	-	-	-
34.86	33.32	33.62	32.84	32.45	33.22	32.99	33.68	33.12	33.30	32.83	33.40	34.52	34.01	33.80	33.88	32.88	34.03	32.93	33.69	33.70	34.57	33.77
0.20	0.36	0.29	0.26	0.25	0.35	0.41	0.40	0.27	0.32	0.39	0.37	0.22	0.40	0.38	0.28	0.30	0.28	0.35	0.34	0.32	0.33	0.36
-	-	-	-	-	-	-	-	-	-	-	-	-	-	-	-	-	-	-	-	-	-	-
88.23	86.91	87.49	85.46	86.76	86.94	87.36	87.51	87.10	87.05	86.06	87.58	87.29	87.69	87.72	86.84	87.18	88.06	85.93	87.81	87.15	88.05	87.72
1.950	1.905	1.915	1.880	1.996	1.891	1.957	1.877	1.907	1.885	1.885	1.912	1.881	1.852	1.927	1.922	1.967	1.886	1.881	1.957	1.902	1.856	1.889
0.000	0.000	0.000	0.000	0.000	0.000	0.000	0.000	0.000	0.000	0.000	0.000	0.000	0.000	0.000	0.000	0.000	0.000	0.000	0.000	0.000	0.000	0.000
0.092	0.223	0.154	0.259	0.129	0.258	0.172	0.259	0.201	0.260	0.247	0.202	0.079	0.109	0.101	0.099	0.138	0.230	0.257	0.108	0.157	0.204	0.256
0.000	0.000	0.000	0.000	0.000	0.000	0.000	0.000	0.000	0.000	0.000	0.000	0.000	0.000	0.000	0.000	0.000	0.000	0.000	0.000	0.000	0.000	0.000
0.348	0.325	0.373	0.318	0.370	0.315	0.346	0.311	0.360	0.317	0.330	0.345	0.418	0.447	0.398	0.386	0.372	0.326	0.320	0.375	0.370	0.344	0.304
0.000	0.000	0.000	0.000	0.000	0.000	0.000	0.000	0.000	0.000	0.000	0.000	0.000	0.000	0.000	0.000	0.000	0.000	0.000	0.000	0.000	0.000	0.000
2.387	2.315	2.329	2.316	2.278	2.305	2.291	2.319	2.304	2.307	2.304	2.308	2.396	2.358	2.341	2.364	2.294	2.331	2.311	2.330	2.341	2.365	2.319
0.010	0.018	0.014	0.013	0.013	0.017	0.020	0.020	0.013	0.016	0.020	0.019	0.011	0.020	0.019	0.014	0.015	0.014	0.018	0.017	0.016	0.016	0.018
0.000	0.000	0.000	0.000	0.000	0.000	0.000	0.000	0.000	0.000	0.000	0.000	0.000	0.000	0.000	0.000	0.000	0.000	0.000	0.000	0.000	0.000	0.000
4.786	4.786	4.786	4.786	4.786	4.786	4.786	4.786	4.786	4.786	4.786	4.786	4.786	4.786	4.786	4.786	4.786	4.786	4.786	4.786	4.786	4.786	4.786
0.127	0.123	0.138	0.121	0.140	0.120	0.131	0.118	0.135	0.121	0.125	0.130	0.149	0.160	0.145	0.140	0.140	0.123	0.122	0.139	0.137	0.127	0.116
0.008	-0.033	0.015	-0.019	-0.121	-0.039	-0.085	-0.013	-0.016	-0.031	-0.016	-0.026	0.158	0.187	0.045	0.056	-0.072	-0.002	-0.018	-0.022	0.039	0.084	-0.034
0.023	-0.102	0.040	-0.059	-0.327	-0.124	-0.246	-0.043	-0.045	-0.097	-0.050	-0.077	0.378	0.419	0.114	0.146	-0.194	-0.008	-0.057	-0.058	0.106	0.243	-0.111

4.786	4.786	4.786	4.786
14	14	14	14
MAC-b 186	MAC-b 187	MAC-b 188	MAC-b 189
40.66	40.93	41.42	42.01
-	-	-	-
4.25	2.09	2.04	1.92
-	-	-	-
8.23	9.96	10.05	9.49
-	-	-	-
33.34	34.75	32.29	33.29
0.27	0.28	0.29	0.32
-	-	-	-
86.74	88.00	86.09	87.03
1.898	1.888	1.970	1.968
0.000	0.000	0.000	0.000
0.234	0.113	0.115	0.106
0.000	0.000	0.000	0.000
0.321	0.384	0.400	0.372
0.000	0.000	0.000	0.000
2.319	2.387	2.287	2.324
0.014	0.014	0.015	0.016
0.000	0.000	0.000	0.000
4.786	4.786	4.786	4.786
0.122	0.139	0.149	0.138
-0.030	0.111	-0.054	-0.043
-0.095	0.289	-0.135	-0.115

Table SM2. EMPA analyses of Fe-rich antigorite from *Green Tinos* meta-ophicarbonate

WDS analyses																					
Σcat	4.786	4.786	4.786	4.786	4.786	4.786	4.786	4.786	4.786	4.786	4.786	4.786	4.786	4.786	4.786	4.786	4.786	4.786	4.786	4.786	4.786
m paramet	14	14	14	14	14	14	14	14	14	14	14	14	14	14	14	14	14	14	14	14	14
Sample	TIN	TIN	TIN	TIN	TIN	TIN	TIN	TIN	TIN	TIN	TIN	TIN	TIN	TIN	TIN	TIN	TIN	TIN	TIN	TIN	TIN
Analyses	124	127	137	156	#82	#84	#85	#86	#87	#88	#89	#91	#93	#94	#95	#96	#97	#98	#99	#111	#112
SiO_2	40.53	40.08	41.26	40.53	39.21	41.50	39.68	40.26	40.84	38.90	41.09	38.52	41.52	40.47	40.44	41.38	42.17	41.67	41.19	43.39	42.26
TiO_2	0.02	0.02	0.00	0.02	0.01	0.06	0.06	0.05	0.06	0.04	0.02	0.03	0.02	0.03	0.03	0.05	0.05	0.04	0.01	0.01	0.01
Al_2O_3	1.97	1.86	2.02	2.08	2.24	2.14	2.25	2.14	2.62	1.84	2.29	2.32	2.32	1.77	2.26	2.25	2.22	1.95	2.37	0.83	0.83
Cr_2O_3	0.35	0.36	0.68	0.38	0.45	0.27	0.33	0.35	0.38	0.35	0.40	0.41	0.31	0.23	0.38	0.32	0.32	0.27	0.35	0.12	0.15
FeO_{tot}	7.29	7.46	8.05	7.44	7.61	7.54	6.94	7.70	7.48	6.80	7.02	6.84	7.50	7.30	7.01	7.24	7.23	7.50	7.17	7.36	7.04
MnO	0.06	0.00	0.05	0.03	0.05	0.05	0.02	0.03	0.00	0.00	0.03	0.03	0.00	0.06	0.04	0.03	0.02	0.06	0.01	0.00	0.04
MgO	34.04	35.11	34.75	34.67	34.86	35.88	34.35	34.38	35.22	32.90	34.37	34.02	35.18	34.66	34.38	35.25	35.78	35.79	35.24	35.69	34.68
NiO	0.20	0.23	0.26	0.30	-	-	-	-	-	-	-	-	-	-	-	-	-	-	-	-	-
CaO	0.35	0.14	0.07	0.17	0.12	0.06	0.11	0.13	0.10	0.21	0.10	0.11	0.08	0.08	0.07	0.09	0.07	0.08	0.08	0.16	0.12
Total	84.81	85.25	87.15	85.62	84.55	87.49	83.73	85.04	86.69	81.03	85.31	82.28	86.92	84.58	84.61	86.62	87.85	87.36	86.41	87.56	85.13
Si	1.929	1.890	1.916	1.908	1.864	1.907	1.904	1.909	1.896	1.933	1.941	1.879	1.924	1.925	1.924	1.923	1.931	1.919	1.917	1.998	2.001
Ti	0.001	0.001	0.000	0.001	0.000	0.002	0.002	0.002	0.002	0.002	0.001	0.001	0.001	0.001	0.001	0.002	0.002	0.001	0.000	0.000	0.000
Al	0.110	0.104	0.110	0.115	0.125	0.116	0.127	0.120	0.144	0.108	0.127	0.133	0.126	0.099	0.127	0.123	0.120	0.106	0.130	0.045	0.046
Cr	0.013	0.014	0.025	0.014	0.017	0.010	0.012	0.013	0.014	0.014	0.015	0.016	0.011	0.008	0.014	0.012	0.011	0.010	0.013	0.004	0.006
Fe_{tot}	0.290	0.294	0.313	0.293	0.302	0.290	0.279	0.305	0.290	0.282	0.277	0.279	0.291	0.290	0.279	0.281	0.277	0.289	0.279	0.283	0.279
Mn	0.002	0.000	0.002	0.001	0.002	0.002	0.001	0.001	0.000	0.000	0.001	0.001	0.000	0.002	0.001	0.001	0.001	0.002	0.000	0.000	0.002
Mg	2.413	2.466	2.404	2.430	2.469	2.456	2.455	2.429	2.436	2.436	2.419	2.471	2.429	2.456	2.436	2.440	2.441	2.455	2.443	2.447	2.446
Ni	0.010	0.011	0.013	0.015	0.000	0.000	0.000	0.000	0.000	0.000	0.000	0.000	0.000	0.000	0.000	0.000	0.000	0.000	0.000	0.000	0.000
Ca	0.018	0.007	0.003	0.008	0.006	0.003	0.005	0.007	0.005	0.011	0.005	0.006	0.004	0.004	0.004	0.005	0.003	0.004	0.004	0.008	0.006
Σcat	4.786	4.786	4.786	4.786	4.786	4.786	4.786	4.786	4.786	4.786	4.786	4.786	4.786	4.786	4.786	4.786	4.786	4.786	4.786	4.786	4.786
XFe	0.107	0.106	0.115	0.107	0.109	0.106	0.102	0.112	0.106	0.104	0.103	0.101	0.107	0.106	0.103	0.103	0.102	0.105	0.102	0.104	0.102
Fe^{+3}calc	0.019	0.103	0.033	0.055	0.130	0.060	0.052	0.049	0.051	0.012	-0.025	0.094	0.014	0.042	0.011	0.020	0.006	0.047	0.023	-0.045	-0.054
$Fe^{+3}/\Sigma Fe$	0.067	0.350	0.105	0.188	0.429	0.206	0.186	0.159	0.175	0.043	-0.089	0.337	0.047	0.145	0.040	0.070	0.023	0.162	0.083	-0.159	-0.194

4.786 14	4.786 14	4.786 14	4.786 14	4.786 14	4.786 14	4.786 14	4.786 14	4.786 14	4.786 14	4.786 14	4.786 14	4.786 14	4.786 14	4.786 14	4.786 14	4.786 14	4.786 14	4.786 14	4.786 14	4.786 14	4.786 14	4.786 14
TIN #113	TIN #115	TIN #121	TIN #122	TIN #123	TIN #124	TIN #125	TIN #126	TIN #127	TIN #128	TIN #130	TIN #131	TIN #132	TIN #133	TIN #134	TIN #135	TIN #136	TIN #137	TIN #140	TIN #147	TIN #147	TIN #152	TIN #156
42.65	41.73	42.17	41.47	42.43	40.53	40.08	41.44	40.08	43.32	40.49	39.65	41.68	42.96	42.08	41.63	42.30	41.26	40.55	40.73	40.73	40.67	40.53
0.00	0.01	0.01	0.00	0.03	0.02	0.03	0.03	0.02	0.00	0.04	0.03	0.02	0.00	0.00	0.01	0.02	0.00	0.03	0.02	0.02	0.06	0.02
1.03	1.76	1.58	1.93	1.61	1.97	2.16	2.05	1.86	1.65	2.66	1.82	1.07	1.07	1.46	1.26	1.63	2.02	1.94	2.11	2.11	1.91	2.08
0.36	0.28	0.70	1.21	0.88	0.35	0.35	0.34	0.36	1.07	0.41	0.70	0.12	0.00	0.20	0.46	0.62	0.68	0.30	0.40	0.40	0.28	0.38
7.20	7.60	7.74	7.85	7.59	7.29	7.23	7.63	7.46	7.56	7.55	7.10	7.67	7.01	8.12	7.34	7.72	8.05	7.16	7.39	7.39	7.33	7.44
0.00	0.02	0.05	0.03	0.03	0.06	0.05	0.03	0.00	0.04	0.02	0.03	0.02	0.10	0.08	0.08	0.03	0.05	0.00	0.00	0.00	0.00	0.03
34.65	34.91	35.08	33.77	34.29	34.04	34.57	35.45	35.11	33.54	34.21	31.61	34.43	35.97	35.06	33.74	35.06	34.75	34.40	34.53	34.53	34.10	34.67
- 0.19	- 0.13	- 0.08	- 0.33	- 0.11	- 0.35	- 0.13	- 0.11	- 0.14	- 0.16	- 0.11	- 0.39	- 0.07	- 0.02	- 0.12	- 0.14	- 0.12	- 0.07	- 0.19	- 0.16	- 0.16	- 0.15	- 0.17
86.07	86.44	87.40	86.58	86.97	84.62	84.59	87.08	85.02	87.34	85.48	81.32	85.09	87.13	87.13	84.66	87.50	86.89	84.56	85.32	85.32	84.50	85.31
2.002	1.947	1.951	1.947	1.979	1.933	1.906	1.917	1.894	2.021	1.911	1.980	1.978	1.981	1.952	1.991	1.955	1.921	1.931	1.924	1.924	1.941	1.914
0.000	0.000	0.000	0.000	0.001	0.001	0.001	0.001	0.001	0.000	0.001	0.001	0.001	0.000	0.000	0.000	0.001	0.000	0.001	0.001	0.001	0.002	0.001
0.057	0.097	0.086	0.107	0.089	0.111	0.121	0.112	0.104	0.091	0.148	0.107	0.060	0.058	0.080	0.071	0.089	0.111	0.109	0.117	0.117	0.107	0.116
0.013	0.010	0.025	0.045	0.033	0.013	0.013	0.012	0.014	0.039	0.015	0.028	0.004	0.000	0.007	0.017	0.023	0.025	0.011	0.015	0.015	0.011	0.014
0.282	0.296	0.299	0.308	0.296	0.291	0.287	0.295	0.295	0.295	0.298	0.296	0.304	0.270	0.315	0.293	0.298	0.313	0.285	0.292	0.292	0.293	0.294
0.000	0.001	0.002	0.001	0.001	0.002	0.002	0.001	0.000	0.002	0.001	0.001	0.001	0.004	0.003	0.003	0.001	0.002	0.000	0.000	0.000	0.000	0.001
2.422	2.427	2.418	2.362	2.383	2.418	2.449	2.442	2.472	2.331	2.406	2.352	2.434	2.471	2.422	2.403	2.414	2.410	2.440	2.430	2.430	2.424	2.438
0.000	0.000	0.000	0.000	0.000	0.000	0.000	0.000	0.000	0.000	0.000	0.000	0.000	0.000	0.000	0.000	0.000	0.000	0.000	0.000	0.000	0.000	0.000
0.010	0.007	0.004	0.017	0.005	0.018	0.007	0.005	0.007	0.008	0.005	0.021	0.004	0.001	0.006	0.007	0.006	0.003	0.010	0.008	0.008	0.008	0.008
4.786	4.786	4.786	4.786	4.786	4.786	4.786	4.786	4.786	4.786	4.786	4.786	4.786	4.786	4.786	4.786	4.786	4.786	4.786	4.786	4.786	4.786	4.786
0.104	0.109	0.110	0.115	0.110	0.107	0.105	0.108	0.106	0.112	0.110	0.112	0.111	0.099	0.115	0.109	0.110	0.115	0.105	0.107	0.107	0.108	0.107
-0.073	-0.002	-0.013	-0.046	-0.079	0.011	0.054	0.042	0.094	-0.172	0.014	-0.095	-0.020	-0.021	0.009	-0.069	-0.021	0.022	0.018	0.020	0.020	0.000	0.042
-0.259	-0.006	-0.045	-0.149	-0.267	0.038	0.188	0.142	0.318	-0.583	0.048	-0.321	-0.067	-0.077	0.027	-0.236	-0.072	0.070	0.065	0.068	0.068	0.000	0.144

TEM-EDS analyses																					
Σcat	4.786	4.786	4.786	4.786	4.786	4.786	4.786	4.786	4.786	4.786	4.786	4.786	4.786	4.786	4.786	4.786	4.786	4.786	4.786	4.786	4.786
m paramet	14	14	14	14	14	14	14	14	14	14	14	14	14	14	14	14	14	14	14	14	14
Sample	TIN	TIN	TIN	TIN	TIN	TIN	TIN	TIN	TIN	TIN	TIN	TIN	TIN	TIN	TIN	TIN	TIN	TIN	TIN	TIN	TIN
Analyses	2	4	5	6	7	9	10	12	13	14	15	16	17	18	19	20	21	22	23	24	25
SiO_2	40.26	41.21	42.56	41.42	41.18	39.90	39.84	41.34	39.71	39.77	39.85	39.86	40.34	40.34	39.95	40.15	40.44	40.76	41.24	41.09	41.04
TiO_2	-	-	-	-	-	-	-	-	-	-	-	-	-	-	-	-	-	-	-	-	-
Al_2O_3	1.53	2.00	2.30	1.80	1.98	2.54	2.28	2.12	2.28	2.13	2.31	2.46	2.38	2.64	2.42	2.14	2.24	2.28	2.47	2.33	2.67
Cr_2O_3	-	-	-	-	-	-	-	-	-	-	-	-	-	-	-	-	-	-	-	-	-
FeO_{tot}	7.64	7.08	7.11	7.29	6.99	6.98	7.27	7.86	7.20	7.40	7.19	7.60	7.07	7.26	7.32	7.37	7.26	6.82	6.66	7.48	7.06
MnO	-	-	-	-	-	-	-	-	-	-	-	-	-	-	-	-	-	-	-	-	-
MgO	34.45	34.96	33.82	35.23	35.36	33.80	34.14	35.20	33.32	33.91	34.13	33.37	33.73	34.30	33.93	34.30	34.32	34.09	32.98	34.04	33.79
NiO	0.30	0.14	0.23	0.22	0.24	0.19	0.26	0.27	0.21	0.20	0.18	0.24	0.20	0.14	0.20	0.21	0.19	0.21	0.09	0.21	0.20
CaO	-	-	-	-	-	-	-	-	-	-	-	-	-	-	-	-	-	-	-	-	-
Total	84.18	85.39	86.03	85.95	85.74	83.41	83.79	86.80	82.71	83.40	83.66	83.52	83.73	84.67	83.82	84.17	84.45	84.17	83.44	85.15	84.76
Si	1.925	1.939	2.000	1.937	1.927	1.923	1.912	1.919	1.934	1.919	1.915	1.926	1.940	1.916	1.918	1.919	1.927	1.948	1.995	1.947	1.952
Ti	0.000	0.000	0.000	0.000	0.000	0.000	0.000	0.000	0.000	0.000	0.000	0.000	0.000	0.000	0.000	0.000	0.000	0.000	0.000	0.000	0.000
Al	0.086	0.111	0.128	0.099	0.109	0.144	0.129	0.116	0.131	0.121	0.131	0.140	0.135	0.148	0.137	0.120	0.126	0.128	0.141	0.130	0.150
Cr	0.000	0.000	0.000	0.000	0.000	0.000	0.000	0.000	0.000	0.000	0.000	0.000	0.000	0.000	0.000	0.000	0.000	0.000	0.000	0.000	0.000
Fe_{tot}	0.306	0.279	0.279	0.285	0.274	0.281	0.292	0.305	0.293	0.298	0.289	0.307	0.284	0.288	0.294	0.295	0.289	0.273	0.269	0.296	0.281
Mn	0.000	0.000	0.000	0.000	0.000	0.000	0.000	0.000	0.000	0.000	0.000	0.000	0.000	0.000	0.000	0.000	0.000	0.000	0.000	0.000	0.000
Mg	2.454	2.450	2.368	2.454	2.465	2.427	2.441	2.433	2.418	2.437	2.443	2.401	2.416	2.427	2.427	2.442	2.435	2.427	2.376	2.403	2.394
Ni	0.015	0.007	0.012	0.011	0.012	0.010	0.013	0.014	0.011	0.010	0.009	0.012	0.010	0.007	0.010	0.011	0.010	0.011	0.005	0.010	0.010
Ca	0.000	0.000	0.000	0.000	0.000	0.000	0.000	0.000	0.000	0.000	0.000	0.000	0.000	0.000	0.000	0.000	0.000	0.000	0.000	0.000	0.000
Σcat	4.786	4.786	4.786	4.786	4.786	4.786	4.786	4.786	4.786	4.786	4.786	4.786	4.786	4.786	4.786	4.786	4.786	4.786	4.786	4.786	4.786
XFe	0.111	0.102	0.106	0.104	0.100	0.104	0.107	0.111	0.108	0.109	0.106	0.113	0.105	0.106	0.108	0.108	0.106	0.101	0.102	0.110	0.105
Fe^{+3}calc	0.063	0.011	-0.127	0.027	0.037	0.009	0.048	0.047	0.002	0.041	0.040	0.008	-0.015	0.020	0.027	0.043	0.021	-0.024	-0.130	-0.023	-0.054
$Fe^{+3}/\Sigma Fe$	0.207	0.039	-0.455	0.094	0.136	0.031	0.163	0.154	0.006	0.138	0.139	0.027	-0.053	0.070	0.091	0.145	0.073	-0.087	-0.484	-0.079	-0.191

4.786 14	4.786 14	4.786 14	4.786 14	4.786 14	4.786 14	4.786 14	4.786 14	4.786 14	4.786 14	4.786 14	4.786 14	4.786 14	4.786 14	4.786 14	4.786 14	4.786 14	4.786 14	4.786 14	4.786 14	4.786 14	4.786 14	4.786 14
TIN 26	TIN 27	TIN 28	TIN 29	TIN 30	TIN 31	TIN 32	TIN 33	TIN 35	TIN 36	TIN 37	TIN 38	TIN 39	TIN 40	TIN 41	TIN 42	TIN 43	TIN 44	TIN 45	TIN 46	TIN 47	TIN 48	TIN 49
41.10	40.28	39.91	40.97	40.27	39.86	41.37	40.15	40.19	39.66	40.10	40.45	39.99	39.89	39.93	40.90	40.39	41.21	41.22	41.07	40.30	41.33	40.24
-	-	-	-	-	-	-	-	-	-	-	-	-	-	-	-	-	-	-	-	-	-	-
2.12	2.18	2.02	2.26	1.56	2.03	0.99	2.47	1.90	1.64	2.23	2.67	2.50	2.51	2.42	2.70	2.10	2.59	2.49	2.72	2.52	2.34	2.50
-	-	-	-	-	-	-	-	-	-	-	-	-	-	-	-	-	-	-	-	-	-	-
7.28	7.24	7.45	7.15	7.89	7.62	7.76	7.16	7.29	7.58	7.19	7.35	7.22	7.31	7.55	7.09	7.45	7.10	7.03	7.31	7.38	7.63	7.13
-	-	-	-	-	-	-	-	-	-	-	-	-	-	-	-	-	-	-	-	-	-	-
34.53	34.05	34.23	33.74	33.47	33.99	35.19	33.78	33.89	33.33	34.57	33.92	33.61	33.83	34.06	32.99	34.60	33.75	33.87	33.88	33.78	34.07	33.70
0.21	0.23	0.27	0.29	0.21	0.26	0.30	0.16	0.13	0.17	0.21	0.18	0.19	0.23	0.14	0.11	0.17	0.17	0.18	0.11	0.29	0.22	0.28
-	-	-	-	-	-	-	-	-	-	-	-	-	-	-	-	-	-	-	-	-	-	-
85.23	83.98	83.88	84.40	83.41	83.76	85.61	83.72	83.39	82.38	84.29	84.58	83.50	83.77	84.10	83.79	84.70	84.81	84.80	85.08	84.27	85.59	83.86
1.941	1.931	1.914	1.957	1.951	1.917	1.946	1.931	1.940	1.942	1.910	1.927	1.929	1.917	1.912	1.972	1.917	1.960	1.960	1.947	1.927	1.949	1.933
0.000	0.000	0.000	0.000	0.000	0.000	0.000	0.000	0.000	0.000	0.000	0.000	0.000	0.000	0.000	0.000	0.000	0.000	0.000	0.000	0.000	0.000	0.000
0.118	0.123	0.114	0.127	0.089	0.115	0.055	0.140	0.108	0.094	0.125	0.150	0.142	0.142	0.137	0.154	0.117	0.145	0.139	0.152	0.142	0.130	0.142
0.000	0.000	0.000	0.000	0.000	0.000	0.000	0.000	0.000	0.000	0.000	0.000	0.000	0.000	0.000	0.000	0.000	0.000	0.000	0.000	0.000	0.000	0.000
0.287	0.290	0.299	0.285	0.320	0.306	0.305	0.288	0.294	0.310	0.286	0.293	0.291	0.294	0.302	0.286	0.296	0.282	0.279	0.290	0.295	0.301	0.286
0.000	0.000	0.000	0.000	0.000	0.000	0.000	0.000	0.000	0.000	0.000	0.000	0.000	0.000	0.000	0.000	0.000	0.000	0.000	0.000	0.000	0.000	0.000
2.429	2.431	2.445	2.401	2.415	2.434	2.465	2.420	2.437	2.431	2.454	2.407	2.414	2.422	2.428	2.369	2.447	2.391	2.398	2.392	2.407	2.394	2.411
0.011	0.012	0.014	0.015	0.011	0.013	0.015	0.008	0.007	0.009	0.011	0.009	0.010	0.012	0.007	0.005	0.009	0.009	0.009	0.005	0.015	0.011	0.014
0.000	0.000	0.000	0.000	0.000	0.000	0.000	0.000	0.000	0.000	0.000	0.000	0.000	0.000	0.000	0.000	0.000	0.000	0.000	0.000	0.000	0.000	0.000
4.786	4.786	4.786	4.786	4.786	4.786	4.786	4.786	4.786	4.786	4.786	4.786	4.786	4.786	4.786	4.786	4.786	4.786	4.786	4.786	4.786	4.786	4.786
0.106	0.107	0.109	0.106	0.117	0.112	0.110	0.106	0.108	0.113	0.104	0.108	0.108	0.108	0.111	0.108	0.108	0.106	0.104	0.108	0.109	0.112	0.106
0.000	0.016	0.057	-0.042	0.009	0.051	0.054	-0.001	0.012	0.022	0.054	-0.004	0.001	0.025	0.040	-0.097	0.048	-0.064	-0.059	-0.046	0.003	-0.029	-0.007
0.000	0.054	0.192	-0.147	0.028	0.167	0.177	-0.004	0.040	0.072	0.189	-0.014	0.003	0.084	0.133	-0.340	0.162	-0.228	-0.211	-0.158	0.011	-0.097	-0.026

4.786 14	4.786 14	4.786 14	4.786 14	4.786 14	4.786 14	4.786 14	4.786 14	4.786 14	4.786 14	4.786 14	4.786 14	4.786 14	4.786 14
TIN 50	TIN 51	TIN 52	TIN 53	TIN 54	TIN 55	TIN 57	TIN 58	TIN 59	TIN 60	TIN 61	TIN 62	TIN 63	TIN 65
40.26	40.89	40.24	39.98	40.55	40.44	40.76	40.33	41.00	40.97	40.52	41.33	40.50	39.80
-	-	-	-	-	-	-	-	-	-	-	-	-	-
1.96	1.73	2.42	2.41	2.57	2.65	2.11	2.38	2.52	2.36	2.15	2.25	2.60	2.12
-	-	-	-	-	-	-	-	-	-	-	-	-	-
7.58	7.57	7.25	7.34	7.23	7.20	7.59	7.48	7.41	7.18	7.41	7.40	7.62	7.82
-	-	-	-	-	-	-	-	-	-	-	-	-	-
34.50	35.27	33.13	33.38	33.94	33.81	34.48	34.18	34.24	33.81	34.03	34.64	34.24	34.91
0.11	0.19	0.16	0.15	0.26	0.17	0.16	0.21	0.19	0.19	0.23	0.28	0.28	0.17
-	-	-	-	-	-	-	-	-	-	-	-	-	-
84.40	85.64	83.19	83.26	84.55	84.27	85.09	84.59	85.35	84.51	84.34	85.89	85.24	84.82
1.919	1.919	1.952	1.936	1.932	1.933	1.929	1.920	1.936	1.955	1.936	1.938	1.915	1.886
0.000	0.000	0.000	0.000	0.000	0.000	0.000	0.000	0.000	0.000	0.000	0.000	0.000	0.000
0.110	0.095	0.138	0.137	0.144	0.149	0.118	0.134	0.140	0.133	0.121	0.124	0.145	0.118
0.000	0.000	0.000	0.000	0.000	0.000	0.000	0.000	0.000	0.000	0.000	0.000	0.000	0.000
0.302	0.297	0.294	0.297	0.288	0.288	0.300	0.298	0.292	0.286	0.296	0.290	0.301	0.310
0.000	0.000	0.000	0.000	0.000	0.000	0.000	0.000	0.000	0.000	0.000	0.000	0.000	0.000
2.449	2.466	2.394	2.408	2.409	2.407	2.431	2.424	2.408	2.403	2.421	2.420	2.411	2.464
0.005	0.010	0.008	0.008	0.013	0.009	0.008	0.011	0.010	0.010	0.012	0.014	0.014	0.008
0.000	0.000	0.000	0.000	0.000	0.000	0.000	0.000	0.000	0.000	0.000	0.000	0.000	0.000
4.786	4.786	4.786	4.786	4.786	4.786	4.786	4.786	4.786	4.786	4.786	4.786	4.786	4.786
0.110	0.107	0.109	0.110	0.107	0.107	0.110	0.109	0.108	0.106	0.109	0.107	0.111	0.112
0.052	0.067	-0.042	-0.009	-0.008	-0.015	0.024	0.026	-0.012	-0.042	0.008	0.000	0.026	0.110
0.172	0.227	-0.142	-0.030	-0.027	-0.052	0.080	0.088	-0.040	-0.147	0.025	-0.001	0.085	0.355

Table SM3. EMPA analyses of Fe-rich antigorite from *Green Verias* meta-ophicarbonate

WDS analyses																					
Σcat	4.824	4.824	4.824	4.824	4.824	4.824	4.824	4.824	4.824	4.824	4.824	4.824	4.824	4.824	4.824	4.824	4.824	4.824	4.824	4.824	4.824
m paramet	17	17	17	17	17	17	17	17	17	17	17	17	17	17	17	17	17	17	17	17	17
Sample	VER	VER	VER	VER	VER	VER	VER	VER	VER	VER	VER	VER	VER	VER	VER	VER	VER	VER	VER	VER	VER
Analyses	47	78	55	#41	#42	#43	#44	#45	#46	#47	#48	#49	#50	#51	#52	#53	#54	#55	#56	#57	#59
SiO_2	41.30	41.15	42.26	40.87	43.72	42.04	42.02	41.57	41.84	41.30	42.29	42.35	41.79	41.81	42.08	42.05	42.07	42.47	43.60	42.59	43.08
TiO_2	0.00	0.02	0.01	0.02	0.00	0.00	0.04	0.05	0.01	0.00	0.00	0.00	0.00	0.00	0.01	0.00	0.02	0.03	0.04	0.03	0.00
Al_2O_3	0.20	0.38	0.28	0.27	0.57	0.30	0.35	0.23	0.30	0.20	0.39	0.27	0.59	0.60	0.47	0.37	0.36	0.54	0.79	0.69	0.43
Cr_2O_3	0.03	0.04	0.02	0.00	0.00	0.02	0.10	0.00	0.07	0.03	0.07	0.05	0.02	0.02	0.00	0.00	0.02	0.07	0.03	0.00	0.01
FeO_{tot}	7.30	5.04	5.71	7.45	4.86	6.07	6.09	6.48	6.21	7.30	5.70	5.80	6.06	5.90	6.02	5.92	5.72	5.73	4.28	4.93	4.55
MnO	0.07	0.05	0.07	0.06	0.06	0.06	0.05	0.06	0.07	0.07	0.07	0.10	0.06	0.07	0.06	0.09	0.08	0.05	0.10	0.09	0.06
MgO	37.55	38.20	38.65	37.67	37.71	38.29	37.84	38.53	38.27	37.55	37.88	38.24	37.86	37.79	37.97	38.02	37.88	37.38	38.06	38.13	38.52
NiO	0.52	0.41	0.37	-	-	-	-	-	-	-	-	-	-	-	-	-	-	-	-	-	-
CaO	0.03	0.10	0.08	0.07	0.13	0.06	0.08	0.06	0.06	0.03	0.07	0.06	0.06	0.05	0.06	0.05	0.07	0.06	0.15	0.14	0.10
Total	87.00	85.39	87.45	86.41	87.06	86.85	86.55	86.98	86.83	86.48	86.46	86.87	86.44	86.25	86.67	86.51	86.22	86.32	87.04	86.60	86.73
Si	1.911	1.921	1.932	1.902	2.012	1.938	1.947	1.913	1.930	1.922	1.959	1.952	1.937	1.942	1.946	1.947	1.954	1.974	2.001	1.965	1.981
Ti	0.000	0.001	0.000	0.001	0.000	0.000	0.001	0.002	0.000	0.000	0.000	0.000	0.000	0.000	0.000	0.000	0.001	0.001	0.001	0.001	0.000
Al	0.011	0.021	0.015	0.015	0.031	0.016	0.019	0.013	0.016	0.011	0.021	0.015	0.032	0.033	0.025	0.020	0.020	0.030	0.043	0.038	0.023
Cr	0.001	0.002	0.001	0.000	0.000	0.001	0.003	0.000	0.003	0.001	0.003	0.002	0.001	0.001	0.000	0.000	0.001	0.003	0.001	0.000	0.000
Fe_{tot}	0.282	0.197	0.218	0.290	0.187	0.234	0.236	0.249	0.240	0.284	0.221	0.223	0.235	0.229	0.232	0.229	0.222	0.223	0.164	0.190	0.175
Mn	0.003	0.002	0.003	0.002	0.002	0.002	0.002	0.002	0.003	0.003	0.003	0.004	0.002	0.003	0.002	0.004	0.003	0.002	0.004	0.004	0.002
Mg	2.588	2.656	2.633	2.611	2.585	2.629	2.612	2.642	2.630	2.602	2.614	2.625	2.614	2.614	2.615	2.622	2.620	2.589	2.603	2.620	2.638
Ni	0.026	0.021	0.018	0.000	0.000	0.000	0.000	0.000	0.000	0.000	0.000	0.000	0.000	0.000	0.000	0.000	0.000	0.000	0.000	0.000	0.000
Ca	0.002	0.005	0.004	0.003	0.006	0.003	0.004	0.003	0.003	0.002	0.004	0.003	0.003	0.002	0.003	0.002	0.004	0.003	0.007	0.007	0.005
Σcat	4.824	4.824	4.824	4.824	4.824	4.824	4.824	4.824	4.824	4.824	4.824	4.824	4.824	4.824	4.824	4.824	4.824	4.824	4.824	4.824	4.824
XFe	0.098	0.069	0.077	0.100	0.067	0.082	0.083	0.086	0.083	0.098	0.078	0.078	0.082	0.081	0.082	0.080	0.078	0.079	0.059	0.068	0.062
Fe^{+3}calc	0.166	0.136	0.119	0.182	-0.055	0.107	0.083	0.160	0.121	0.145	0.058	0.080	0.093	0.083	0.083	0.086	0.072	0.019	-0.046	0.033	0.015
$Fe^{+3}/\Sigma Fe$	0.586	0.693	0.548	0.627	-0.295	0.457	0.353	0.644	0.505	0.510	0.263	0.359	0.395	0.362	0.358	0.376	0.324	0.084	-0.280	0.173	0.088

4.824	4.824	4.824	4.824	4.824	4.824	4.824	4.824	4.824	4.824	4.824	4.824	4.824	4.824	4.824	4.824	4.824	4.824	4.824	4.824	4.824	4.824	4.824
17	17	17	17	17	17	17	17	17	17	17	17	17	17	17	17	17	17	17	17	17	17	17
VER #60	VER #61	VER #62	VER #63	VER #64	VER #65	VER #66	VER #67	VER #68	VER #70	VER #71	VER #72	VER #73	VER #74	VER #75	VER #76	VER #77	VER #78	VER #79	VER #80	VER #82	VER #84	VER #86
43.13	43.43	42.96	42.87	42.75	43.03	43.48	43.69	43.24	41.02	41.11	40.41	41.47	41.91	42.20	41.05	41.42	41.15	41.46	41.21	42.05	42.75	42.47
0.02	0.04	0.01	0.04	0.06	0.01	0.03	0.00	0.03	0.03	0.01	0.01	0.02	0.02	0.00	0.02	0.00	0.02	0.00	0.01	0.02	0.01	0.00
0.47	0.63	0.46	0.43	0.48	0.42	0.42	0.51	0.48	0.33	0.32	0.27	0.53	0.35	0.44	0.40	0.30	0.38	0.37	0.34	0.30	0.39	1.15
0.00	0.05	0.01	0.00	0.03	0.01	0.01	0.05	0.01	0.04	0.03	0.07	0.04	0.03	0.11	0.00	0.07	0.04	0.05	0.02	0.05	0.03	0.09
4.42	3.89	4.72	4.99	4.82	4.35	3.71	3.58	4.08	5.15	4.93	5.78	4.68	4.28	4.19	4.87	4.75	5.04	4.93	4.93	5.66	5.05	4.99
0.08	0.05	0.13	0.14	0.09	0.07	0.08	0.08	0.07	0.08	0.05	0.02	0.05	0.08	0.06	0.03	0.05	0.05	0.01	0.10	0.03	0.05	0.07
38.21	38.48	38.08	37.97	38.08	38.38	38.93	38.80	38.48	38.16	38.37	38.01	38.11	38.28	38.39	38.06	38.56	38.20	38.21	38.03	38.11	38.37	36.84
-	-	-	-	-	-	-	-	-	-	-	-	-	-	-	-	-	-	-	-	-	-	-
0.10	0.14	0.11	0.12	0.12	0.09	0.09	0.12	0.09	0.13	0.10	0.06	0.12	0.07	0.07	0.07	0.07	0.10	0.13	0.06	0.08	0.10	0.15
86.44	86.71	86.47	86.55	86.44	86.36	86.75	86.83	86.47	84.94	84.92	84.61	85.01	85.01	85.46	84.51	85.22	84.98	85.15	84.70	86.30	86.74	85.75
1.991	1.995	1.985	1.981	1.976	1.986	1.992	2.001	1.992	1.924	1.926	1.905	1.943	1.961	1.965	1.934	1.933	1.929	1.939	1.939	1.949	1.968	1.986
0.001	0.001	0.000	0.001	0.002	0.000	0.001	0.000	0.001	0.001	0.000	0.000	0.001	0.001	0.000	0.001	0.000	0.001	0.000	0.000	0.001	0.000	0.000
0.026	0.034	0.025	0.023	0.026	0.023	0.023	0.028	0.026	0.018	0.018	0.015	0.029	0.019	0.024	0.022	0.017	0.021	0.021	0.019	0.016	0.021	0.064
0.000	0.002	0.000	0.000	0.001	0.000	0.000	0.002	0.000	0.002	0.001	0.003	0.001	0.001	0.004	0.000	0.003	0.002	0.002	0.001	0.002	0.001	0.003
0.171	0.149	0.182	0.193	0.186	0.168	0.142	0.137	0.157	0.202	0.193	0.228	0.183	0.167	0.163	0.192	0.185	0.198	0.193	0.194	0.219	0.194	0.195
0.003	0.002	0.005	0.005	0.004	0.003	0.003	0.003	0.003	0.003	0.002	0.001	0.002	0.003	0.002	0.001	0.002	0.002	0.000	0.004	0.001	0.002	0.003
2.628	2.633	2.621	2.614	2.623	2.639	2.658	2.647	2.641	2.667	2.678	2.670	2.659	2.668	2.662	2.671	2.681	2.667	2.663	2.665	2.632	2.632	2.566
0.000	0.000	0.000	0.000	0.000	0.000	0.000	0.000	0.000	0.000	0.000	0.000	0.000	0.000	0.000	0.000	0.000	0.000	0.000	0.000	0.000	0.000	0.000
0.005	0.007	0.005	0.006	0.006	0.004	0.004	0.006	0.004	0.006	0.005	0.003	0.006	0.004	0.003	0.004	0.004	0.005	0.006	0.003	0.004	0.005	0.008
4.824	4.824	4.824	4.824	4.824	4.824	4.824	4.824	4.824	4.824	4.824	4.824	4.824	4.824	4.824	4.824	4.824	4.824	4.824	4.824	4.824	4.824	4.824
0.061	0.054	0.065	0.069	0.066	0.060	0.051	0.049	0.056	0.070	0.067	0.079	0.064	0.059	0.058	0.067	0.065	0.069	0.068	0.068	0.077	0.069	0.071
-0.008	-0.026	0.005	0.014	0.020	0.004	-0.008	-0.031	-0.011	0.131	0.129	0.172	0.084	0.058	0.042	0.110	0.114	0.120	0.099	0.103	0.083	0.041	-0.038
-0.046	-0.177	0.025	0.073	0.109	0.026	-0.057	-0.229	-0.068	0.649	0.666	0.754	0.461	0.344	0.259	0.575	0.617	0.607	0.513	0.533	0.380	0.212	-0.197

4.824	4.824	4.824	4.824	4.824	4.824	4.824	4.824	4.824	4.824	4.824	4.824	4.824	4.824	4.824	4.824	4.824	4.824	4.824	4.824	4.824	4.824	4.824
17	17	17	17	17	17	17	17	17	17	17	17	17	17	17	17	17	17	17	17	17	17	17
VER #45	VER #46	VER #47	VER #48	VER #49	VER #50	VER #51	VER #52	VER #53	VER #54	VER #55	VER #56	VER #57	VER #58	VER #59	VER #60	VER #61	VER #62	VER #63	VER #64	VER #65	VER #66	VER #67
42.26	42.43	42.41	44.68	42.28	41.96	42.65	42.37	42.28	43.71	42.26	42.84	42.75	42.28	42.32	42.44	43.10	42.23	43.89	43.23	44.13	43.15	42.71
0.03	0.03	0.01	0.01	0.04	0.00	0.00	0.02	0.00	0.03	0.01	0.05	0.00	0.01	0.01	0.01	0.00	0.02	0.00	0.00	0.01	0.01	0.00
0.25	0.22	0.27	0.74	0.27	0.22	0.29	0.39	0.24	0.45	0.28	0.26	0.31	0.30	0.29	0.29	0.48	0.35	0.59	0.57	0.45	0.45	0.31
0.05	0.04	0.05	0.02	0.05	0.00	0.05	0.04	0.01	0.02	0.02	0.02	0.04	0.05	0.00	0.00	0.07	0.05	0.10	0.04	0.00	0.03	0.00
5.81	5.86	5.64	3.87	5.89	6.11	5.57	5.70	6.11	4.48	5.71	5.24	5.60	5.65	5.79	5.20	4.95	6.43	4.31	4.89	4.02	4.87	5.46
0.06	0.01	0.08	0.11	0.09	0.06	0.00	0.07	0.05	0.11	0.07	0.06	0.07	0.08	0.10	0.05	0.24	0.05	0.15	0.07	0.04	0.06	0.11
38.34	38.60	38.35	38.66	38.36	38.18	38.49	37.98	38.16	39.25	38.65	38.67	38.50	38.13	38.17	38.24	38.56	38.04	38.55	38.05	39.09	38.18	38.69
-	-	-	-	-	-	-	-	-	-	-	-	-	-	-	-	-	-	-	-	-	-	-
0.09	0.04	0.16	0.18	0.05	0.12	0.07	0.08	0.06	0.09	0.08	0.08	0.08	0.09	0.09	0.05	0.14	0.08	0.15	0.15	0.11	0.10	0.11
86.88	87.22	86.97	88.28	87.02	86.65	87.12	86.65	86.92	88.13	87.07	87.22	87.34	86.59	86.78	86.27	87.55	87.24	87.73	87.00	87.84	86.85	87.39
1.947	1.946	1.951	2.020	1.945	1.939	1.958	1.958	1.949	1.977	1.940	1.962	1.958	1.954	1.952	1.965	1.968	1.943	1.998	1.988	2.001	1.986	1.953
0.001	0.001	0.000	0.000	0.001	0.000	0.000	0.001	0.000	0.001	0.000	0.002	0.000	0.000	0.000	0.000	0.000	0.001	0.000	0.000	0.000	0.000	0.000
0.013	0.012	0.015	0.040	0.014	0.012	0.016	0.021	0.013	0.024	0.015	0.014	0.017	0.016	0.016	0.016	0.026	0.019	0.032	0.031	0.024	0.024	0.017
0.002	0.001	0.002	0.001	0.002	0.000	0.002	0.001	0.000	0.001	0.001	0.001	0.001	0.002	0.000	0.000	0.002	0.002	0.004	0.001	0.000	0.001	0.000
0.224	0.225	0.217	0.146	0.226	0.236	0.214	0.220	0.235	0.169	0.219	0.201	0.214	0.218	0.223	0.201	0.189	0.247	0.164	0.188	0.152	0.187	0.209
0.002	0.000	0.003	0.004	0.003	0.002	0.000	0.003	0.002	0.004	0.003	0.002	0.003	0.003	0.004	0.002	0.009	0.002	0.006	0.003	0.001	0.002	0.004
2.630	2.637	2.628	2.604	2.629	2.628	2.632	2.615	2.621	2.644	2.643	2.639	2.627	2.625	2.623	2.637	2.622	2.607	2.614	2.606	2.640	2.618	2.636
0.000	0.000	0.000	0.000	0.000	0.000	0.000	0.000	0.000	0.000	0.000	0.000	0.000	0.000	0.000	0.000	0.000	0.000	0.000	0.000	0.000	0.000	0.000
0.005	0.002	0.008	0.009	0.002	0.006	0.003	0.004	0.003	0.004	0.004	0.004	0.004	0.004	0.005	0.002	0.007	0.004	0.007	0.008	0.005	0.005	0.005
4.824	4.824	4.824	4.824	4.824	4.824	4.824	4.824	4.824	4.824	4.824	4.824	4.824	4.824	4.824	4.824	4.824	4.824	4.824	4.824	4.824	4.824	4.824
0.078	0.079	0.076	0.053	0.079	0.082	0.075	0.078	0.082	0.060	0.077	0.071	0.075	0.077	0.078	0.071	0.067	0.087	0.059	0.067	0.055	0.067	0.073
0.091	0.095	0.081	-0.081	0.093	0.109	0.067	0.060	0.088	0.022	0.105	0.061	0.065	0.073	0.080	0.054	0.036	0.093	-0.031	-0.008	-0.025	0.003	0.077
0.408	0.423	0.374	-0.553	0.411	0.463	0.315	0.274	0.374	0.129	0.478	0.302	0.305	0.335	0.356	0.267	0.191	0.378	-0.189	-0.042	-0.164	0.017	0.368

																	TEM-EDS analyses					
4.824	4.824	4.824	4.824	4.824	4.824	4.824	4.824	4.824	4.824	4.824	4.824	4.824	4.824	4.824	4.824		Σcat	4.824	4.824	4.824	4.824	4.824
17	17	17	17	17	17	17	17	17	17	17	17	17	17	17	17		m paramet	17	17	17	17	17
VER	VER	VER	VER	VER	VER	VER	VER	VER	VER	VER	VER	VER	VER	VER	VER		Sample	VER	VER	VER	VER	VER
#68	#69	#70	#71	#73	#74	#75	#77	#78	#79	#80	#81	#82	#83	#84	#85		Analyses	1	3	5	8	5
42.48	43.31	44.03	44.08	42.90	44.51	42.74	44.34	42.32	44.34	43.86	43.03	44.61	43.06	42.58	44.75		SiO_2	42.97	42.61	43.10	45.43	43.10
0.00	0.04	0.02	0.00	0.02	0.01	0.00	0.01	0.01	0.00	0.02	0.00	0.02	0.03	0.03	0.02		TiO_2	-	-	-	-	-
0.44	0.50	0.36	0.52	0.43	0.73	0.44	0.21	0.39	0.34	0.59	0.36	0.31	0.45	0.33	0.40		Al_2O_3	0.43	0.23	0.28	0.49	0.28
0.03	0.05	0.06	0.00	0.03	0.00	0.03	0.00	0.04	0.00	0.03	0.02	0.01	0.05	0.04	0.02		Cr_2O_3	-	-	-	-	-
5.25	5.15	4.38	4.26	5.12	3.74	5.41	4.94	4.30	4.75	4.40	5.05	4.65	5.13	5.36	3.19		FeO_{tot}	4.50	5.99	5.68	4.35	5.68
0.59	0.07	0.08	0.15	0.09	0.13	0.07	0.13	0.11	0.09	0.05	0.08	0.15	0.12	0.09	0.13		MnO	-	-	-	-	-
37.84	38.24	38.00	38.94	38.24	38.78	37.98	38.22	36.74	38.17	38.39	38.42	38.41	38.45	38.68	39.90		MgO	36.45	38.53	38.50	38.90	38.50
-	-	-	-	-	-	-	-	-	-	-	-	-	-	-	-		NiO	0.41	0.42	0.52	0.37	0.52
0.15	0.14	0.93	0.16	0.09	0.13	0.11	0.24	2.57	0.21	0.16	0.14	0.08	0.14	0.09	0.08		CaO	-	-	-	-	-
86.78	87.49	87.86	88.10	86.90	88.03	86.77	88.09	86.48	87.91	87.49	87.09	88.24	87.44	87.19	88.48		Total	84.76	87.78	88.08	89.53	88.08
1.962	1.981	2.007	1.996	1.974	2.016	1.972	2.018	1.963	2.020	2.003	1.974	2.024	1.970	1.951	2.007		Si	2.033	1.944	1.960	2.030	1.960
0.000	0.001	0.001	0.000	0.001	0.000	0.000	0.000	0.000	0.000	0.001	0.000	0.001	0.001	0.001	0.001		Ti	0.000	0.000	0.000	0.000	0.000
0.024	0.027	0.019	0.028	0.023	0.039	0.024	0.011	0.021	0.018	0.032	0.019	0.017	0.024	0.018	0.021		Al	0.024	0.012	0.015	0.026	0.015
0.001	0.002	0.002	0.000	0.001	0.000	0.001	0.000	0.002	0.000	0.001	0.001	0.000	0.002	0.001	0.001		Cr	0.000	0.000	0.000	0.000	0.000
0.203	0.197	0.167	0.161	0.197	0.141	0.209	0.188	0.167	0.181	0.168	0.194	0.176	0.196	0.205	0.120		Fe_{tot}	0.178	0.228	0.216	0.163	0.216
0.023	0.003	0.003	0.006	0.003	0.005	0.003	0.005	0.004	0.004	0.002	0.003	0.006	0.004	0.003	0.005		Mn	0.000	0.000	0.000	0.000	0.000
2.604	2.606	2.580	2.626	2.621	2.616	2.610	2.591	2.539	2.591	2.611	2.626	2.596	2.619	2.640	2.666		Mg	2.569	2.619	2.608	2.589	2.608
0.000	0.000	0.000	0.000	0.000	0.000	0.000	0.000	0.000	0.000	0.000	0.000	0.000	0.000	0.000	0.000		Ni	0.021	0.021	0.025	0.017	0.025
0.007	0.007	0.045	0.008	0.005	0.006	0.005	0.012	0.127	0.010	0.008	0.007	0.004	0.007	0.004	0.004		Ca	0.000	0.000	0.000	0.000	0.000
4.824	4.824	4.824	4.824	4.824	4.824	4.824	4.824	4.824	4.824	4.824	4.824	4.824	4.824	4.824	4.824		Σcat	4.824	4.824	4.824	4.824	4.824
0.072	0.070	0.061	0.058	0.070	0.051	0.074	0.068	0.062	0.065	0.060	0.069	0.064	0.070	0.072	0.043		XFe	0.065	0.080	0.076	0.059	0.076
0.051	0.008	-0.035	-0.019	0.028	-0.071	0.031	-0.046	0.051	-0.059	-0.038	0.032	-0.065	0.034	0.079	-0.036		Fe^{+3}calc	-0.090	0.099	0.065	-0.085	0.065
0.249	0.043	-0.209	-0.117	0.145	-0.500	0.149	-0.246	0.305	-0.325	-0.227	0.164	-0.371	0.175	0.384	-0.300		$Fe^{+3}/\Sigma Fe$	-0.504	0.435	0.302	-0.521	0.302

4.824	4.824	4.824	4.824	4.824	4.824	4.824	4.824	4.824	4.824	4.824	4.824	4.824	4.824	4.824	4.824	4.824	4.824	4.824	4.824	4.824	4.824	4.824
17	17	17	17	17	17	17	17	17	17	17	17	17	17	17	17	17	17	17	17	17	17	17
VER 11	VER 12	VER 13	VER 14	VER 16	VER 17	VER 18	VER 20	VER 21	VER 23	VER 24	VER 26	VER 29	VER 30	VER 31	VER 32	VER 33	VER 36	VER 37	VER 38	VER 39	VER 40	VER 41
42.60	45.07	42.94	41.51	42.59	43.89	41.71	42.62	41.95	42.56	42.27	42.84	42.04	41.32	42.52	42.87	41.14	46.21	42.50	41.92	41.19	44.05	42.29
-	-	-	-	-	-	-	-	-	-	-	-	-	-	-	-	-	-	-	-	-	-	-
0.32	0.28	0.29	0.52	0.30	0.41	0.22	0.35	1.14	1.11	1.12	0.41	0.47	0.32	0.25	0.24	0.32	0.39	0.57	0.50	0.32	0.30	0.44
-	-	-	-	-	-	-	-	-	-	-	-	-	-	-	-	-	-	-	-	-	-	-
4.96	5.26	5.01	5.13	4.71	4.66	6.44	4.55	5.65	5.67	5.86	5.02	4.70	5.64	5.39	6.38	5.13	4.42	4.71	5.11	6.02	6.51	4.49
-	-	-	-	-	-	-	-	-	-	-	-	-	-	-	-	-	-	-	-	-	-	-
38.43	39.98	38.45	35.84	38.21	38.70	37.57	36.17	36.20	36.33	35.88	37.29	36.70	36.56	38.75	39.15	35.86	41.14	36.74	37.18	36.95	40.25	36.10
0.43	0.50	0.44	0.41	0.31	0.35	0.37	0.32	0.36	0.37	0.52	0.55	0.44	0.47	0.43	0.49	0.39	0.42	0.39	0.35	0.45	0.54	0.40
-	-	-	-	-	-	-	-	-	-	-	-	-	-	-	-	-	-	-	-	-	-	-
86.73	91.08	87.14	83.41	86.11	88.00	86.30	84.01	85.31	86.04	85.65	86.11	84.35	84.31	87.34	89.14	82.85	92.58	84.91	85.06	84.92	91.64	83.72
1.960	1.979	1.969	1.998	1.973	1.992	1.940	2.035	1.978	1.991	1.990	1.994	1.995	1.966	1.944	1.927	1.991	1.989	2.005	1.972	1.946	1.925	2.025
0.000	0.000	0.000	0.000	0.000	0.000	0.000	0.000	0.000	0.000	0.000	0.000	0.000	0.000	0.000	0.000	0.000	0.000	0.000	0.000	0.000	0.000	0.000
0.017	0.014	0.016	0.030	0.016	0.022	0.012	0.020	0.063	0.061	0.062	0.023	0.026	0.018	0.013	0.013	0.018	0.020	0.032	0.028	0.018	0.015	0.025
0.000	0.000	0.000	0.000	0.000	0.000	0.000	0.000	0.000	0.000	0.000	0.000	0.000	0.000	0.000	0.000	0.000	0.000	0.000	0.000	0.000	0.000	0.000
0.191	0.193	0.192	0.206	0.182	0.177	0.250	0.182	0.223	0.222	0.231	0.195	0.186	0.224	0.206	0.240	0.208	0.159	0.186	0.201	0.238	0.238	0.180
0.000	0.000	0.000	0.000	0.000	0.000	0.000	0.000	0.000	0.000	0.000	0.000	0.000	0.000	0.000	0.000	0.000	0.000	0.000	0.000	0.000	0.000	0.000
2.634	2.615	2.626	2.569	2.637	2.617	2.603	2.572	2.542	2.532	2.516	2.585	2.594	2.592	2.639	2.621	2.586	2.637	2.582	2.605	2.600	2.620	2.575
0.021	0.023	0.022	0.021	0.016	0.017	0.018	0.016	0.018	0.019	0.026	0.027	0.022	0.024	0.021	0.024	0.020	0.019	0.020	0.018	0.023	0.025	0.020
0.000	0.000	0.000	0.000	0.000	0.000	0.000	0.000	0.000	0.000	0.000	0.000	0.000	0.000	0.000	0.000	0.000	0.000	0.000	0.000	0.000	0.000	0.000
4.824	4.824	4.824	4.824	4.824	4.824	4.824	4.824	4.824	4.824	4.824	4.824	4.824	4.824	4.824	4.824	4.824	4.824	4.824	4.824	4.824	4.824	4.824
0.068	0.069	0.068	0.074	0.065	0.063	0.088	0.066	0.081	0.080	0.084	0.070	0.067	0.080	0.072	0.084	0.074	0.057	0.067	0.072	0.084	0.083	0.065
0.062	0.028	0.047	-0.025	0.038	-0.006	0.107	-0.089	-0.019	-0.043	-0.041	-0.010	-0.016	0.049	0.098	0.133	-0.001	0.003	-0.042	0.028	0.091	0.134	-0.074
0.325	0.145	0.243	-0.123	0.207	-0.032	0.429	-0.489	-0.083	-0.193	-0.177	-0.053	-0.088	0.220	0.478	0.556	-0.006	0.018	-0.225	0.140	0.381	0.564	-0.414

4.824	4.824	4.824	4.824	4.824	4.824	4.824
17	17	17	17	17	17	17
VER	VER	VER	VER	VER	VER	VER
42	44	51	52	66	67	70
41.64	42.20	41.71	42.06	42.16	42.20	41.62
-	-	-	-	-	-	-
0.27	0.47	0.47	0.38	0.32	0.44	0.35
-	-	-	-	-	-	-
5.70	4.08	5.72	5.87	5.38	5.12	4.61
-	-	-	-	-	-	-
37.14	36.89	36.74	37.17	37.89	37.17	36.84
0.37	0.42	0.49	0.45	0.32	0.50	0.29
-	-	-	-	-	-	-
85.12	84.05	85.14	85.93	86.08	85.42	83.71
1.961	2.004	1.967	1.965	1.959	1.979	1.986
0.000	0.000	0.000	0.000	0.000	0.000	0.000
0.015	0.026	0.026	0.021	0.018	0.024	0.020
0.000	0.000	0.000	0.000	0.000	0.000	0.000
0.224	0.162	0.225	0.229	0.209	0.201	0.184
0.000	0.000	0.000	0.000	0.000	0.000	0.000
2.605	2.610	2.581	2.587	2.622	2.596	2.619
0.018	0.021	0.025	0.022	0.016	0.025	0.015
0.000	0.000	0.000	0.000	0.000	0.000	0.000
4.824	4.824	4.824	4.824	4.824	4.824	4.824
0.079	0.058	0.080	0.081	0.074	0.072	0.066
0.064	-0.035	0.040	0.050	0.065	0.019	0.008
0.283	-0.216	0.178	0.217	0.309	0.094	0.041

Table SM4. EMPA analyses of Fe-rich antigorite from *Verde Acceglio* meta-ophicarbonate

WDS analyses																					
Σcat	4.750	4.750	4.750	4.750	4.750	4.750	4.750	4.750	4.750	4.750	4.750	4.750	4.750	4.750	4.750	4.750	4.750	4.750	4.750	4.750	4.750
m paramete	12	12	12	12	12	12	12	12	12	12	12	12	12	12	12	12	12	12	12	12	12
Sample	ACC	ACC	ACC	ACC	ACC	ACC	ACC	ACC	ACC	ACC	ACC	ACC	ACC	ACC	ACC	ACC	ACC	ACC	ACC	ACC	ACC
Analyses	71	160	247	250	#128	#129	#130	#131	#132	#133	#134	#135	#136	#137	#138	#139	#140	#141	#142	#143	#144
SiO_2	40.29	40.60	40.21	39.85	41.56	42.10	41.48	41.84	41.32	41.34	42.32	42.26	40.41	40.38	42.04	41.77	41.07	43.62	43.81	42.45	42.14
TiO_2	0.03	0.00	0.05	0.00	0.03	0.01	0.00	0.02	0.00	0.00	0.00	0.00	0.01	0.00	0.00	0.00	0.00	0.00	0.00	0.01	0.00
Al_2O_3	1.23	2.20	1.17	1.05	0.27	0.27	0.22	0.23	0.16	0.11	0.42	0.38	0.16	0.12	0.24	0.41	0.20	0.57	0.69	0.50	0.35
Cr_2O_3	0.00	0.00	0.05	0.07	0.00	0.00	0.02	0.00	0.00	0.04	0.03	0.05	0.03	0.00	0.00	0.00	0.05	0.10	0.08	0.08	0.05
FeO_{tot}	8.46	6.47	11.31	12.23	5.82	5.52	5.72	5.21	6.17	5.80	5.01	5.01	6.82	7.21	5.37	5.80	6.93	4.10	3.55	5.11	5.25
MnO	0.03	0.06	0.06	0.02	0.03	0.05	0.06	0.05	0.06	0.08	0.08	0.08	0.06	0.08	0.09	0.07	0.04	0.07	0.05	0.06	0.06
MgO	36.01	37.07	34.27	33.94	38.04	37.97	38.03	37.96	38.10	37.98	38.01	38.01	37.79	37.47	38.57	37.66	37.91	38.49	38.26	38.02	38.16
NiO	0.07	0.24	0.34	0.11	-	-	-	-	-	-	-	-	-	-	-	-	-	-	-	-	-
CaO	0.04	0.05	0.05	0.07	0.04	0.06	0.03	0.07	0.05	0.03	0.10	0.07	0.05	0.02	0.05	0.08	0.06	0.11	0.10	0.08	0.08
Total	86.16	86.69	87.50	87.33	85.79	85.98	85.55	85.39	85.86	85.37	85.97	85.86	85.31	85.28	86.37	85.79	86.24	87.05	86.54	86.31	86.08
Si	1.865	1.851	1.861	1.853	1.907	1.928	1.908	1.927	1.896	1.906	1.936	1.936	1.869	1.872	1.913	1.920	1.881	1.968	1.986	1.936	1.926
Ti	0.001	0.000	0.002	0.000	0.001	0.000	0.000	0.001	0.000	0.000	0.000	0.000	0.000	0.000	0.000	0.000	0.000	0.000	0.000	0.000	0.000
Al	0.067	0.118	0.064	0.057	0.015	0.015	0.012	0.013	0.009	0.006	0.022	0.021	0.008	0.007	0.013	0.022	0.011	0.030	0.037	0.027	0.019
Cr	0.000	0.000	0.002	0.003	0.000	0.000	0.001	0.000	0.000	0.002	0.001	0.002	0.001	0.000	0.000	0.000	0.002	0.003	0.003	0.003	0.002
Fe_{tot}	0.327	0.247	0.437	0.475	0.223	0.211	0.220	0.201	0.236	0.223	0.192	0.192	0.264	0.279	0.204	0.223	0.265	0.155	0.135	0.195	0.200
Mn	0.001	0.002	0.002	0.001	0.001	0.002	0.002	0.002	0.002	0.003	0.003	0.003	0.002	0.003	0.003	0.003	0.002	0.003	0.002	0.002	0.002
Mg	2.483	2.518	2.362	2.352	2.601	2.591	2.606	2.604	2.604	2.609	2.591	2.593	2.603	2.588	2.614	2.578	2.587	2.586	2.583	2.583	2.597
Ni	0.003	0.012	0.017	0.006	0.000	0.000	0.000	0.000	0.000	0.000	0.000	0.000	0.000	0.000	0.000	0.000	0.000	0.000	0.000	0.000	0.000
Ca	0.002	0.002	0.002	0.003	0.002	0.003	0.002	0.003	0.002	0.002	0.005	0.003	0.002	0.001	0.003	0.004	0.003	0.005	0.005	0.004	0.004
Σcat	4.750	4.750	4.750	4.750	4.750	4.750	4.750	4.750	4.750	4.750	4.750	4.750	4.750	4.750	4.750	4.750	4.750	4.750	4.750	4.750	4.750
XFe	0.116	0.089	0.156	0.168	0.079	0.075	0.078	0.072	0.083	0.079	0.069	0.069	0.092	0.097	0.073	0.080	0.093	0.056	0.050	0.070	0.072
Fe^{+3}calc	0.203	0.180	0.212	0.233	0.171	0.128	0.172	0.134	0.199	0.180	0.104	0.106	0.253	0.249	0.162	0.138	0.225	0.031	-0.011	0.098	0.128
$Fe^{+3}/\Sigma Fe$	0.619	0.729	0.485	0.491	0.765	0.608	0.780	0.666	0.842	0.807	0.542	0.552	0.960	0.891	0.792	0.619	0.848	0.202	-0.085	0.504	0.638

4.750	4.750	4.750	4.750	4.750	4.750	4.750	4.750	4.750	4.750	4.750	4.750	4.750	4.750	4.750	4.750	4.750	4.750	4.750	4.750	4.750	4.750	4.750
12	12	12	12	12	12	12	12	12	12	12	12	12	12	12	12	12	12	12	12	12	12	12
ACC #145	ACC #146	ACC #147	ACC #148	ACC #149	ACC #150	ACC #151	ACC #152	ACC #153	ACC #154	ACC #155	ACC #156	ACC #157	ACC #158	ACC #159	ACC #160	ACC #161	ACC #162	ACC #163	ACC #164	ACC #165	ACC #166	ACC #167
42.74	42.57	42.66	42.25	42.48	43.39	42.10	41.71	42.16	41.64	41.83	42.21	43.20	42.23	41.59	41.76	42.66	43.38	42.82	42.20	42.41	41.98	42.26
0.02	0.02	0.00	0.00	0.00	0.01	0.00	0.00	0.01	0.05	0.01	0.00	0.00	0.01	0.03	0.03	0.03	0.01	0.02	0.00	0.02	0.00	0.00
0.44	0.42	0.38	0.41	0.48	0.81	0.80	0.42	0.35	0.31	0.30	0.27	0.50	0.39	0.35	0.32	0.56	0.64	0.63	0.61	0.58	0.33	0.49
0.07	0.11	0.06	0.08	0.04	0.23	0.07	0.05	0.03	0.05	0.05	0.07	0.06	0.04	0.03	0.07	0.02	0.02	0.01	0.05	0.02	0.00	0.05
4.87	5.21	4.76	5.30	5.01	4.09	5.15	5.50	5.36	5.88	5.36	5.45	4.37	5.09	5.71	5.81	3.22	3.17	3.59	4.02	4.23	4.28	3.64
0.08	0.03	0.06	0.05	0.11	0.07	0.05	0.09	0.06	0.06	0.00	0.02	0.04	0.04	0.05	0.10	0.08	0.05	0.12	0.08	0.02	0.00	0.12
38.49	38.24	38.27	38.07	37.95	38.28	37.32	37.96	38.15	37.87	38.00	38.41	38.28	38.18	37.89	38.06	38.65	38.53	38.48	37.39	37.82	38.51	38.19
-	-	-	-	-	-	-	-	-	-	-	-	-	-	-	-	-	-	-	-	-	-	-
0.09	0.10	0.11	0.09	0.12	0.07	0.11	0.06	0.06	0.05	0.07	0.07	0.07	0.07	0.10	0.06	0.13	0.12	0.12	0.13	0.16	0.06	0.08
86.80	86.71	86.28	86.25	86.18	86.94	85.61	85.78	86.16	85.90	85.62	86.49	86.53	86.04	85.73	86.21	85.35	85.93	85.79	84.47	85.25	85.16	84.82
1.935	1.933	1.943	1.928	1.940	1.961	1.939	1.914	1.925	1.911	1.922	1.920	1.961	1.929	1.911	1.909	1.952	1.974	1.953	1.961	1.952	1.929	1.949
0.001	0.001	0.000	0.000	0.000	0.000	0.000	0.000	0.000	0.002	0.000	0.000	0.000	0.000	0.001	0.001	0.001	0.000	0.001	0.000	0.001	0.000	0.000
0.024	0.023	0.020	0.022	0.026	0.043	0.043	0.023	0.019	0.017	0.016	0.014	0.027	0.021	0.019	0.017	0.030	0.035	0.034	0.033	0.032	0.018	0.027
0.003	0.004	0.002	0.003	0.001	0.008	0.003	0.002	0.001	0.002	0.002	0.003	0.002	0.001	0.001	0.003	0.001	0.001	0.000	0.002	0.001	0.000	0.002
0.184	0.198	0.181	0.202	0.191	0.155	0.198	0.211	0.205	0.225	0.206	0.207	0.166	0.195	0.219	0.222	0.123	0.121	0.137	0.156	0.163	0.164	0.140
0.003	0.001	0.002	0.002	0.004	0.003	0.002	0.003	0.002	0.002	0.000	0.001	0.002	0.001	0.002	0.004	0.003	0.002	0.005	0.003	0.001	0.000	0.005
2.596	2.586	2.596	2.588	2.582	2.577	2.560	2.594	2.595	2.589	2.600	2.602	2.589	2.599	2.593	2.592	2.634	2.612	2.615	2.588	2.593	2.636	2.624
0.000	0.000	0.000	0.000	0.000	0.000	0.000	0.000	0.000	0.000	0.000	0.000	0.000	0.000	0.000	0.000	0.000	0.000	0.000	0.000	0.000	0.000	0.000
0.005	0.005	0.005	0.004	0.006	0.004	0.005	0.003	0.003	0.002	0.004	0.003	0.004	0.003	0.005	0.003	0.006	0.006	0.006	0.006	0.008	0.003	0.004
4.750	4.750	4.750	4.750	4.750	4.750	4.750	4.750	4.750	4.750	4.750	4.750	4.750	4.750	4.750	4.750	4.750	4.750	4.750	4.750	4.750	4.750	4.750
0.066	0.071	0.065	0.072	0.069	0.057	0.072	0.075	0.073	0.080	0.073	0.074	0.060	0.070	0.078	0.079	0.045	0.044	0.050	0.057	0.059	0.059	0.051
0.103	0.108	0.092	0.118	0.093	0.027	0.077	0.148	0.130	0.160	0.138	0.144	0.049	0.119	0.159	0.162	0.066	0.017	0.059	0.043	0.063	0.124	0.074
0.561	0.547	0.507	0.586	0.486	0.177	0.389	0.699	0.633	0.710	0.671	0.695	0.293	0.611	0.725	0.731	0.532	0.140	0.432	0.272	0.385	0.757	0.524

			TEM-EDS analyses																	
4.750	4.750	4.750	Σcat	4.750	4.750	4.750	4.750	4.750	4.750	4.750	4.750	4.750	4.750	4.750	4.750	4.750	4.750	4.750	4.750	4.750
12	12	12	m paramet	12	12	12	12	12	12	12	12	12	12	12	12	12	12	12	12	12
ACC	ACC	ACC	Sample	ACC	ACC	ACC	ACC	ACC	ACC	ACC	ACC	ACC	ACC	ACC	ACC	ACC	ACC	ACC	ACC	ACC
#168	#169	#170	Analyses	70	71	72	73	74	75	76	77	78	79	80	81	82	83	84	85	86	87
41.94	41.87	41.51	SiO_2	40.86	40.29	40.95	42.00	41.50	40.91	40.54	40.98	40.75	40.60	40.93	41.30	42.02	41.28	40.87	41.57	41.45	42.62
0.02	0.00	0.01	TiO_2	-	-	-	-	-	-	-	-	-	-	-	-	-	-	-	-	-	-
0.49	0.44	0.37	Al_2O_3	1.16	1.23	1.20	1.09	1.10	1.39	1.15	1.75	0.79	0.68	1.16	0.94	0.91	1.11	1.19	1.03	1.58	1.47
0.01	0.08	0.00	Cr_2O_3	-	-	-	-	-	-	-	-	-	-	-	-	-	-	-	-	-	-
4.09	4.19	4.49	FeO_{tot}	8.89	8.46	7.57	6.72	7.38	7.66	8.20	7.76	7.71	8.03	8.26	7.65	6.52	8.12	8.02	7.42	6.90	6.62
0.08	0.02	0.09	MnO	-	-	-	-	-	-	-	-	-	-	-	-	-	-	-	-	-	-
38.02	38.46	38.16	MgO	35.51	36.01	36.54	36.89	36.06	36.43	35.95	34.61	35.94	36.05	36.01	37.47	37.15	36.40	35.81	36.68	36.98	36.12
-	-	-	NiO	0.13	0.07	0.23	0.38	0.13	0.36	0.29	0.29	0.05	0.02	0.34	0.40	0.10	0.22	0.33	0.23	0.17	0.08
0.11	0.12	0.09	CaO	-	-	-	-	-	-	-	-	-	-	-	-	-	-	-	-	-	-
84.74	85.18	84.72	Total	86.55	86.06	86.49	87.06	86.16	86.75	86.13	85.39	85.24	85.38	86.70	87.76	86.71	87.13	86.22	86.93	87.08	86.91
1.939	1.924	1.919	Si	1.890	1.867	1.882	1.914	1.917	1.875	1.877	1.920	1.903	1.894	1.884	1.868	1.919	1.888	1.891	1.901	1.887	1.951
0.001	0.000	0.000	Ti	0.000	0.000	0.000	0.000	0.000	0.000	0.000	0.000	0.000	0.000	0.000	0.000	0.000	0.000	0.000	0.000	0.000	0.000
0.027	0.024	0.020	Al	0.063	0.067	0.065	0.058	0.060	0.075	0.063	0.097	0.044	0.037	0.063	0.050	0.049	0.060	0.065	0.056	0.085	0.079
0.000	0.003	0.000	Cr	0.000	0.000	0.000	0.000	0.000	0.000	0.000	0.000	0.000	0.000	0.000	0.000	0.000	0.000	0.000	0.000	0.000	0.000
0.158	0.161	0.173	Fe_{tot}	0.344	0.327	0.291	0.256	0.285	0.294	0.317	0.304	0.301	0.313	0.318	0.289	0.249	0.311	0.310	0.283	0.263	0.253
0.003	0.001	0.004	Mn	0.000	0.000	0.000	0.000	0.000	0.000	0.000	0.000	0.000	0.000	0.000	0.000	0.000	0.000	0.000	0.000	0.000	0.000
2.618	2.632	2.629	Mg	2.447	2.485	2.501	2.504	2.482	2.488	2.479	2.415	2.500	2.505	2.469	2.524	2.528	2.481	2.468	2.498	2.507	2.463
0.000	0.000	0.000	Ni	0.006	0.003	0.011	0.018	0.006	0.018	0.014	0.014	0.003	0.001	0.017	0.019	0.005	0.011	0.016	0.011	0.008	0.004
0.005	0.006	0.005	Ca	0.000	0.000	0.000	0.000	0.000	0.000	0.000	0.000	0.000	0.000	0.000	0.000	0.000	0.000	0.000	0.000	0.000	0.000
4.750	4.750	4.750	Σcat	4.750	4.750	4.750	4.750	4.750	4.750	4.750	4.750	4.750	4.750	4.750	4.750	4.750	4.750	4.750	4.750	4.750	4.750
0.057	0.058	0.062	XFe	0.123	0.116	0.104	0.093	0.103	0.106	0.113	0.112	0.107	0.111	0.114	0.103	0.090	0.111	0.112	0.102	0.095	0.093
0.096	0.125	0.141	Fe^{+3}calc	0.157	0.199	0.172	0.114	0.105	0.174	0.184	0.064	0.150	0.175	0.170	0.215	0.112	0.164	0.154	0.142	0.142	0.020
0.606	0.780	0.814	$Fe^{+3}/\Sigma Fe$	0.456	0.608	0.590	0.447	0.370	0.593	0.578	0.210	0.499	0.560	0.535	0.744	0.450	0.526	0.495	0.502	0.539	0.077

4.750	4.750	4.750	4.750	4.750	4.750	4.750	4.750	4.750	4.750	4.750	4.750	4.750	4.750	4.750	4.750	4.750	4.750	4.750	4.750	4.750	4.750	4.750
12	12	12	12	12	12	12	12	12	12	12	12	12	12	12	12	12	12	12	12	12	12	12
ACC 88	ACC 89	ACC 90	ACC 91	ACC 92	ACC 107	ACC 108	ACC 109	ACC 110	ACC 111	ACC 112	ACC 113	ACC 114	ACC 115	ACC 116	ACC 117	ACC 118	ACC 119	ACC 120	ACC 121	ACC 122	ACC 123	ACC 124
41.84	41.86	41.12	40.60	41.46	41.72	41.12	41.28	40.28	41.21	40.51	41.45	40.84	41.81	41.19	40.59	41.51	40.83	41.56	41.10	41.28	41.53	41.17
-	-	-	-	-	-	-	-	-	-	-	-	-	-	-	-	-	-	-	-	-	-	-
0.89	0.86	1.10	1.56	0.82	1.21	1.18	1.32	1.22	1.36	1.54	1.35	1.13	1.18	1.19	1.30	1.32	1.33	1.12	1.48	1.60	1.74	1.62
-	-	-	-	-	-	-	-	-	-	-	-	-	-	-	-	-	-	-	-	-	-	-
6.33	7.18	7.88	8.61	7.71	8.37	8.39	7.77	7.80	8.16	6.74	6.91	7.22	7.45	7.41	7.35	7.21	7.24	6.99	6.92	6.78	6.32	7.23
-	-	-	-	-	-	-	-	-	-	-	-	-	-	-	-	-	-	-	-	-	-	-
37.36	37.29	35.87	35.82	36.02	35.86	36.00	36.15	36.27	36.24	36.40	36.29	35.86	35.80	36.62	36.21	36.04	36.47	37.45	36.77	36.68	37.28	37.09
0.27	0.20	0.19	0.29	0.06	0.17	0.13	0.24	0.17	0.34	0.29	0.26	0.26	0.29	0.20	0.10	0.31	0.29	0.37	0.15	0.25	0.39	0.32
-	-	-	-	-	-	-	-	-	-	-	-	-	-	-	-	-	-	-	-	-	-	-
86.69	87.39	86.15	86.89	86.07	87.32	86.82	86.75	85.73	87.30	85.47	86.26	85.31	86.52	86.61	85.55	86.38	86.16	87.49	86.42	86.57	87.26	87.42
1.909	1.900	1.903	1.867	1.919	1.910	1.891	1.896	1.868	1.883	1.877	1.909	1.904	1.927	1.889	1.885	1.913	1.881	1.882	1.885	1.890	1.882	1.868
0.000	0.000	0.000	0.000	0.000	0.000	0.000	0.000	0.000	0.000	0.000	0.000	0.000	0.000	0.000	0.000	0.000	0.000	0.000	0.000	0.000	0.000	0.000
0.048	0.046	0.060	0.084	0.045	0.065	0.064	0.071	0.067	0.073	0.084	0.073	0.062	0.064	0.064	0.071	0.071	0.072	0.059	0.080	0.086	0.093	0.086
0.000	0.000	0.000	0.000	0.000	0.000	0.000	0.000	0.000	0.000	0.000	0.000	0.000	0.000	0.000	0.000	0.000	0.000	0.000	0.000	0.000	0.000	0.000
0.241	0.272	0.305	0.331	0.298	0.320	0.322	0.298	0.302	0.312	0.261	0.266	0.281	0.287	0.284	0.285	0.278	0.279	0.265	0.265	0.259	0.239	0.274
0.000	0.000	0.000	0.000	0.000	0.000	0.000	0.000	0.000	0.000	0.000	0.000	0.000	0.000	0.000	0.000	0.000	0.000	0.000	0.000	0.000	0.000	0.000
2.539	2.521	2.473	2.454	2.484	2.446	2.466	2.473	2.505	2.466	2.513	2.489	2.490	2.458	2.502	2.504	2.473	2.503	2.526	2.512	2.502	2.517	2.506
0.013	0.010	0.009	0.014	0.003	0.008	0.006	0.012	0.008	0.016	0.015	0.013	0.013	0.014	0.010	0.005	0.015	0.014	0.018	0.007	0.012	0.019	0.016
0.000	0.000	0.000	0.000	0.000	0.000	0.000	0.000	0.000	0.000	0.000	0.000	0.000	0.000	0.000	0.000	0.000	0.000	0.000	0.000	0.000	0.000	0.000
4.750	4.750	4.750	4.750	4.750	4.750	4.750	4.750	4.750	4.750	4.750	4.750	4.750	4.750	4.750	4.750	4.750	4.750	4.750	4.750	4.750	4.750	4.750
0.087	0.098	0.110	0.119	0.107	0.116	0.116	0.108	0.108	0.112	0.094	0.097	0.102	0.105	0.102	0.102	0.101	0.100	0.095	0.095	0.094	0.087	0.099
0.135	0.153	0.134	0.182	0.116	0.114	0.154	0.137	0.198	0.162	0.161	0.110	0.131	0.082	0.157	0.160	0.103	0.165	0.177	0.150	0.134	0.143	0.178
0.559	0.562	0.438	0.551	0.389	0.355	0.477	0.459	0.654	0.519	0.617	0.413	0.465	0.285	0.552	0.560	0.373	0.593	0.667	0.565	0.515	0.598	0.651

4.750	4.750	4.750	4.750	4.750	4.750	4.750	4.750	4.750	4.750	4.750	4.750	4.750	4.750	4.750	4.750	4.750	4.750	4.750	4.750	4.750	4.750	4.750
12	12	12	12	12	12	12	12	12	12	12	12	12	12	12	12	12	12	12	12	12	12	12
ACC 125	ACC 126	ACC 127	ACC 128	ACC 129	ACC 130	ACC 132	ACC 133	ACC 134	ACC 135	ACC 136	ACC 137	ACC 138	ACC 139	ACC 140	ACC 141	ACC 142	ACC 143	ACC 144	ACC 145	ACC 148	ACC 149	ACC 150
42.17	41.84	41.15	40.85	40.95	40.68	40.93	40.25	41.00	41.16	41.58	41.32	41.23	41.25	41.64	41.30	41.19	41.56	42.01	41.69	41.73	41.82	41.53
-	-	-	-	-	-	-	-	-	-	-	-	-	-	-	-	-	-	-	-	-	-	-
1.48	1.06	1.08	1.83	1.47	1.43	1.60	2.37	1.56	1.32	1.42	1.23	2.06	1.23	1.39	1.25	1.35	1.94	1.07	1.29	0.99	0.88	0.90
-	-	-	-	-	-	-	-	-	-	-	-	-	-	-	-	-	-	-	-	-	-	-
6.64	6.65	7.10	7.11	7.54	7.42	7.53	7.08	6.87	7.31	7.43	7.79	7.23	6.92	7.67	7.33	6.77	5.80	6.18	6.50	7.23	6.63	6.99
-	-	-	-	-	-	-	-	-	-	-	-	-	-	-	-	-	-	-	-	-	-	-
36.88	37.06	36.51	36.71	36.21	36.33	36.86	35.65	35.54	36.59	36.47	36.36	35.19	36.42	36.59	37.05	36.21	37.15	38.03	36.16	37.00	37.24	36.39
0.17	0.39	0.20	0.21	0.17	0.25	0.30	0.17	0.13	0.23	0.32	0.20	0.10	0.12	0.22	0.29	0.29	0.24	0.01	0.39	0.35	0.26	0.23
-	-	-	-	-	-	-	-	-	-	-	-	-	-	-	-	-	-	-	-	-	-	-
87.33	86.99	86.03	86.71	86.34	86.10	87.21	85.52	85.10	86.61	87.22	86.91	85.80	85.95	87.50	87.22	85.81	86.70	87.31	86.04	87.29	86.83	86.04
1.915	1.906	1.899	1.868	1.887	1.877	1.864	1.870	1.916	1.888	1.897	1.893	1.916	1.905	1.894	1.879	1.906	1.893	1.899	1.924	1.898	1.907	1.917
0.000	0.000	0.000	0.000	0.000	0.000	0.000	0.000	0.000	0.000	0.000	0.000	0.000	0.000	0.000	0.000	0.000	0.000	0.000	0.000	0.000	0.000	0.000
0.079	0.057	0.058	0.099	0.080	0.077	0.086	0.130	0.086	0.072	0.076	0.066	0.113	0.067	0.074	0.067	0.074	0.104	0.057	0.070	0.053	0.047	0.049
0.000	0.000	0.000	0.000	0.000	0.000	0.000	0.000	0.000	0.000	0.000	0.000	0.000	0.000	0.000	0.000	0.000	0.000	0.000	0.000	0.000	0.000	0.000
0.252	0.253	0.274	0.272	0.290	0.286	0.286	0.275	0.268	0.280	0.283	0.298	0.281	0.267	0.291	0.279	0.262	0.221	0.234	0.251	0.275	0.253	0.270
0.000	0.000	0.000	0.000	0.000	0.000	0.000	0.000	0.000	0.000	0.000	0.000	0.000	0.000	0.000	0.000	0.000	0.000	0.000	0.000	0.000	0.000	0.000
2.495	2.515	2.509	2.501	2.485	2.497	2.500	2.467	2.474	2.499	2.478	2.482	2.436	2.505	2.479	2.511	2.495	2.520	2.560	2.486	2.507	2.530	2.503
0.008	0.019	0.010	0.010	0.009	0.012	0.015	0.009	0.006	0.011	0.016	0.010	0.005	0.006	0.011	0.014	0.014	0.012	0.000	0.019	0.017	0.013	0.012
0.000	0.000	0.000	0.000	0.000	0.000	0.000	0.000	0.000	0.000	0.000	0.000	0.000	0.000	0.000	0.000	0.000	0.000	0.000	0.000	0.000	0.000	0.000
4.750	4.750	4.750	4.750	4.750	4.750	4.750	4.750	4.750	4.750	4.750	4.750	4.750	4.750	4.750	4.750	4.750	4.750	4.750	4.750	4.750	4.750	4.750
0.092	0.091	0.098	0.098	0.105	0.103	0.103	0.100	0.098	0.101	0.103	0.107	0.103	0.096	0.105	0.100	0.095	0.081	0.084	0.092	0.099	0.091	0.097
0.090	0.131	0.144	0.165	0.147	0.168	0.187	0.131	0.083	0.153	0.130	0.147	0.056	0.123	0.137	0.174	0.115	0.110	0.145	0.082	0.150	0.138	0.117
0.358	0.518	0.527	0.606	0.506	0.587	0.654	0.476	0.308	0.545	0.460	0.492	0.199	0.461	0.471	0.626	0.441	0.498	0.623	0.327	0.547	0.547	0.433

4.750 12	4.750 12	4.750 12	4.750 12	4.750 12	4.750 12	4.750 12	4.750 12	4.750 12	4.750 12	4.750 12	4.750 12	4.750 12	4.750 12	4.750 12	4.750 12	4.750 12	4.750 12	4.750 12	4.750 12	4.750 12	4.750 12	4.750 12
ACC 151	ACC 152	ACC 153	ACC 154	ACC 155	ACC 156	ACC 157	ACC 158	ACC 159	ACC 160	ACC 161	ACC 162	ACC 163	ACC 164	ACC 165	ACC 166	ACC 167	ACC 168	ACC 169	ACC 170	ACC 171	ACC 172	ACC 173
41.57	41.68	41.03	41.37	40.77	40.90	41.51	41.14	41.01	40.60	41.52	40.54	40.77	41.14	40.77	40.99	40.82	41.12	41.49	41.87	41.56	41.49	41.55
-	-	-	-	-	-	-	-	-	-	-	-	-	-	-	-	-	-	-	-	-	-	-
1.26	1.22	1.25	1.27	1.36	1.77	1.49	1.86	1.91	2.20	0.95	1.21	1.13	1.22	1.08	1.35	1.11	0.88	1.04	0.96	1.68	1.30	1.14
-	-	-	-	-	-	-	-	-	-	-	-	-	-	-	-	-	-	-	-	-	-	-
7.42	6.43	6.41	7.15	6.85	6.78	6.58	6.35	6.50	6.47	7.90	7.75	8.64	7.85	8.19	8.05	8.02	7.45	6.18	5.86	6.93	6.22	5.91
-	-	-	-	-	-	-	-	-	-	-	-	-	-	-	-	-	-	-	-	-	-	-
36.33	36.84	36.70	36.25	36.17	37.13	36.86	36.91	36.66	37.07	35.93	35.89	35.43	35.44	35.80	35.89	36.10	37.09	36.71	37.61	37.37	36.98	37.49
0.43	0.21	0.37	0.12	0.31	0.06	0.14	0.33	0.38	0.24	0.06	0.10	0.28	0.16	0.37	0.22	0.21	0.25	0.57	0.15	0.30	0.10	0.34
-	-	-	-	-	-	-	-	-	-	-	-	-	-	-	-	-	-	-	-	-	-	-
87.00	86.38	85.76	86.15	85.45	86.63	86.58	86.58	86.46	86.58	86.35	85.48	86.25	85.81	86.21	86.49	86.26	86.78	85.99	86.46	87.85	86.09	86.42
1.902	1.911	1.894	1.908	1.893	1.868	1.899	1.879	1.878	1.853	1.918	1.888	1.891	1.914	1.887	1.890	1.886	1.880	1.910	1.911	1.874	1.905	1.897
0.000	0.000	0.000	0.000	0.000	0.000	0.000	0.000	0.000	0.000	0.000	0.000	0.000	0.000	0.000	0.000	0.000	0.000	0.000	0.000	0.000	0.000	0.000
0.068	0.066	0.068	0.069	0.075	0.095	0.080	0.100	0.103	0.118	0.052	0.066	0.062	0.067	0.059	0.073	0.060	0.047	0.057	0.052	0.089	0.071	0.061
0.000	0.000	0.000	0.000	0.000	0.000	0.000	0.000	0.000	0.000	0.000	0.000	0.000	0.000	0.000	0.000	0.000	0.000	0.000	0.000	0.000	0.000	0.000
0.284	0.246	0.247	0.276	0.266	0.259	0.252	0.243	0.249	0.247	0.305	0.301	0.335	0.305	0.317	0.310	0.310	0.285	0.238	0.224	0.261	0.239	0.225
0.000	0.000	0.000	0.000	0.000	0.000	0.000	0.000	0.000	0.000	0.000	0.000	0.000	0.000	0.000	0.000	0.000	0.000	0.000	0.000	0.000	0.000	0.000
2.476	2.516	2.523	2.491	2.501	2.526	2.512	2.512	2.501	2.520	2.472	2.489	2.448	2.456	2.469	2.465	2.484	2.526	2.518	2.557	2.511	2.530	2.550
0.021	0.010	0.018	0.006	0.015	0.003	0.007	0.016	0.018	0.012	0.003	0.005	0.014	0.008	0.018	0.011	0.010	0.012	0.028	0.007	0.014	0.005	0.016
0.000	0.000	0.000	0.000	0.000	0.000	0.000	0.000	0.000	0.000	0.000	0.000	0.000	0.000	0.000	0.000	0.000	0.000	0.000	0.000	0.000	0.000	0.000
4.750	4.750	4.750	4.750	4.750	4.750	4.750	4.750	4.750	4.750	4.750	4.750	4.750	4.750	4.750	4.750	4.750	4.750	4.750	4.750	4.750	4.750	4.750
0.103	0.089	0.089	0.100	0.096	0.093	0.091	0.088	0.091	0.089	0.110	0.108	0.120	0.111	0.114	0.112	0.111	0.101	0.086	0.080	0.094	0.086	0.081
0.129	0.112	0.145	0.114	0.139	0.170	0.121	0.141	0.140	0.176	0.112	0.158	0.155	0.105	0.167	0.146	0.168	0.192	0.123	0.127	0.162	0.118	0.145
0.454	0.453	0.586	0.414	0.524	0.656	0.482	0.581	0.564	0.713	0.369	0.524	0.464	0.345	0.526	0.470	0.544	0.676	0.519	0.567	0.620	0.497	0.643

4.750	4.750	4.750	4.750	4.750	4.750	4.750	4.750	4.750	4.750	4.750	4.750	4.750	4.750	4.750	4.750	4.750	4.750	4.750	4.750	4.750	4.750	4.750
12	12	12	12	12	12	12	12	12	12	12	12	12	12	12	12	12	12	12	12	12	12	12
ACC 174	ACC 175	ACC 176	ACC 177	ACC 178	ACC 180	ACC 182	ACC 183	ACC 184	ACC 185	ACC 186	ACC 187	ACC 188	ACC 189	ACC 190	ACC 191	ACC 192	ACC 193	ACC 194	ACC 195	ACC 196	ACC 197	ACC 198
41.41	41.17	41.43	40.24	42.61	41.65	40.77	41.62	41.79	39.22	40.08	39.73	41.17	40.47	41.25	42.54	42.27	41.53	41.82	40.48	40.25	39.11	38.76
-	-	-	-	-	-	-	-	-	-	-	-	-	-	-	-	-	-	-	-	-	-	-
1.33	1.22	1.17	1.21	2.17	1.54	1.42	1.38	1.53	0.53	1.10	0.79	0.89	1.19	1.26	1.47	0.95	1.30	1.29	1.02	1.09	0.83	0.86
-	-	-	-	-	-	-	-	-	-	-	-	-	-	-	-	-	-	-	-	-	-	-
6.27	6.66	7.42	7.87	7.57	6.65	5.60	6.61	5.66	11.82	10.93	10.67	9.20	9.33	8.37	8.29	7.57	8.61	8.78	9.18	10.66	12.00	11.98
-	-	-	-	-	-	-	-	-	-	-	-	-	-	-	-	-	-	-	-	-	-	-
37.78	37.27	36.35	35.98	33.86	36.68	37.46	36.26	36.94	34.43	34.68	34.56	35.39	35.33	35.62	35.55	36.23	35.56	35.20	35.16	34.43	34.56	34.59
0.24	0.35	0.20	0.40	0.12	0.32	0.31	0.17	0.23	0.16	0.37	0.23	0.37	0.07	0.12	0.09	0.22	0.17	0.21	0.24	0.14	0.08	0.28
-	-	-	-	-	-	-	-	-	-	-	-	-	-	-	-	-	-	-	-	-	-	-
87.02	86.66	86.58	85.70	86.32	86.84	85.55	86.05	86.15	86.14	87.15	85.99	87.02	86.38	86.62	87.95	87.23	87.19	87.30	86.08	86.57	86.58	86.47
1.878	1.879	1.904	1.869	1.983	1.902	1.875	1.920	1.916	1.841	1.856	1.863	1.898	1.878	1.904	1.938	1.932	1.907	1.923	1.885	1.876	1.827	1.812
0.000	0.000	0.000	0.000	0.000	0.000	0.000	0.000	0.000	0.000	0.000	0.000	0.000	0.000	0.000	0.000	0.000	0.000	0.000	0.000	0.000	0.000	0.000
0.071	0.066	0.063	0.066	0.119	0.083	0.077	0.075	0.083	0.029	0.060	0.044	0.048	0.065	0.068	0.079	0.051	0.071	0.070	0.056	0.060	0.045	0.047
0.000	0.000	0.000	0.000	0.000	0.000	0.000	0.000	0.000	0.000	0.000	0.000	0.000	0.000	0.000	0.000	0.000	0.000	0.000	0.000	0.000	0.000	0.000
0.238	0.254	0.285	0.305	0.295	0.254	0.215	0.255	0.217	0.464	0.423	0.418	0.355	0.362	0.323	0.316	0.289	0.331	0.337	0.357	0.415	0.469	0.468
0.000	0.000	0.000	0.000	0.000	0.000	0.000	0.000	0.000	0.000	0.000	0.000	0.000	0.000	0.000	0.000	0.000	0.000	0.000	0.000	0.000	0.000	0.000
2.552	2.534	2.488	2.489	2.347	2.495	2.567	2.491	2.523	2.408	2.392	2.414	2.430	2.442	2.449	2.413	2.467	2.433	2.410	2.439	2.391	2.405	2.409
0.012	0.017	0.010	0.020	0.006	0.016	0.015	0.008	0.011	0.008	0.019	0.012	0.018	0.003	0.006	0.004	0.011	0.008	0.010	0.012	0.007	0.004	0.014
0.000	0.000	0.000	0.000	0.000	0.000	0.000	0.000	0.000	0.000	0.000	0.000	0.000	0.000	0.000	0.000	0.000	0.000	0.000	0.000	0.000	0.000	0.000
4.750	4.750	4.750	4.750	4.750	4.750	4.750	4.750	4.750	4.750	4.750	4.750	4.750	4.750	4.750	4.750	4.750	4.750	4.750	4.750	4.750	4.750	4.750
0.085	0.091	0.103	0.109	0.111	0.092	0.077	0.093	0.079	0.161	0.150	0.148	0.127	0.129	0.117	0.116	0.105	0.120	0.123	0.128	0.148	0.163	0.163
0.174	0.176	0.129	0.195	-0.085	0.113	0.172	0.085	0.085	0.288	0.228	0.231	0.155	0.179	0.124	0.044	0.084	0.115	0.085	0.173	0.187	0.300	0.329
0.730	0.693	0.454	0.639	-0.290	0.444	0.800	0.333	0.392	0.621	0.539	0.553	0.438	0.494	0.385	0.141	0.292	0.347	0.253	0.484	0.451	0.641	0.704

4.750	4.750	4.750	4.750	4.750	4.750	4.750	4.750	4.750	4.750	4.750	4.750	4.750	4.750	4.750	4.750	4.750	4.750	4.750	4.750	4.750	4.750	4.750
12	12	12	12	12	12	12	12	12	12	12	12	12	12	12	12	12	12	12	12	12	12	12
ACC 199	ACC 200	ACC 201	ACC 202	ACC 203	ACC 204	ACC 205	ACC 206	ACC 207	ACC 208	ACC 209	ACC 210	ACC 211	ACC 212	ACC 213	ACC 214	ACC 215	ACC 216	ACC 217	ACC 218	ACC 219	ACC 220	ACC 221
41.28	38.40	38.63	40.09	39.17	39.79	41.05	39.83	40.19	39.65	39.34	39.69	41.64	39.12	39.34	39.59	38.41	39.24	39.70	40.66	40.19	39.64	40.44
-	-	-	-	-	-	-	-	-	-	-	-	-	-	-	-	-	-	-	-	-	-	-
1.50	1.08	1.13	1.21	1.16	1.34	1.18	1.32	1.34	1.07	1.21	1.17	1.45	1.99	1.09	1.17	1.07	1.12	1.17	1.31	1.18	1.66	1.22
-	-	-	-	-	-	-	-	-	-	-	-	-	-	-	-	-	-	-	-	-	-	-
9.39	11.47	11.58	10.94	11.02	10.61	9.11	9.51	10.86	11.02	11.10	11.39	10.02	10.34	10.95	11.97	11.90	11.71	10.57	10.40	10.32	8.44	10.19
-	-	-	-	-	-	-	-	-	-	-	-	-	-	-	-	-	-	-	-	-	-	-
34.54	32.87	33.70	33.78	34.57	34.89	35.64	34.43	34.84	33.98	34.33	34.88	34.94	32.35	33.57	33.79	33.53	34.04	34.78	34.88	35.34	33.01	34.63
0.08	0.12	0.27	0.40	0.18	0.16	0.34	0.16	0.22	0.08	0.23	0.23	0.18	0.00	0.18	0.14	0.36	0.26	0.16	0.05	0.22	0.17	0.16
-	-	-	-	-	-	-	-	-	-	-	-	-	-	-	-	-	-	-	-	-	-	-
86.78	83.93	85.31	86.42	86.09	86.79	87.32	85.26	87.44	85.80	86.20	87.37	88.24	83.79	85.13	86.66	85.26	86.37	86.38	87.29	87.25	82.92	86.63
1.914	1.855	1.833	1.878	1.835	1.846	1.884	1.877	1.854	1.868	1.842	1.834	1.902	1.891	1.869	1.854	1.826	1.840	1.851	1.877	1.852	1.921	1.881
0.000	0.000	0.000	0.000	0.000	0.000	0.000	0.000	0.000	0.000	0.000	0.000	0.000	0.000	0.000	0.000	0.000	0.000	0.000	0.000	0.000	0.000	0.000
0.082	0.062	0.063	0.067	0.064	0.073	0.064	0.073	0.073	0.059	0.067	0.064	0.078	0.113	0.061	0.065	0.060	0.062	0.064	0.071	0.064	0.095	0.067
0.000	0.000	0.000	0.000	0.000	0.000	0.000	0.000	0.000	0.000	0.000	0.000	0.000	0.000	0.000	0.000	0.000	0.000	0.000	0.000	0.000	0.000	0.000
0.364	0.463	0.459	0.428	0.431	0.412	0.349	0.375	0.419	0.434	0.435	0.440	0.383	0.418	0.435	0.468	0.473	0.459	0.412	0.401	0.397	0.342	0.396
0.000	0.000	0.000	0.000	0.000	0.000	0.000	0.000	0.000	0.000	0.000	0.000	0.000	0.000	0.000	0.000	0.000	0.000	0.000	0.000	0.000	0.000	0.000
2.386	2.365	2.382	2.357	2.411	2.411	2.436	2.417	2.394	2.385	2.395	2.401	2.378	2.329	2.376	2.357	2.374	2.377	2.415	2.399	2.426	2.383	2.399
0.004	0.006	0.014	0.020	0.009	0.008	0.017	0.008	0.011	0.004	0.012	0.011	0.009	0.000	0.009	0.007	0.018	0.013	0.008	0.002	0.011	0.009	0.008
0.000	0.000	0.000	0.000	0.000	0.000	0.000	0.000	0.000	0.000	0.000	0.000	0.000	0.000	0.000	0.000	0.000	0.000	0.000	0.000	0.000	0.000	0.000
4.750	4.750	4.750	4.750	4.750	4.750	4.750	4.750	4.750	4.750	4.750	4.750	4.750	4.750	4.750	4.750	4.750	4.750	4.750	4.750	4.750	4.750	4.750
0.132	0.164	0.162	0.154	0.152	0.146	0.125	0.134	0.149	0.154	0.154	0.155	0.139	0.152	0.155	0.166	0.166	0.162	0.146	0.143	0.141	0.126	0.142
0.089	0.229	0.272	0.177	0.267	0.235	0.169	0.173	0.220	0.205	0.249	0.268	0.117	0.105	0.201	0.228	0.289	0.259	0.234	0.175	0.232	0.063	0.172
0.245	0.495	0.592	0.414	0.619	0.570	0.484	0.461	0.525	0.472	0.572	0.610	0.306	0.252	0.461	0.488	0.611	0.565	0.568	0.437	0.584	0.185	0.434

4.750	4.750	4.750	4.750	4.750	4.750	4.750	4.750	4.750	4.750	4.750	4.750	4.750	4.750	4.750	4.750	4.750	4.750	4.750	4.750	4.750	4.750	4.750
12	12	12	12	12	12	12	12	12	12	12	12	12	12	12	12	12	12	12	12	12	12	12
ACC 222	ACC 223	ACC 224	ACC 225	ACC 226	ACC 227	ACC 228	ACC 229	ACC 230	ACC 231	ACC 232	ACC 233	ACC 234	ACC 235	ACC 236	ACC 237	ACC 238	ACC 239	ACC 240	ACC 241	ACC 242	ACC 243	ACC 244
40.59	39.14	39.72	40.19	39.84	38.66	39.08	39.82	40.66	41.40	40.47	40.68	41.03	40.57	40.30	40.09	38.69	40.01	40.07	40.72	39.82	39.76	40.73
-	-	-	-	-	-	-	-	-	-	-	-	-	-	-	-	-	-	-	-	-	-	-
1.19	1.29	1.27	1.43	1.41	1.14	1.22	1.27	1.35	1.63	1.56	1.68	1.19	1.35	1.33	1.82	0.31	1.13	1.16	1.32	1.29	1.26	1.23
-	-	-	-	-	-	-	-	-	-	-	-	-	-	-	-	-	-	-	-	-	-	-
10.12	12.06	11.70	11.01	10.10	11.97	11.75	10.99	9.66	9.38	8.74	9.20	10.05	10.66	10.67	10.72	12.74	10.69	10.39	9.72	10.15	9.72	10.81
-	-	-	-	-	-	-	-	-	-	-	-	-	-	-	-	-	-	-	-	-	-	-
34.20	34.28	33.93	34.13	32.75	33.37	33.35	34.27	34.10	35.51	33.63	34.54	34.94	34.69	34.17	34.17	33.54	34.87	34.75	34.51	33.95	34.26	35.09
0.16	0.31	0.24	0.22	0.20	0.10	0.16	0.14	0.14	0.10	0.06	0.24	0.31	0.31	0.39	0.30	0.16	0.38	0.25	0.14	0.16	0.21	0.21
-	-	-	-	-	-	-	-	-	-	-	-	-	-	-	-	-	-	-	-	-	-	-
86.26	87.08	86.87	86.98	84.30	85.23	85.57	86.49	85.92	88.02	84.45	86.33	87.52	87.57	86.85	87.09	85.44	87.07	86.63	86.42	85.37	85.21	88.07
1.898	1.820	1.853	1.869	1.913	1.840	1.853	1.860	1.907	1.888	1.927	1.894	1.888	1.870	1.875	1.859	1.841	1.852	1.863	1.897	1.881	1.877	1.865
0.000	0.000	0.000	0.000	0.000	0.000	0.000	0.000	0.000	0.000	0.000	0.000	0.000	0.000	0.000	0.000	0.000	0.000	0.000	0.000	0.000	0.000	0.000
0.066	0.071	0.070	0.079	0.080	0.064	0.068	0.070	0.075	0.088	0.087	0.092	0.065	0.073	0.073	0.099	0.017	0.062	0.064	0.072	0.072	0.070	0.066
0.000	0.000	0.000	0.000	0.000	0.000	0.000	0.000	0.000	0.000	0.000	0.000	0.000	0.000	0.000	0.000	0.000	0.000	0.000	0.000	0.000	0.000	0.000
0.395	0.469	0.456	0.428	0.405	0.476	0.466	0.429	0.379	0.357	0.348	0.358	0.387	0.411	0.415	0.415	0.507	0.414	0.404	0.378	0.401	0.383	0.414
0.000	0.000	0.000	0.000	0.000	0.000	0.000	0.000	0.000	0.000	0.000	0.000	0.000	0.000	0.000	0.000	0.000	0.000	0.000	0.000	0.000	0.000	0.000
2.382	2.375	2.358	2.364	2.342	2.365	2.355	2.384	2.382	2.412	2.385	2.395	2.395	2.381	2.368	2.361	2.377	2.404	2.407	2.395	2.389	2.409	2.394
0.008	0.016	0.012	0.011	0.010	0.005	0.008	0.007	0.007	0.005	0.003	0.012	0.015	0.015	0.019	0.015	0.008	0.019	0.013	0.007	0.008	0.011	0.010
0.000	0.000	0.000	0.000	0.000	0.000	0.000	0.000	0.000	0.000	0.000	0.000	0.000	0.000	0.000	0.000	0.000	0.000	0.000	0.000	0.000	0.000	0.000
4.750	4.750	4.750	4.750	4.750	4.750	4.750	4.750	4.750	4.750	4.750	4.750	4.750	4.750	4.750	4.750	4.750	4.750	4.750	4.750	4.750	4.750	4.750
0.142	0.165	0.162	0.153	0.148	0.168	0.165	0.153	0.137	0.129	0.127	0.130	0.139	0.147	0.149	0.150	0.176	0.147	0.144	0.136	0.144	0.137	0.147
0.138	0.289	0.223	0.184	0.095	0.257	0.226	0.211	0.111	0.137	0.059	0.121	0.159	0.188	0.177	0.182	0.302	0.235	0.210	0.133	0.167	0.176	0.203
0.348	0.616	0.490	0.431	0.234	0.539	0.485	0.491	0.293	0.383	0.170	0.338	0.411	0.457	0.427	0.438	0.595	0.567	0.521	0.353	0.416	0.459	0.490

4.750	4.750	4.750	4.750	4.750	4.750	4.750	4.750	4.750	4.750	4.750	4.750	4.750	4.750	4.750	4.750	4.750	4.750	4.750	4.750	4.750	4.750	4.750
12	12	12	12	12	12	12	12	12	12	12	12	12	12	12	12	12	12	12	12	12	12	12
ACC 245	ACC 246	ACC 247	ACC 248	ACC 249	ACC 250	ACC 252	ACC 253	ACC 254	ACC 255	ACC 256	ACC 257	ACC 258	ACC 259	ACC 260	ACC 261	ACC 262	ACC 263	ACC 264	ACC 265	ACC 285	ACC 286	ACC 287
40.24	40.15	40.21	39.56	40.14	39.85	39.19	39.80	39.51	39.86	40.05	40.12	39.68	39.96	39.77	39.38	39.39	39.04	39.54	39.52	41.25	41.71	41.40
-	-	-	-	-	-	-	-	-	-	-	-	-	-	-	-	-	-	-	-	-	-	-
1.24	1.13	1.17	1.14	1.12	1.05	1.12	1.13	1.28	1.18	1.49	1.28	1.18	1.29	1.37	1.20	1.12	1.12	1.27	1.11	1.25	1.46	1.57
-	-	-	-	-	-	-	-	-	-	-	-	-	-	-	-	-	-	-	-	-	-	-
10.72	10.59	11.31	11.38	11.86	12.23	10.87	10.44	11.48	10.99	10.79	10.98	10.77	11.20	10.35	10.88	11.25	11.37	11.06	11.49	9.05	8.55	8.73
-	-	-	-	-	-	-	-	-	-	-	-	-	-	-	-	-	-	-	-	-	-	-
34.60	34.42	34.27	33.40	33.60	33.94	34.04	34.23	34.20	34.54	34.18	34.18	34.41	34.10	34.56	33.65	34.13	34.07	34.55	33.79	35.62	35.18	35.48
0.33	0.35	0.34	0.16	0.30	0.11	0.31	0.27	0.15	0.25	0.24	0.16	0.25	0.45	0.13	0.25	0.16	0.08	0.18	0.05	0.09	0.00	0.09
-	-	-	-	-	-	-	-	-	-	-	-	-	-	-	-	-	-	-	-	-	-	-
87.13	86.65	87.30	85.64	87.02	87.18	85.53	85.87	86.61	86.82	86.75	86.72	86.29	87.00	86.18	85.36	86.05	85.67	86.60	85.95	87.27	86.89	87.27
1.864	1.870	1.864	1.873	1.874	1.856	1.850	1.869	1.845	1.853	1.865	1.871	1.855	1.859	1.858	1.865	1.850	1.842	1.842	1.862	1.894	1.924	1.900
0.000	0.000	0.000	0.000	0.000	0.000	0.000	0.000	0.000	0.000	0.000	0.000	0.000	0.000	0.000	0.000	0.000	0.000	0.000	0.000	0.000	0.000	0.000
0.068	0.062	0.064	0.064	0.062	0.057	0.062	0.062	0.070	0.065	0.081	0.070	0.065	0.071	0.076	0.067	0.062	0.062	0.070	0.061	0.068	0.079	0.085
0.000	0.000	0.000	0.000	0.000	0.000	0.000	0.000	0.000	0.000	0.000	0.000	0.000	0.000	0.000	0.000	0.000	0.000	0.000	0.000	0.000	0.000	0.000
0.415	0.412	0.438	0.450	0.463	0.476	0.429	0.410	0.448	0.427	0.420	0.428	0.421	0.435	0.404	0.431	0.442	0.449	0.431	0.452	0.347	0.330	0.335
0.000	0.000	0.000	0.000	0.000	0.000	0.000	0.000	0.000	0.000	0.000	0.000	0.000	0.000	0.000	0.000	0.000	0.000	0.000	0.000	0.000	0.000	0.000
2.387	2.388	2.367	2.355	2.336	2.355	2.393	2.395	2.379	2.392	2.371	2.374	2.397	2.363	2.406	2.374	2.388	2.394	2.398	2.372	2.436	2.417	2.426
0.016	0.017	0.017	0.008	0.015	0.006	0.015	0.013	0.007	0.012	0.012	0.008	0.013	0.022	0.006	0.012	0.008	0.004	0.009	0.003	0.004	0.000	0.004
0.000	0.000	0.000	0.000	0.000	0.000	0.000	0.000	0.000	0.000	0.000	0.000	0.000	0.000	0.000	0.000	0.000	0.000	0.000	0.000	0.000	0.000	0.000
4.750	4.750	4.750	4.750	4.750	4.750	4.750	4.750	4.750	4.750	4.750	4.750	4.750	4.750	4.750	4.750	4.750	4.750	4.750	4.750	4.750	4.750	4.750
0.148	0.147	0.156	0.160	0.165	0.168	0.152	0.146	0.158	0.151	0.150	0.153	0.149	0.156	0.144	0.154	0.156	0.158	0.152	0.160	0.125	0.120	0.121
0.204	0.198	0.207	0.191	0.190	0.231	0.237	0.199	0.239	0.228	0.188	0.189	0.225	0.211	0.208	0.203	0.238	0.255	0.246	0.215	0.144	0.073	0.115
0.492	0.480	0.473	0.424	0.411	0.484	0.553	0.485	0.534	0.535	0.448	0.441	0.534	0.486	0.515	0.470	0.539	0.568	0.570	0.475	0.415	0.221	0.344

4.750	4.750	4.750	4.750	4.750	4.750	4.750	4.750	4.750	4.750	4.750	4.750	4.750
12	12	12	12	12	12	12	12	12	12	12	12	12
ACC	ACC	ACC	ACC	ACC	ACC	ACC	ACC	ACC	ACC	ACC	ACC	ACC
288	289	290	311	312	313	314	315	316	317	318	319	320
40.81	41.06	41.59	41.46	41.06	41.61	42.13	41.27	41.26	42.12	41.90	41.76	40.10
-	-	-	-	-	-	-	-	-	-	-	-	-
1.48	1.48	1.55	1.00	1.57	1.15	1.01	1.04	1.31	1.21	1.29	1.27	0.88
-	-	-	-	-	-	-	-	-	-	-	-	-
8.85	8.23	8.37	9.12	9.66	8.74	8.44	8.04	8.72	8.54	8.58	8.52	10.34
-	-	-	-	-	-	-	-	-	-	-	-	-
34.94	35.16	35.03	35.46	35.21	35.46	36.01	35.64	35.72	35.43	36.21	35.90	35.40
0.31	0.01	0.28	0.25	0.30	0.14	0.21	0.22	0.14	0.03	0.33	0.37	0.22
-	-	-	-	-	-	-	-	-	-	-	-	-
86.39	85.94	86.82	87.29	87.79	87.10	87.80	86.20	87.14	87.33	88.31	87.83	86.93
1.894	1.911	1.920	1.905	1.880	1.914	1.920	1.912	1.895	1.933	1.898	1.903	1.854
0.000	0.000	0.000	0.000	0.000	0.000	0.000	0.000	0.000	0.000	0.000	0.000	0.000
0.081	0.081	0.084	0.054	0.084	0.063	0.054	0.057	0.071	0.065	0.069	0.068	0.048
0.000	0.000	0.000	0.000	0.000	0.000	0.000	0.000	0.000	0.000	0.000	0.000	0.000
0.343	0.320	0.323	0.350	0.370	0.336	0.321	0.311	0.335	0.328	0.325	0.325	0.400
0.000	0.000	0.000	0.000	0.000	0.000	0.000	0.000	0.000	0.000	0.000	0.000	0.000
2.416	2.438	2.409	2.428	2.401	2.430	2.444	2.459	2.443	2.422	2.443	2.437	2.438
0.016	0.000	0.014	0.012	0.015	0.007	0.010	0.011	0.007	0.001	0.016	0.018	0.011
0.000	0.000	0.000	0.000	0.000	0.000	0.000	0.000	0.000	0.000	0.000	0.000	0.000
4.750	4.750	4.750	4.750	4.750	4.750	4.750	4.750	4.750	4.750	4.750	4.750	4.750
0.124	0.116	0.118	0.126	0.133	0.121	0.116	0.112	0.120	0.119	0.117	0.118	0.141
0.131	0.097	0.075	0.135	0.156	0.109	0.106	0.120	0.140	0.068	0.136	0.127	0.244
0.381	0.304	0.233	0.386	0.421	0.323	0.331	0.385	0.418	0.207	0.418	0.390	0.611